ANALYSIS OF THE EFFECTS OF XANTHOHUMOL ON HEPATIC HOMEOSTASIS, INFLAMMATION, FIBROSIS AND CANCEROGENESIS

DISSERTATION

ZUR ERLANGUNG DES DOKTORGRADES DER NATURWISSENSCHAFTEN (DR. RER. NAT.) DER FAKULTÄT CHEMIE UND PHARMAZIE DER UNIVERSITÄT REGENSBURG

vorgelegt von

Christoph Michael Dorn

aus Höchstädt a.d. Donau

im Jahr 2009

Promotionsgesuch eingereicht: Januar 2007

Die Arbeit wurde angeleitet von: Herrn PD Dr. Claus Hellerbrand

Prüfungsausschuss:

Vorsitzender:	Herr Prof. Dr. Elz
1. Gutachter (1. Prüfer):	Herr Prof. Dr. Jörg Heilmann
2. Gutachter (2. Prüfer):	Herr PD Dr. Claus Hellerbrand
3. Prüfer:	Herr Prof. Dr. Schlossmann

für meine Familie

Table of Contents

1 SUMMARY 1

2 INTRODUCTION 3

2.1 HOP 3
2.1.1 BOTANY 3
2.1.2 MEDICAL USE 4
2.1.3 PHYTOCHEMISTRY 5
2.2 FLAVONOIDS 6
2.3 XANTHOHUMOL 8
2.3.1 DIETARY EXPOSURE 8
2.3.2 BIOAVAILABILITY AND METABOLISM 9
2.4 BIOLOGICAL EFFECTS OF XANTHOHUMOL 11
2.4.1 ANTI-INFLAMMATORY EFFECTS 11
2.4.2 ANTI-ANGIOGENIC EFFECTS 12
2.4.3 ANTI-CANCEROUS EFFECTS 14
2.4.4 ANTIOXIDANT PROPERTIES 17
2.4.5 ANTI-INFECTIVE PROPERTIES 18
2.4.5.1 Anti-bacterial effects 18
2.4.5.2 Anti-fungal effects 19
2.4.5.3 Anti-malarial effects 19
2.4.5.4 Anti-viral effects 20
2.4.6 (ANTI)ESTROGENIC POTENTIAL 21
2.4.7 EFFECTS ON LIPID AND CARBOHYDRATE METABOLISM 22
2.4.8 EFFECTS ON BONE RESORPTION 23
2.5 XANTHOHUMOL SAFETY STUDIES 23
2.6 EFFECTS OF XANTHOHUMOL ON THE LIVER 25
2.6.1 EFFECTS OF ORAL ADMINISTERED XANTHOHUMOL ON THE LIVER 26
2.6.2 EFFECTS OF XANTHOHUMOL ON HEPATOCELLULAR CARCINOMA CELLS 26
2.6.3 EFFECTS OF XANTHOHUMOL ON HEPATOCYTES 27
2.6.4 EFFECTS OF XANTHOHUMOL ON NON-PARENCHYMAL LIVER CELLS 27
2.7 LIVER DISEASES 28
2.7.1 DEFINITION AND NATURAL COURSE OF LIVER DISEASE 28
2.7.2 LIVER FIBROSIS 28
2.7.3 LIVER CIRRHOSIS 30

2.7.4 LIVER CANCER 31
2.7.4.1 Hepatocellular cancer 31
2.7.4.1.1 Prevalence and incidence 31
2.7.4.1.2 Etiology 31
2.7.4.1.3 Therapy and prognosis 32
2.7.5 CAUSES FOR CHRONIC LIVER DISEASES 32
2.7.5.1 Alcohol induced liver disease 33
2.7.5.2 Drug induced liver injury 34
2.7.5.3 Autoimmune related mechanisms and genetic defects 34
2.7.5.4 Viral hepatitis 35
2.7.5.4.1 Hepatitis A 35
2.7.5.4.2 Hepatitis B 35
2.7.5.4.3 Hepatitis C 36
2.7.5.5 Non-alcoholic fatty liver disease (NAFLD) 36
2.7.5.5.1 Definition 36
2.7.5.5.2 Prevalence of NAFLD/NASH 37
2.7.5.5.3 Etiology and pathogenesis 38
2.7.5.5.4 Prognosis and therapy 38
2.7.5.5.5 Experimental NASH models 39
2.8 AIM OF THE THESIS 40

3 MATERIALS AND METHODS 41

3.1 CHEMICALS AND REAGENTS 41
3.2 LABORATORY EXPENDABLES 41
3.3 LABORATORY INSTRUMENTS 42
3.4 BUFFERS 43
3.5 CELL CULTURE 43
3.5.1 CELL CULTURE MEDIUM 43
3.5.2 CULTIVATION OF CELL LINES 44
3.5.3 HUMAN HEPATOCELLULAR CARCINOMA CELL LINES 44
3.5.4 ISOLATION OF PRIMARY HUMAN HEPATOCYTES 44
3.5.5 ISOLATION OF PRIMARY MURINE HEPATOCYTES 45
3.5.6 ISOLATION OF HUMAN HEPATIC STELLATE CELLS 47
3.5.7 DETERMINATION OF CELL NUMBER AND VIABILITY 48
3.5.8 FREEZING CELLS FOR STORAGE 48
3.6 ISOLATION AND ANALYSIS OF RNA 49
3.6.1 RNA ISOLATION AND DETERMINATION OF RNA CONCENTRATION 49

3.6.2 REVERSE TRANSCRIPTION OF RNA TO CDNA 50
3.6.3 QUANTITATIVE REAL TIME POLYMERASE CHAIN REACTION 50
3.7 PROTEIN ANALYSIS 53
3.7.1 PREPARATION OF WHOLE CELL PROTEIN EXTRACTS 53
3.7.2 PREPARATION OF NUCLEAR PROTEIN EXTRACTS 53
3.7.3 DETERMINATION OF PROTEIN CONCENTRATION 54
3.7.4 SDS POLYACRYLAMID GEL ELECTROPHORESIS 55
3.7.5 WESTERN BLOTTING 56
3.7.6 QUANTIFICATION OF NFκB ACTIVITY 57
3.7.7 QUANTIFICATION OF CASPASE-3/7 ACTIVITY 57
3.7.8 ANALYSIS OF CELL CULTURE SUPERNATANTS 58
3.8 FLOW CYTOMETRY 58
3.8.1 ANNEXIN V / PROPIDIUM IODIDE DOUBLE STAINING 59
3.8.2 CELL VIABILITY ANALYSIS VIA PROPIDIUM IODIDE STAINING 60
3.8.3 FLOW CYTOMETRICAL ANALYSIS OF CASPASE-3 ACTIVITY 61
3.9 FUNCTIONAL ASSAYS 62
3.9.1 XTT-PROLIFERATION ASSAY 62
3.9.2 MIGRATION ASSAY 62
3.10 ANIMAL EXPERIMENTS 63
3.10.1 ANIMAL TREATMENT AND SAMPLE ASSERVATION 63
3.10.2 MURINE NASH MODEL 64
3.10.3 TOXICITY STUDY 64
3.11 HISTOLOGY AND IMMUNOHISTOCHEMISTRY 64
3.11.1 HEMATOXYLIN/EOSIN STAINING 64
3.11.2 IMMUNOHISTOCHEMICAL ANALYSIS OF α-SMOOTH MUSCLE ACTIN 65
3.12 SEROLOGY 66
3.13 LIMULUS AMEBOCYTE LYSATE ASSAY 66
3.14 GLYCOGEN ASSAY 67
3.15 CHOLESTEROL ASSAY 67
3.16 REAGENT PREPARATION FOR *IN VITRO* EXPERIMENTS 68
3.16.1 PALMITIC ACID PREPARATION 68
3.16.2 XANTHOHUMOL PREPARATION 69
3.17 STATISTICAL ANALYSIS 69

4 RESULTS 70

4.1 EFFECTS OF XANTHOHUMOL ON HEPATIC INFLAMMATION AND FIBROSIS 70

4.1.1 MOTIVATION 70
4.1.2 EFFECTS OF XANTHOHUMOL ON HSC 71
4.1.2.1 Effects on HSC activation *in vitro* 71
4.1.2.2 Induction of apoptosis in activated HSC *in vitro* 72
4.1.2.3 Inhibition of NFκB activity and proinflammatory gene expression in HSC *in vitro* 73
4.1.3 EFFECTS OF XANTHOHUMOL ON PRIMARY HUMAN HEPATOCYTES 75
4.1.4 *IN VIVO* EFFECTS OF XANTHOHUMOL IN A MURINE NASH MODEL 77
4.1.4.1 No affection of hepatic steatosis in the murine NASH model 77
4.1.4.2 Inhibition of hepatic inflammation in a murine NASH model 79
4.1.4.3 Inhibition of HCS activation and hepatic fibrosis *in vivo* 81
4.1.5 SUMMARY 82
4.2 EFFECTS OF XANTHOHUMOL ON HEPATOCELLULAR CARCINOMA CELLS 83
4.2.1 MOTIVATION 83
4.2.2 INDUCTION OF CELL DEATH IN HCC CELLS BUT NOT IN PHH 83
4.2.3 INDUCTION OF APOPTOSIS IN HCC CELLS 85
4.2.4 INHIBITION OF HCC CELL PROLIFERATION AND MIGRATION 87
4.2.5 INHIBITION OF NFκB ACTIVATION AND IL-8 EXPRESSION IN HCC CELLS 88
4.2.6 SUMMARY 90
4.3 SAFETY PROFILE OF ORALLY APPLIED XANTHOHUMOL 91
4.3.1 MOTIVATION 91
4.3.2 IN-LIFE PARAMETERS 91
4.3.3 EFFECTS ON FUNCTION AND HOMEOSTASIS OF INNER ORGANS 93
4.3.4 EFFECTS ON LIVER FUNCTION AND HOMEOSTASIS 95
4.3.5 COMPARISON OF CYTOTOXICITY IN MURINE AND HUMAN HEPATOCYTES *IN VITRO* 98
4.3.6 SUMMARY 99

5 DISCUSSION 100

5.1 XANTHOHUMOL AND HEPATIC INFLAMMATION AND FIBROSIS 100
5.1.1 *IN VITRO* EFFECTS OF XANTHOHUMOL ON PRIMARY HUMAN LIVER CELLS 100
5.1.2 *IN VIVO* EFFECTS OF XANTHOHUMOL IN A MURINE NASH MODEL 101
5.1.3 XANTHOHUMOL AS A THERAPEUTIC AGENT FOR CHRONIC LIVER DISEASES 102
5.2 XANTHOHUMOL AND HEPATOCELLULAR CARCINOMA 103
5.2.1 EFFECTS OF XANTHOHUMOL ON HCC CELL VIABILITY 103
5.2.2 FUNCTIONAL EFFECTS OF XANTHOHUMOL ON HCC CELLS 104
5.2.3 EFFECTS ON NFκB ACTIVITY AND IL-8 EXPRESSION IN HCC CELLS 104
5.2.4 EFFECTS OF XANTHOHUMOL ON NON-MALIGNANT CELLS 106

5.2.5 XANTHOHUMOL AS THERAPEUTIC AGENT FOR HCC TREATMENT 107
5.3 SAFETY PROFILE OF XANTHOHUMOL 108
5.3.1 PREVIOUSLY PERFORMED SAFETY STUDIES 108
5.3.2 EFFECTS OF XANTHOHUMOL ON INNER ORGANS 109
5.3.3 EFFECTS OF XANTHOHUMOL ON LIVER FUNCTION 109
5.4 CONCLUSION 112

6 REFERENCES 115

7 ABBREVIATIONS 135

8 APPENDIX 138

8.1 CURRICULUM VITAE 138
8.2 ADVANCED TRAINING COURSES 139
8.3 PUBLICATIONS 139
8.4 PRESENTATIONS 140
8.4.1 ORAL PRESENTATIONS 140
8.4.2 POSTER PRESENTATIONS 141
8.5 AWARDS/GRANTS 142
8.6 DANKSAGUNG 142
8.7 EIDESSTATTLICHE ERKLÄRUNG 144

1 Summary

Xanthohumol is the major prenylated chalcone found in hops, and it has been shown to exhibit various biological effects. However, xanthohumol effects on liver cells or in liver diseases, respectively, are widely unknown.

In the present work, first the effects of xanthohumol on hepatic stellate cells (HSC), the central mediators of liver fibrogenesis, were analyzed. Xanthohumol inhibited the activation of primary human HSC and induces apoptosis in activated HSC *in vitro* in a dose dependent manner (0-20 µM). In contrast, xanthohumol doses as high as 100 µM did not impair viability of primary human hepatocytes (PHH). However, in both cell types xanthohumol inhibited NFκB activation and expression of NFκB dependent proinflammatory chemokines. *In vivo*, feeding of xanthohumol reduced levels of serum transaminases and hepatic expression of proinflammatory genes in a murine model of non-alcoholic steatohepatitis (NASH). Moreover, xanthohumol treatment significantly inhibited hepatic expression of profibrogenic genes and activation of HSC *in vivo*.

Next, xanthohumol effects on hepatocellular carcinoma (HCC) cells were investigated. Xanthohumol concentration of 25 µM induced apoptosis in two HCC cell lines (HepG2 and Huh7). Furthermore, xanthohumol repressed proliferation and migration, as well as TNF induced activation of the transcription factor NFκB and interleukin-8 expression in both cell lines at even lower concentrations.

Finally, to evaluate the safety profile of xanthohumol female BALB/c mice were fed with a xanthohumol enriched diet for three weeks, achieving a daily dose of approximately 1000 mg xanthohumol /kg body weight per day. Macroscopical and histopathological examination of liver, kidney, colon, lung, heart, spleen and thymus revealed no signs of xanthohumol-toxicity, and biochemical serum analysis confirmed normal organ function. Further, serum glucose levels and hepatic glycogen content as well as hepatic CYP2E1 mRNA expression levels were unaffected by xanthohumol treatment. In addition, also mRNA expression of several genes indicative of early hepatic inflammation and fibrosis, a hallmark of chronic liver injury, did not differ between xanthohumol treated and control mice.

In conclusion, xanthohumol has the potential to ameliorate NASH induced liver injury as well as different pro-tumorigenic mechanisms known to promote HCC

progression. Together with the good safety profile these data suggest the potential use of xanthohumol as a functional nutrient or therapeutic agent to prevent or treat chronic liver diseases like NASH or HCC.

2 Introduction

2.1 Hop

2.1.1 Botany

The hop plant (*Humulus lupulus* L.) is well-known as a raw material in the brewing industry. The female inflorescences, rich in polyphenolic compounds and acyl phloroglucinols are widely used to preserve beer and to give it a characteristic aroma and flavor. From a taxonomic point of view, the genus *Humulus* belongs to the family *Cannabaceae* of the order *Urticales*, but in 2003 it was incorporated in the order *Rosales* (Van Cleemput et al. 2009, Bremer et al. 2003). Hop is a dioecious, wind pollinated, perennial climbing bine. The stems regrow each spring from the rhizomes of an underground rootstock and die off each autumn, whereas the cold-hardy rootstock itself can reach an age of up to 50 years. The slender, flexible, climbing stems twist around their support in a clockwise direction growing up to 6-9 m in length, often with stout-hooked hairs. The wire-haired leaves are heart-shaped and lobed, on foot-stalks, and placed opposite one another on the stem. They are of a dark-green color with their edges coarsely toothed. Blooming period ranges from early to mid July. The male inflorescences are loose, panicle-like cymes. Female inflorescences are cone-shaped spikes of pistillate flowers (aments) growing from the axils of the leaves and are also known as hop strobiles, hop cones or “hops” (Figure 2.1). They consist of overlapping green ovate bracts with a pair of pistillate flowers tucked between each adjacent pair of bracts.

Figure 2.1 Development of the female inflorescences of *Humulus lupulus* from the flower (left) to the ripe strobile (right). Pictures from Nagel, 2009 (Nagel 2009).

Hop resin a.k.a. lupulin is secreted by glandular trichomes, also called lupulin glands, and can be found on the adaxial surfaces of the cone bracts (Figure 2.2).

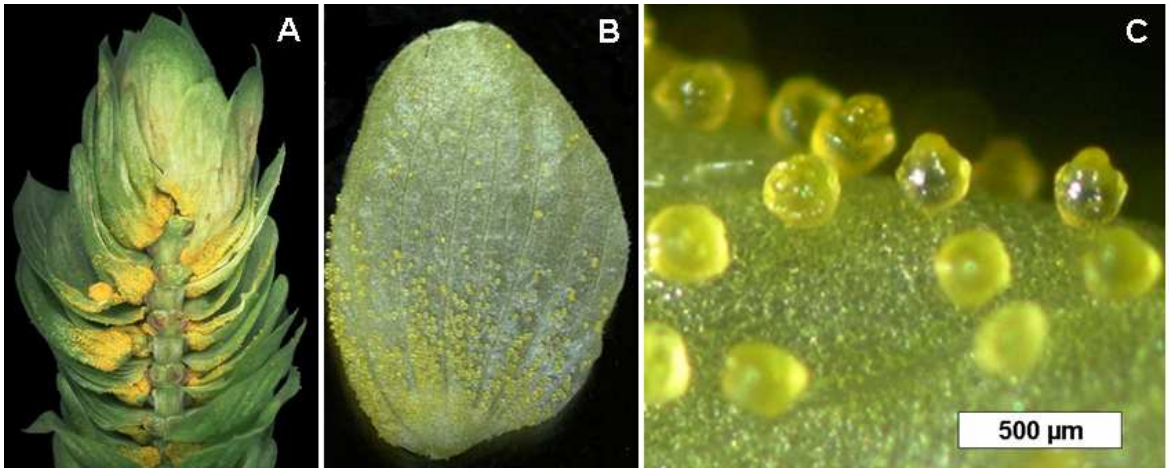

Figure 2.2 (A) Longitudinal section of a hop cone showing lupulin glands at the base of bracteoles. (B) A single bract showing trichomes mainly on the lower third of the bract. (C) Ripe lupulin glands. Pictures from Nagel, 2009 (Nagel 2009).

2.1.2 Medical use

Humulus lupulus has a long history as a medicinal remedy to treat a wide range of complaints (Zanoli and Zavatti 2008). It has been mainly recommended as a mild sedative useful to treat sleeplessness and nervousness (Blumenthal 1998). Traditionally, hops were used to treat excitability and restlessness associated to tension headache, to improve appetite and digestion and to relieve toothache, earache and neuralgia (Barnes et al. 2002; Grieve 1971). In addition hops have been reputed to exert diuretic, antispasmodic and anaphrodisiac effects (Blumenthal 1998; Duke 1985; Weiss 2009). Native American tribes used hops as a sedative, antirheumatic, analgesic and as a diuretic (Blumenthal 1998; Bown 2001; Hamel and Chiltoskey 1975). Further, they used heated hops as a poultice in the treatment of pneumonia (Carr and Westey 1945) and a decoction of hops was recommended for intestinal pain and fevers (Bown 2001). In India, the Ayurvedic Pharmacopoeia recommends hops to treat restlessness associated with nervous tension, headache and indigestion (Karnick 1994). In traditional Chinese medicine hops are used to treat insomnia, restlessness, dyspepsia and lack of appetite. Alcoholic extracts of hops have been clinically used in China to treat leprosy, pulmonary tuberculosis, acute bacterial dysentery, silicosis and asbestosis with positive outcomes (Blumenthal et al. 2000). Topically, hops were

used to treat crural ulcers and skin injuries and to relieve muscle spasms and nerve pain (Lawless 1995). In aromatherapy hops have been used for skin care, breathing conditions, nervousness, nerve pain and stress-related conditions (Lawless 1995). The Committee on Herbal Medicinal Products (HMPC) of the European Medicines Agency (EMEA) reports the traditional use of *Humulus lupulus flos* for relief of mild symptoms of mental stress and insomnia. The German Commission E and European Scientific Cooperative on Phytotherapy (ESCOP) approved hops as a treatment for excitability, mood and sleep disturbances (Blumenthal 1998).

2.1.3 Phytochemistry

Starting from the second half of the 20th century, several phytochemical studies were performed to investigate the composition of hop cones and other parts of the plant, leading to the isolation and identification of pharmacologically relevant compounds. The main structural classes of chemical compounds identified from hop cones include terpenes, bitter acids and chalcones. Hops are also rich in flavonol glycosides (kaempferol, quercetin, quercitrin, rutin) (Sagesser and Deinzer 1996) and catechins (catechin gallate, epicatechin gallate) (Gorissen et al. 1968).

Hundreds of terpenoid components were identified in the volatile oil (0.3–1.0% of hop strobile weight): primarily β-caryophyllene, farnesene and humulene (sesquiterpenes) and myrcene (monoterpene) (Eri et al. 2000; Malizia et al. 1999).

The bitter acids (5–20% of hop strobile weight) are phloroglucinol derivatives usually classified as α-acids and β-acids. β-acids are structurally different from α-acids for one more prenyl group. The bitter acids are present in hops as a complex mixture of variable composition and concentrations. The main α-acids are humulone (35–70% of total α-acids), cohumulone (20–65%) and adhumulone (10–15%); the corresponding β-acids are lupulone (30–55% of total β-acids), colupulone and adlupulone. In addition to the two series of normal, co- and ad-homologs, there exist some other minor bitter acids.

Aside from volatile oil and bitter acids, several prenylated flavonoids were identified from hop cones.

2.2 Flavonoids

Flavonoids are widely common products of secondary metabolism in plants, but are totally absent in animals, bacteria, fungi and algae. Beside of phenolic acids, lignans and stilbens, the flavonoids represent a major part of plant polyphenols. The name derives from the Latin word for “yellow” *(flavus*), which reflects the fact that most (but not all) flavonoids have a yellow color. Flavonoids are formed in plants from malonate and the aromatic amino acids phenylalanine and tyrosine (Harborne 1986). The basic flavonoid structure is the flavane (2-phenylchromane) (Figure 2.3), which consists of 15 carbon atoms arranged in three rings; two aromatic rings (which are labeled A and B) and an O-heterocyclic C-ring (C6−C3−C6 structure).

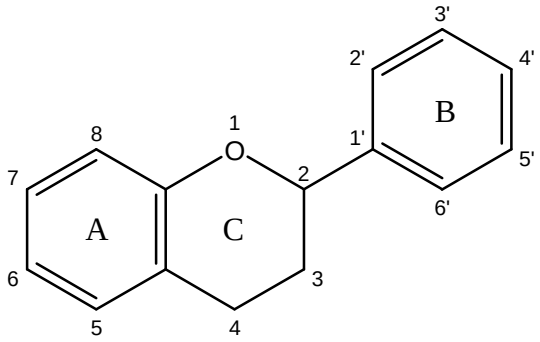

Figure 2.3 Flavane (2-phenylchromane)

Depending on the level of oxidation and pattern of substitution of the C-ring, flavonoids are subdivided into various classes: flavanes, flavanoles (3-hydroxy-flavanes), flavandioles (3,4-dihydroxy-flavanes), flavanones (4-oxo-flavanes), flavones (3-oxo-flav-2-enes), flavonoles (3-hydroxy-4-oxo-flav-2-enes), flavanonoles (3-hydroxy-4-oxo-flavanes) and flavylium salts also known as anthocyanidines. A special group of flavonoids are the chalcones, which are derivatives of phenyl styryl ketone (Figure 2.4). Chalcones are precursors of flavanones in the biosynthesis of flavane derivatives.

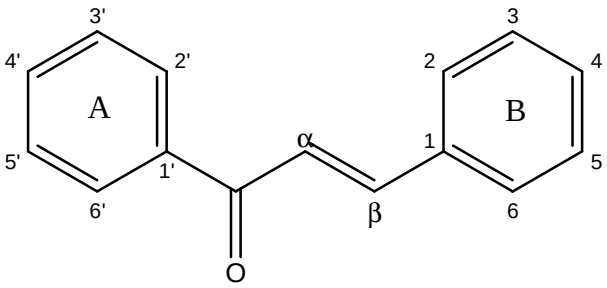

Figure 2.4 Chalcone (phenyl styryl ketone)

Prenylated chalcones are the principle component of the phenolic fraction of hops. Xanthohumol (XN) (Figure 2.5) is the most abundant chalcone found in hops (0.1–1% of dry weight) and was first described by Power *et al*. in 1913 (Power et al. 1913). Other chalcones can also be found in hops, but they occur at 10 to 100-fold lower concentrations. XN accounts for approximately 82−89% of all prenylated flavonoids in hops (Rodriguez et al. 2001; Stevens et al. 2003; Stevens and Page 2004).

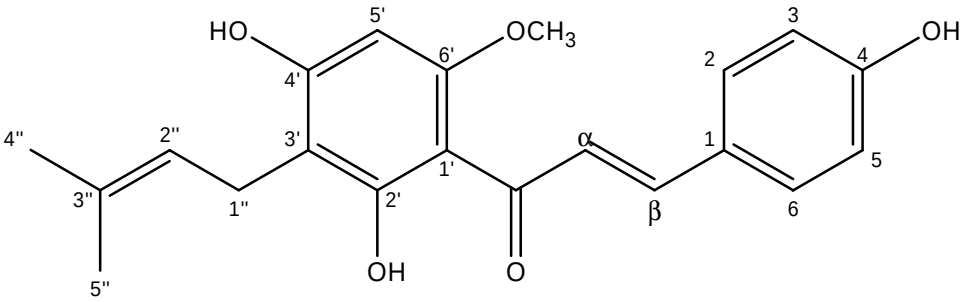

Figure 2.5 Xanthohumol

Most of the chalcones found in hops contain a free 2'-hydroxy group and can therefore isomerize to their corresponding flavanones. XN can be converted to the prenylflavanone isoxanthohumol (IX) (Figure 2.6) in consequence of thermal treatment (*e.g.* during the brewing process of beer) or increased pH value (Stevens et al. 1999). Due to this, IX is the main prenylflavonoid present in beer.

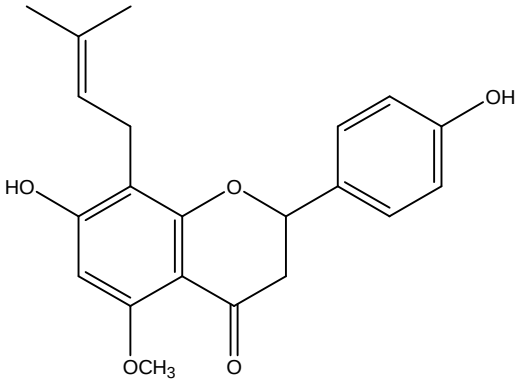

Figure 2.6 Isoxanthohumol

Over the past few years, hop research has been largely dedicated to prenylflavonoids in view of their extremely interesting bioactivities. Whereas xanthohumol has received much attention mostly as a cancer chemopreventive agent, 8-prenylnaringenin (8-PN), an isomerization product of desmethyl-

xanthohumol (DMX), also present in beer, enjoys fame as the most potent phytoestrogen isolated to date, whereas 6-prenylnaringenin (6-PN), another isomerization product of DMX shows only slight estrogenic activity (Milligan et al. 2002; Milligan et al. 2000; Milligan et al. 1999) (Figure 2.7).

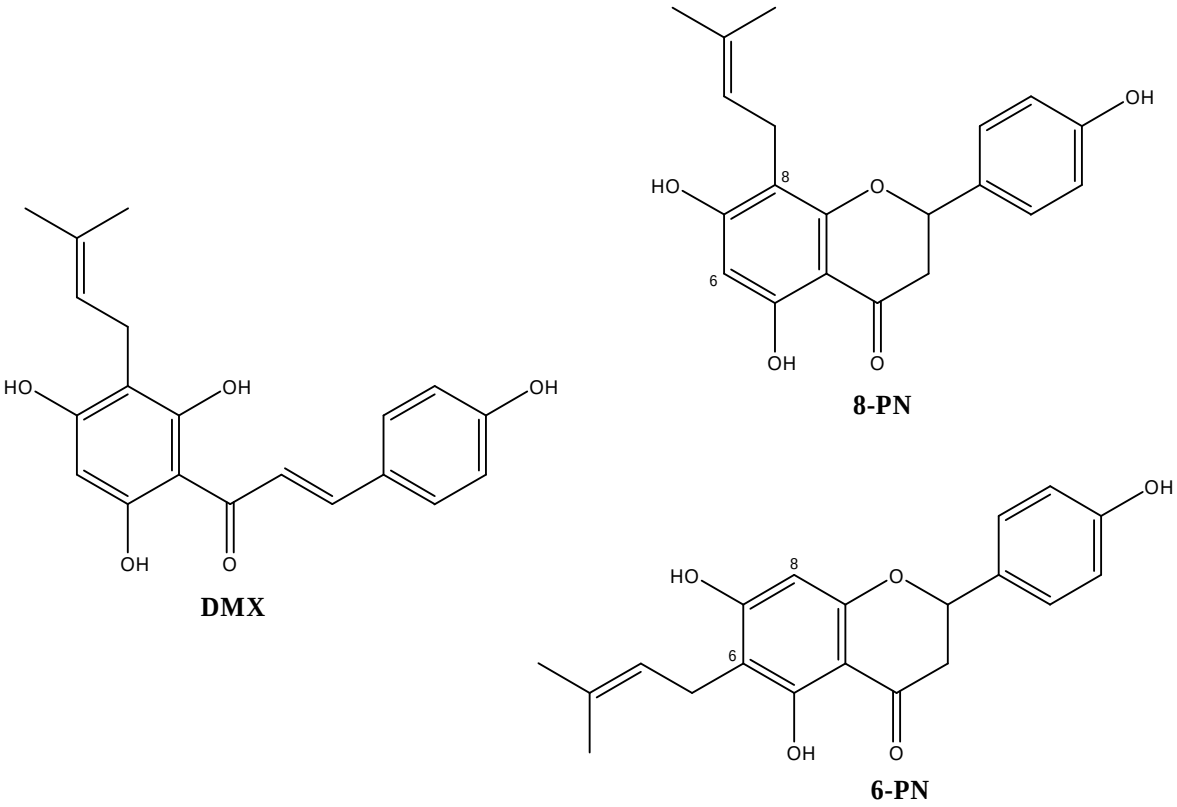

Figure 2.7 Desmethylxanthohumol (DMX), 8-prenylnaringenin (8-PN), 6-prenylnaringenin (6-PN)

2.3 Xanthohumol

Xanthohumol (2',4',4-trihydroxy 6'-methoxy 3'-prenyl chalcone) is a structurally simple prenylated chalcone. The distribution of xanthohumol (XN) (Figure 2.5) is limited to and ubiquitous within *Humulus lupulus,* respectively. XN is secreted as part of the hop resin, which is accumulated in the glandular trichomes (see also Figure 2.2). Furthermore, XN can also be found in the trichomes on the underside of young leaves.

2.3.1 Dietary exposure

Beer is the most important dietary source of XN and related prenylflavonoids. The average person in Germany consumed 0.31 liters of beer per day in 2006

(Statistisches Bundesamt Deutschland, 2007). Based on the assumption that the mean XN concentration in beer is 0.03 mg/l (Forster et al. 2002), the daily intake of XN would be about 9.3 µg. Compared to the total polyphenol content of beer, the fraction of prenylflavonoids is relatively small (Gerhäuser 2005a; Vinson et al. 2003). Based on this, one might conclude that prenylflavonoids contribute little to the antioxidant properties of beer. On the other hand, prenylflavonoids differ from other beer polyphenols, such as proanthocyanidins, flavonol glycosides, and phenolic acids, in that they are more lipophilic, and therefore, may be more effective antioxidants at lipophilic surfaces such as membranes and low-density lipoproteins (Stevens et al. 2003; Stevens and Page 2004).

2.3.2 Bioavailability and metabolism

The metabolism of prenylated flavonoids is not very well documented. The biotransformation of flavonoids occurs at several places in the body, but mainly in the liver and the gut lumen. Thus, the gut flora might play a significant role as well. In general, monomeric flavonoids reach the small intestine unchanged (Spencer 2003), where absorption from the gut in the mesenteric circulation can take place. However, the extent of dietary polyphenol absorption in the small intestine is rather limited (10-20%) (Kuhnle et al. 2000; Spencer et al. 1999), thereby implying that a large proportion reaches the colon. Incubation of XN with human faecal samples or with *Eubacterium limosum*, a bacterial species occurring in human faeces, revealed no transformation of XN by the intestinal microbiota (Possemiers et al. 2008). Further, Hanske *et al*. observed no influence on diversity of the intestinal microbial flora after oral application of XN to Sprague Dawley rats (Hanske et al. 2005).

Several studies showed that flavonoids are mostly excreted as glucuronides in humans and animals. Glucuronidation is the most important reaction route for the phase II detoxification process for most xenobiotics. This functionalization is catalyzed by the membrane-bound UDP-glucuronosyltransferase, mainly in the endoplasmatic reticulum of the liver.

A few studies analyzed the *in vitro* metabolism of XN using liver microsome preparations. Yilmazer *et al*. studied the biotransformation of XN by rat liver microsomes (Yilmazer et al. 2001b). Several metabolites with cyclized and/or

oxidized prenyl substituents were described. Aromatic hydroxylation of the B-ring of XN was also observed. In a subsequent study, Yilmazer *et al*. investigated the *in vitro* metabolism of XN by rat and human liver microsomes, respectively, in the presence of uridine 5'-diphosphoglucuronic acid (Yilmazer et al. 2001a). Four glucuronic acid metabolites were detected by LC–MS, of which the two major metabolites were identified as the 4'-O- and 4-O-monoglucuronides of XN (approximately 89% and 10%, respectively, of the total glucuronides generated in the incubations).

The biotransformation of XN and IX by human liver microsomes was reinvestigated by Nikolic *et al*. (Nikolic et al. 2005). Six metabolites of XN and 13 metabolites of IX were identified. The authors described hydroxylation of a prenyl methyl group as the primary route of oxidative metabolism of both compounds. Importantly, IX was partly demethylated to form 8-PN. This might be relevant for the reported estrogenic effect of hop extracts. Further, to mimic reactions that could take place in the stomach, XN was incubated with diluted hydrochloric acid, and cyclization to the isomeric flavanone IX could be observed (Nikolic et al. 2005).

In a study peformed by Nookandeh at al. (Nookandeh et al. 2004), fecal samples from 12 female Sprague-Dawley rats were collected 24 and 48 h after a single dose application of XN (1000 mg/kg b.w.). XN was largely recovered in unchanged form (89% of the total of recovered flavonoids). However, 22 metabolites were isolated from the faeces and characterized by spectroscopic methods. Biotransformation resulted in the formation of cyclic prenyl moieties that included the oxygen at C-4' or at C-2' as well as metabolites with non-cyclic oxidized prenyl substituents. Further, XN-4'-O-glucuronide, XN-4-O-methyl ether, XN-4-O-acetate, IX and an IX metabolites were identified.

After oral administration of XN to male rats (50 mg/kg b.w.), Yilmazer could detect XN in the plasma mainly in form of two mono-glucuronides (4'-O and 4-O-monoglucuronides) whose maximum concentrations reached 180 and 65 nM after 4 h (Yilmazer 2001). The cumulative amounts of both XN glucuronides excreted in the urine reached a plateau at 12 h after oral XN administration and accounted for 0.3% and 0.05% of the administered dose, respectively. The recovery of unchanged XN from the urine was 0.2%. Other metabolites of XN, formed by cytochrome P450 enzymes, were detected in plasma and urine samples at much

lower levels than the glucuronides. These findings suggest that XN's bioavailability, defined as the fraction of the administered dose that is ultimately absorbed intact, is very low.

Pharmacokinetics of XN in male Wistar rats were also investigated by Avula and co workers (Avula et al. 2004). In a first experiment, rats received either oral or intravenous administration of a low dose of XN (20 mg/kg b.w.). In a second experiment, rats received a single oral administration of up to 500 mg XN/kg b.w. Plasma, urine, and faeces were collected at varying time points and assayed for their XN content by HPLC. XN and its metabolites were excreted mainly in faeces within 24 h of administration. Plasma levels of XN fell rapidly within 60 min after i.v. administration. At these doses, no XN was detected in plasma after oral administration.

2.4 Biological effects of xanthohumol

2.4.1 Anti-inflammatory effects

The transcriptional factor NFκB plays a key role in regulating immune responses and cell survival. Incorrect regulation of NFκB has been linked to cancer and inflammation. A decrease in NFκB activity is mainly considered as having anti-inflammatory and pro-apoptotic effects. NFκB consists of a heterotrimer composed of two members of the RelA family, mainly p50 and p65. In its inactive form NFκB is bound in the cytoplasm to members of the IκB family, and here mostly, to IκBα. Proinflammatory stimuly lead to rapid phosphorylation of IκBα by the protein kinase complex IKK. The phosphorylation of IκBα leads to its ubiquitination and rapid degradation that consequently frees the p50-p65 NFκB heterodimer to translocate to the nucleus and to activate NFκB-dependent genes (Vallabhapurapu and Karin 2009; Wong and Tergaonkar 2009).

Immunofluorescent staining done by Albini *et al*. (Albini et al. 2006) showed that NFκB was largely localized in the cytoplasm of unstimulated HUVEC (Human Umbilical Vein Endothelial Cells), and that XN treatment had little effect on this localization. Treatment with 10 ng/ml TNF for 15 min resulted in translocation of NFκB to the nucleus. However, pretreatment with 10 µM XN completely inhibited NFκB activation and translocation. Western blot analysis indicated that XN

significantly repressed the levels of phosphorylated IκBα present in HUVEC after stimulation with TNF, indicating an inhibitory effect on IKK.

Colgate *et al*. determined the NFκB activity in nuclear extracts of prostate epithelial cells and showed that treatment with 20 mM XN resulted in a 42% decrease of NFκB activity (Colgate et al. 2007). Further, Monteiro *et al*. described inhibitiory effects of XN on NFκB activity *in vivo* in a murine cancer model (Monteiro et al. 2008).

In a study performed by Gerhäuser *et al*. (Gerhäuser et al. 2002) XN exhibited anti-inflammatory potential by inhibition of cyclooxygenase (COX) activity with IC_{50} values of 16.6 µM for the constitutive form of cyclooxygenase COX-1 and 41.5 µM for the inducible COX-2, which is linked to inflammation as well as to carcinogenesis and angiogenesis. Cyclooxygenases convert arachidonic acid to prostaglandin H_2 which is the precursor of prostanoids (prostaglandins, prostacyclin and thromboxanes). The latter play important roles as mediators of inflammation.

XN also suppressed the protein expression of the inducible nitric oxide synthase (iNOS) in LPS-stimulated murine macrophages which leads to decreased nitric oxid (NO) release (Zhao et al. 2003; Zhao et al. 2005). NO acts as a signal for a variety of cellular functions throughout the body, including the triggering of inflammation and dilatation of blood vessels. Kim *et al*. described a binding interaction of iNOS and COX-2 (Kim et al. 2005). iNOS inhibitors, which also inhibit COX-2 activation, may decrease pro-inflammatory prostaglandin formation in a synergistic way.

In a recently published study by Gao *et al*., XN revealed immunosuppressive effects on T cell proliferation, development of IL-2 activated killer cells and cytotoxic T lymphocytes as well as on production of Th1 cytokines (IL-2, IFN-γ and TNF). These effect were caused, at least in part, due to inhibition of NFκB through suppression of phosphorylation of IκBα (Gao et al. 2009).

2.4.2 Anti-angiogenic effects

Angiogenesis exhibits a critical role in the progression of cancer. Solid tumors smaller than 1 to 2 mm^3 are not vascularized, however, to spread they need to be supplied by blood vessels that deliver oxygen and nutrients and remove metabolic

waste, respectively. Beyond the critical volume of 2 mm^3, oxygen and nutrients have difficulty diffusing to the cells in the center of the tumor, causing a state of cellular hypoxia that marks the onset of tumoral angiogenesis (Sooriakumaran and Kaba 2005). In addition to its role in tumor growth, (neo)vascularization influences the dissemination of cancer cells, eventually leading to metastasis formation.

Prostaglandins are also known to initiate formation of new blood vessels (angiogenesis), an important pathophysiological mechanism of tumor growth. Furthermore, excessive and prolonged NO generation promotes the production of vascular endothelial growth factor (VEGF), a known inducer of angiogenesis. Considering the studies of Zhao *et al*. (inhibition of iNOS protein expression) and Gerhäuser *et al*. (inhibition of COX activity), mentioned in the previous chapter (2.4.1), anti-angiongenic effects of XN could be assumed (Gerhäuser et al. 2002; Zhao et al. 2003; Zhao et al. 2005).

Indeed, a study of Albini *et al*. (Albini et al. 2006) showed the ability of XN to significantly inhibit angiogenesis in a matrigel sponge implanted to mice by adding XN to the drinking water at concentrations as low as 2 µM. At higher concentrations (up to 200 µM) XN displayed a more marked inhibition of angiogenesis without any detectable adverse effects on animal health parameters.

Bertl at al. could show that XN effectively inhibited microcapillary formation of human microvascular endothelial cells on a membrane matrix at XN-doses of 1, 5 and 10 µM, respectively, whereas at a dose of 0.1 µM, some tubes started to form within the incubation period of 6 h (Bertl et al. 2004). In another study performed by Bertl, an inhibition of angiogenesis (33% in comparison with controls) in female immuno-deficient mice implanted with human breast tumor xenograft was reported after subcutane injection of XN at the daily dose of 1000 mg/kg b.w. for 14 days (Bertl 2005). In a similiar *in vivo* experiment oral administration of XN to nude mice inoculated with breast cancer cells resulted in decreased tumor microvessel density. Anti-angiogenic effects of XN were further confirmed by immunoblotting for Factor VIII expression, a marker for active endothelial cells, in XN-treated and untreated tumors (Monteiro et al. 2008).

2.4.3 Anti-cancerous effects

One of the mechanisms through which XN may exhibit anti-cancerous effects is anti-angiogenic activity. Indeed, the studies performed by Bertl (Bertl 2005), Albini *et al.* (Albini et al. 2006) and Monteiro *et al.* (Monteiro et al. 2008) mentioned in the previous chapter (2.4.2 Anti-angiogenic effects), showed that XN exerts anti-cancerous effects *in vivo*. The growth of human breast tumor xenograft implanted in immuno-deficient mice was significantly inhibited (inhibition by 83% compared to controls) by subcutaneous injection of XN at the daily dose of 1000 mg/kg b.w. for 14 days (Bertl 2005). Oral administration of XN (20 µM in the drinking water) significantly inhibited the growth rate of Kaposi's sarcoma cells in male nude mice (Albini et al. 2006). Furthermore, Monteiro *et al*. observed positive effects of orally applied XN (100 µM in the drinking water) in immuno-deficient mice inoculated with breast cancer cells, *i.e.* central necrosis within tumors, reduced inflammatory cell number, increased percentage of apoptotic cells and decreased microvessel density (Monteiro et al. 2008). As anti-cancerous mechanisms the anti-angiogenic properties but also the NFκB inhibiting effects of XN were discussed.

A common strategy of cancer cells to evade apoptosis is to upregulate NFκB activity (Shen and Tergaonkar 2009). Thus, NFκB inhibitors like XN may have beneficial effects in cancer treatment and prevention. Colgate *et al*. described inhibitory effects of XN on NFκB activity in benign prostate hyperplasia cells (Colgate et al. 2007). Pro-apoptotic effects as well as a loss of viability in both benign prostate hyperplasia cells and prostate cancer cells were observed. In general, the various anti-inflammatory effects of XN described in chapter 2.4.1 may contribute to its anti-cancerous effects. Epidemiological studies have established that many tumors occur in association with chronic infectious diseases, and it is also known that persistent inflammation increases the risk, and accelerates the development of cancer, respectively (Berasain et al. 2009).

In addition to the anti-angiogenic and anti-inflammatory effects of XN also other XN-mediated effects may contribute to its anti-cancerous properties.
Plazar *et al*. and Kac *et al*. described antigenotoxic/antimutagenic effects. XN efficiently protected human hepatoma cells against the genotoxic effects of the two pro-carcinogens 2-amino-3-methylimidazo[4,5-f]quinoline and benzo(a)pyrene

which are both found in cooked meat and are dependent on cytochrome P450 mediated metabolic activation (Kac et al. 2008; Plazar et al. 2008; Plazar et al. 2007). In line with these studies, Miranda *et al* found that XN prevents the metabolic activation of 2-amino-3-methylimidazo[4,5-f]quinoline most likely due to inhibition of cytochrome P450 enzymes, in particular Cyp1A2 (Henderson et al. 2000; Miranda et al. 2000c). XN also inhibits activity of Cyp1A1 and Cyp1B1, but not Cyp2E1 and Cyp3A4 at low micromolar concentrations as shown by Henderson *et al*. (Henderson et al. 2000). These cytochrome P450 enzymes form a group of enzymes (phase 1 enzymes) that mediate the metabolic activation of many chemical carcinogens, and the inhibitory effects of XN may offer an explanation for the reported inhibitory effects of beer on mutagenesis and DNA adduct formation induced by carcinogens (Arimoto-Kobayashi et al. 1999).

In addition to inhibition of phase 1 enzymes, the activation of phase 2 enzymes represents another target for cancer chemoprevention. These enzymes are responsible for detoxification of xenobiotics including carcinogens. Phase 2 enzymes mediate the conjugation of xenobiotics to endogenous ligands, such as glutathione, glucuronic acid, acetate and sulfate, to facilitate excretion. NAD(P)H:quinone reductase is a phase 2 enzyme that is involved in the detoxification of quinones by reductive conversion into hydroquinones, which are suitable substrates for enzymatic conjugation. Quinone reductase activity in cultured mouse hepatoma cells was significantly induced by XN at a dose of approximately 2 µM (Dietz et al. 2005; Miranda et al. 2000a), and Gerhäuser *et al*. characterized XN as a monofunctional inducer, that is, it selectively induces quinone reductase without simultaneously causing transcriptional activation of the phase 1 enzyme Cyp1A1 (Gerhäuser et al. 2002).

Furthermore, XN seems to affect not only development but also the progression of cancers. In two different invasion assays with breast cancer cells a significant anti-invasive effect of XN at a dose of 5 µM could be demonstrated by Vanhoecke *et al.* (Vanhoecke et al. 2005a). As a mechanism, involvement of the E-cadherin/catenin invasion-suppressor complex could be identified. In addition, a XN-mediated (5 µM) stimulation of aggregation, which could be completely

inhibited by an antibody against E-cadherin, was observed (Vanhoecke et al. 2005a).

Apparently, XN seems to affect several different pro-cancerogenic processes, and hence, appears as a broad-spectrum chemopreventive agent. Further, it exhibits these effects on a variety of cancer cells regardless of the origin of the cancer. Interestingly, the effective dose seems to vary depending on the type of cancer.
Lust *et al*. and Dell'Eva *et al*. described anti-proliferative (IC_{50} values between 2.5 and 10 µM XN) and cytotoxic (approx. 25 µM XN) effects of XN on various leukemia cell lines (Dell'Eva et al. 2007; Lust et al. 2005). A similar result was obtained in a study by Gerhäuser *et al.* (Gerhäuser et al. 2002). Here, the growth inhibitory effect of XN on leukaemia cells (IC_{50} value of 3.7 µM) was accompanied by an induction of nonspecific acid esterase expression, a marker for cell differentiation. In the same study, treatment of mammary adenocarcinoma cells with 25 µM XN decreased proliferation to approximately 40% compared to control cells. Pan *et al*. observed anti-proliferative effects of XN on human colon cancer cells in concentrations lower than 10 µM (Pan et al. 2005). Monteiro *et al*. reported significant anti-proliferative and cytotoxic effects of XN on a breast cancer cell line in doses of 1 µM and 50 µm, respectively (Monteiro et al. 2008). XN-mediated growth inhibition of prostate cancer cell lines (IC_{50} values of approx. 13 µM XN) were described by Delmulle *at al.* (Delmulle et al. 2006; Delmulle et al. 2008), whereas Miranda *et al*. found inhibited proliferation of breast and ovarian cancer cells with IC_{50} values of 13 and 0.52 µM XN, respectively (Miranda et al. 1999).

One explanation for the anti-proliferative effects of XN in various fast replicating cancer cells could be the XN-mediated inhibition of human DNA polymerase α activity (IC_{50} value of 23 µM) and/or on DNA topoisomerase I activity described by Gerhäuser *et al.* (Gerhäuser et al. 2002) and Lee *et al.* (Lee et al. 2007), respectively.

Some studies point to a particularly effective anti-cancerogenic effect of XN under hypoxic conditions. Thus, proliferation and motility of human fibrosarcoma cells was significantly suppressed in the presence of XN at a dose of 3 µM under hypoxic, but not under normoxic conditions (Goto et al. 2005). Hypoxia is an

important feature of the microenvironment of a wide range of solid tumours (Airley and Mobasheri 2007; Rademakers et al. 2008).

In summary, anti-angiogenic, anti-inflammatory and antigenotoxic/antimutagenic effects, anti-invasive and anti-proliferative effects in cancer cells, and inhibition of cytochrome P450 enzymes (phase 1 enzymes) together with induction of phase 2 enzymes should result in enhanced protection against carcinogenesis and carcinoma progression.

Aside from direct effects on cancer cells also other effects of XN may be useful for cancer treatment. Lee *et al.* could demonstrate that XN clearly decreases the mRNA levels of the drug efflux genes ABCB1 (MDR1), ABCC1 (MRP1), ABCC2 (MRP2), and ABCC3 (MRP3), which are known to be responsible for drug resistances (Lee et al. 2007).

Finally, also the antioxidant properties of XN should be mentioned when evaluating its chemopreventive potential (see next chapter).

2.4.4 Antioxidant properties

Many flavonoids exhibit antioxidant properties (Lotito and Frei 2004; Lotito and Frei 2006; Pietta 2000). Scavenging of reactive oxygen species (ROS; hydroxyl, peroxyl, and superoxide anion radicals) represents one of the mechanisms by which flavonoids exert their antioxidant activities. Free radicals can initiate reactions that modify polyunsaturated lipids, proteins and nucleic acids, which have been associated with the early stages of atherosclerosis and carcinogenesis, and with the development of neurodegenerative diseases (Stevens and Page 2004). Scavenging of ROS by XN was studied by Gerhäuser *et al*. (Gerhäuser et al. 2002), who found that XN was approximately 3 and 9-fold more potent than the reference compound trolox (a water soluble vitamin E analogue) at a concentration of 1 µM with respect to scavenging of hydroxyl and peroxyl radicals, respectively, in the ORAC (oxygen radical absorbance capacity) fluorescein assay (Davalos et al. 2004). XN was also shown to scavenge superoxide anion radicals, generated by xanthine oxidase, without directly inhibiting xanthine oxidase activity.

Furthermore, XN inhibited superoxide anion radical formation by 12-O-tetradecanoylphorbol-13-acetate stimulation in differentiated human promyelocytic leukemia cells with an IC_{50} of 2.6 µM (Gerhäuser et al. 2002). In studies performed by Vogel *et al*. a trolox equivalent antioxidative capacity of 2.3 was determined for XN (Vogel and Heilmann 2008; Vogel et al. 2008). Miranda *et al*. could show that prenylated chalcones from hops protect low density lipoproteins (LDL) from Cu^{2+}-induced oxidation *in vitro*. At a concentration of 5 µM XN decreased conjugated diene formation, a marker of lipid peroxidation, by more than 70% (Miranda et al. 2000b). Similarly, inhibitory effects of XN on liver microsomal lipid peroxidation, induced by Fe^{2+}-ascorbate, Fe^{3+}-ADP/NADPH, or *tert*-butyl hydroperoxide, could be seen (Rodriguez et al. 2001). Further, XN showed high total oxygen radical absorbance capacity as well as singlet oxygen absorbance capacity (Yamaguchi et al. 2009). In a study by Plazar *et al*. hepatoma cells pre-treated with XN (1 µM for 20 min) revealed significantly reduced levels of *tert*-butyl hydroperoxide-induced DNA strand breaks, indicating that its protective effect is mediated by induction of cellular defense mechanisms against oxidative stress (Plazar et al. 2007).

2.4.5 Anti-infective properties

Serveral anti-infective properties of XN are described. Thus, XN acts as a broad spectrum anti-infective agent against Gram-positive bacteria (*Staphylococcus aureus*, *Streptococcus mutans*), viruses (cytomegalovirus, *herpes simplex* virus type 1 and 2, human immunodeficiency virus 1), fungi (*Trichophyton spp.*) and malarial protozoa (*Plasmodium falciparum*) (Gerhäuser 2005b). However, the mechanisms of the observed inhibitory activities are still under investigation.

2.4.5.1 Anti-bacterial effects

Mizobuchi and Sato (Mizobuchi and Sato 1984) investigated the potential of XN to inhibit the growth of Gram-positive *Staphylococcus aureus*, a pathogen often found in pneumonia and sepsis, in comparison to the antibiotic activity against *E. coli*. A minimal inhibitory concentration (MIC) of 17.7 µM was determined for XN, whereas no antiproliferative effect on *E. coli* could be seen. Bhattacharya *et al*. (Bhattacharya et al. 2003) tested XN against three strains of *Streptococcus* in a

disc diffusion assay. XN demonstrated antimicrobial activity against *S. mutans*, one of the causative agents of dental caries, *S. salivarius* and *S. sanguis*. At a dose of 50 µg per disc, XN produced similar zones of inhibition against all three strains as thymol, a well-known additive to popular mouthwashs. The lowest concentration to prevent visible bacterial growth was determined in a turbidity assay. At a pH of 7.5, XN inhibited the growth of *S. mutans* with an MIC of 35 µM. When the pH was lowered to 6.5 by addition of ascorbic or hydrochloric acid, the MIC of XN decreased to a concentration as low as 6 µM.

2.4.5.2 Anti-fungal effects

Investigations on anti-fungal activity of hop constituents are limited. Mizobuchi and Sato (Mizobuchi and Sato 1984) tested XN against five human pathogenic fungi, *i.e. Trichophyton mentagrophytes*, *Trichophyton rubrum*, *Candida albicans*, *Fusarium oxysporum* and *Mucor rouxianus*. With a MIC of 8.8 µM XN inhibited the growth of the dermatophytic fungi *T. mentagrophytes* and *T. rubrum* more efficiently than the positive control griseofulvin (MIC 17.8 µM), Isoxanthohumol was basically inactive. Also, weak inhibition of *M. rouxianus* was observed (MIC 141 µM XN). *C. albicans* and the opportunistic human pathogen *F. oxysporum* were not responsive to XN.

2.4.5.3 Anti-malarial effects

Malaria is caused by infection with *Plasmodium falciparum*. Chalcones are among the structural classes for which antiplasmodial activity has been reported and are thought to act against malarial cysteine proteases which are responsible for haemoglobin degradation (Li et al. 1995; Liu et al. 2001). The malarial aspartyl and cysteine proteases represent promising targets for the development of anti-malarial compounds (Li et al. 1995; Steele et al. 2002). Herath *et al*. determined the anti-malarial activity of XN against the chloroquine-sensitive *Plasmodium falciparum* strain D6 and the chloroquine-resistant strain W2 (Herath et al. 2003). Plasmodial lactate dehydrogenase activity was measured as an indicator of the number of parasites remaining in infected red blood cells. XN was active against both strains, with IC_{50} values of approximately 9 µM against strain D6, and 3 µM against strain W2, respectively. Anti-malarial activity was confirmed in a study by

Frölich *et al*. (Frölich et al. 2005). *In vitro* antiplasmodial activity of XN was evaluated against the chloroquine-sensitive strain poW and the multiresistant clone Dd2, using a ^{3}H-hypoxanthine incorporation assay. In addition, the influence on glutathione-dependent haemin degradation was analyzed (Frölich et al. 2005). Inhibited haemin degradation leads to a decrease of parasite replication by the subsequent accumulation of toxic by-products. XN showed activity with IC_{50} values of 8 µM (poW) and 24 µM (Dd2), respectively. For comparison, chloroquine was tested as a positive control, and IC_{50} values of 0.015 and 0.14 µM were determined in the two strains, respectively.

2.4.5.4 Anti-viral effects

XN was shown to possess anti-viral activity against a series of DNA and RNA viruses (Gerhäuser 2005b).

In a study performed by Wang *et al*. (Wang et al. 2004), the potential of XN to inhibit various steps essential for the replication of HIV-1 was tested. During replication, many viruses destroy not only the infected host cells but also neighbouring uninfected cells by cytopathic effects. XN was able to inhibit HIV-1-induced cytopathic effects, as well as the production of viral p24 antigen and reverse transcriptase activity as indicators of active retroviral replication, with IC_{50} values of 2.3, 3.6 and 1.4 µM, respectively, in lymphocytes infected with HIV-1IIIB. Further, XN inhibited HIV-1 replication in peripheral blood mononuclear cells with an IC_{50} value of approx. 60 µM. The activity of recombinant HIV-1 reverse transcriptase and HIV-1 entry into cells were not inhibited. From these results it was concluded that the targets of XN on HIV-1 may be situated post reverse transcription.

Buckwold *et al*. tested XN against a series of DNA and RNA viruses *in vitro* (Buckwold et al. 2004). Bovine viral diarrhea virus (BVDV) as a surrogate model of hepatitis C virus and human rhinovirus (HRV) were included as RNA viruses. Further, the DNA herpes viruses cytomegalovirus (CMV) as well as *herpes simplex* virus types 1 and 2 (HSV-1 and -2) were utilized to assess anti-viral activity. Inhibitory effects of XN against BVDV, HRV, HSV-1 and HSV-2 were tested using cell-based assays designed to assess inhibition of cytopathic effects. CMV was tested in a plaque reduction assay. XN inhibited the growth of BVDV, CMV, HSV-1 and HSV-2 more potently than its isomerization product

isoxanthohumol. Half-maximal inhibitory concentrations of XN to inhibit viral replication were in the range of 4–8 µM. Concomitantly, the half-maximal toxic concentrations (TC_{50}) to reduce the number of viable host cells used to propagate the viruses were about 3 to 6-fold higher than the IC_{50} values and ranged from 17–25 µM. XN did not have any anti-viral activity against HRV. In the same study, an XN-enriched extract was tested. XN contained in the extract appeared to account for almost all of the anti-viral activity of the extract, since the therapeutic indices ($TI = TC_{50}/IC_{50}$) of pure XN against BVDV, HSV-1 and HSV-2 were similar to those of the XN-enriched extract.

2.4.6 (Anti)estrogenic potential

Hop extracts have repeatedly been reported to possess estrogenic properties (Chadwick et al. 2006). Gerhäuser *et al*. investigated the pro- and antiestrogenic properties of XN and isoxanthohumol (IX) in Ishikawa cells. This human endometrial cancer cell line responds to estrogens with elevated alkaline phosphatase activity (Holinka et al. 1986a; Holinka et al. 1986b; Holinka et al. 1986c). Concomitant treatment with estrogens and test compounds allows the identification of estrogenic as well as antiestrogenic effects. XN efficiently inhibited estrogen-mediated induction of alkaline phosphatase without possessing intrinsic estrogenic potential, whereas IX was identified as a weak estrogen agonist (Gerhäuser et al. 2002). XN and IX revealed very low affinity for both estrogen receptors (ERα and ERβ) in competitive receptor binding assays (Milligan et al. 2000). In addition, inhibiting effects of XN on human recombinant aromatase (CYP19) activity was described by Gerhäuser *et al*. (Gerhäuser 2005a), and therefore, XN might reduce endogenous estrogen levels.

Possemiers *et al*. have discovered that intestinal microbiota are able to transform IX efficiently into 8-prenynaringenin (8-PN) (Possemiers et al. 2008; Possemiers et al. 2006; Possemiers et al. 2005). 8-PN has been identified as one of the most potent phytoestrogens (Milligan et al. 2002; Milligan et al. 1999). Hence, the antiestrogenic XN may exhibit an estrogenic effect only indirectly through its isomeric IX.

Vanhoecke *et al*. could detect no differences in uterotrophic activity in mice after 4 weeks of treatment with XN, which was added to the drinking water in a

concentration of 0.5 mM. Furthermore, no chances in circulating estradiol and progesteron concentrations could be measured (Vanhoecke et al. 2005b). In a toxicity study performed by Hussong *et al*., no alteration of plasma testosterone levels could be detected in Sprague Dawley rats after 4 weeks of treatment with XN at high daily doses of up to 1000 mg/kg b.w. (Hussong et al. 2005). These data suggest that XN do not exhibit (anti)estrogenicity *in vivo*.

2.4.7 Effects on lipid and carbohydrate metabolism

Casachi *et al*. examined the role of XN on apolipoprotein B (apoB) and triglyceride (TG) synthesis and secretion, using hepatoma cells as model system (Casaschi et al. 2004). The results indicated that XN decrease apoB secretion in a dose-dependent manner under both basal and lipid-rich conditions (decrease by approx. 40% at a dose of 15 µM XN). This decrease was associated with increased cellular apoB degradation. Furthermore, XN inhibited the synthesis of TG in the microsomal membrane and the transfer of this newly synthesized TG to the microsomal lumen (decreases of approx. 25 and 60%, respectively, under lipid-rich conditions). TG availability is a major factor in the regulation of apoB secretion. The inhibition of TG synthesis was caused by a reduction in diacylglycerol acyltransferase (DGAT) activity, which was corresponded to a decrease in DGAT-1 mRNA expression, but not DGAT-2 expression. DGAT is a key enzyme in TG synthesis. In addition, XN decreased microsomal TG transfer protein (MTP) activity in a dose-dependent manner. MTP may also control the rate of TG transfer from the microsomal membrane to the active lumenal pool. Whether TG accumulation in the microsomal lumen is predominantly reduced due to DGAT or MTP activity could not be determined. These results were also confirmed by Tabata *et al*., who could show that XN inhibited DGAT activity in rat liver microsomes with an IC_{50} value of 50 µM (Tabata et al. 1997). Goto *et al*. described increased synthesis of TGs and formation of lipid droplets in the cytoplasm of human fibrosarcoma cells induced by hypoxic conditions, however, the treatment of XN (3 µM) downregulated the TG synthesis and completely canceled the appearance of lipid droplets (Goto et al. 2005). Nozawa *et al*. could demonstrate that XN ameliorates lipid and glucose metabolism in KK-A^y mice which spontaneously develop severe obesity, hyperlipidemia and insulin resistance

(Iwatsuka et al. 1970; Nozawa 2005). XN-fed KK-A^y mice exhibited lowered levels of plasma glucose as well as plasma and hepatic triglyceride levels. Further, they showed a decreased water intake, lowered weights of white adipose tissue, and increased levels of plasma adiponectin, indicating that XN attenuated diabetes in KK-A^y mice. Additionally, lowered expression levels of the sterol regulatory element-binding protein-1c gene *SREBP-1c,* including its targets involved in fatty acid synthesis, as well as lowered expression levels of gluconeogenetic genes could be noticed. The authors suggested that XN may act as a farnesoid X receptor (FXR) ligand.

Yang *et al*. and Mendes *et al*. described effects of XN on preadipocytes and mature adipocytes respectively (Mendes et al. 2008; Yang et al. 2007). XN inhibits differentiation of preadipocytes and induces apoptosis in mature adipocytes which both leads to a decreased number of adipocytes.

2.4.8 Effects on bone resorption

Tobe *et al*. reported inhibiting effects of XN on bone resorption with an IC_{50} value of about 1 µM assessed in a so-called osteoclast pit assay (Boyde et al. 1984; Tobe et al. 1997). However, the underlying mechanism remains unclear.

2.5 Xanthohumol safety studies

So far, two safety studies have been performed, one in mice and one in rats with in part discrepant results.

Vanhoecke *et al*. treated female C3H mice orally with XN by adding it to the drinking water (0.5 mM XN) (Vanhoecke et al. 2005b) resulting in a daily dose of approx. 30-35 mg XN/kg body weight. After 4 weeks, analysis of various haematological and biochemical blood parameters did not reveal significant differences. Furthermore, no signs of liver toxicity, as indicated by aspartate transferase, lactate dehydrogenase and of cholestasis, as indicated by alkaline phosphatase activities, were noticed after treatment. Also, no indications of myolysis were found by creatine kinase activity measurements. Amylase and lipase activities excluded toxicity in the exocrine pancreas, while blood urea nitrogen and creatinine concentrations suggested an intact kidney function.

Further, the metabolism of carbohydrates (glucose, insulin, glucagon, haemoglobin A1c), lipids (cholesterol, triglycerides), proteins and uric acid was not disturbed. As mentioned in chapter 2.4.6, the data related to uterotrophic activity and concentrations of circulating estradiol and progesterone suggest that XN is also devoid of (anti)estrogenicity *in vivo*. Levels of free thyroxin and triiodothyronine indicate that the thyroid function was not affected by the treatment. In a second study, Hussong *et al*. could demonstrate that treatment with 100 mg/kg b.w. XN per day did not affect either fertility or mating and nursing abilities of Sprague Dawley rats (Hussong et al. 2005). Also development of the XN treated rats' offspring was not different from control rats' offspring. Furthermore, at daily doses of up to 1000 mg/kg b.w. no changes in relative weights of kidney, lung, heart, stomach, and spleen as well as in total body weights were noticeable. However, a decrease in relative liver weight and hepatic glycogen content, assessed by histological investigation, was described. The authors interpreted these findings as suggestive of mild hepatotoxicity, but it could be also caused by an altered carbohydrate metabolism (see chapter 2.4.7). The concentrations chosen in this toxicity study were actually considered as maximum tolerable doses to detect potentially harmful effects of XN. Generally, it is unlikely that animals or humans are naturally exposed to XN doses that high under normal circumstances.

Several other *in vivo* studies have been performed with markedly lower XN concentrations (Albini et al. 2006; Avula et al. 2004; Hanske et al. 2005; Monteiro et al. 2008) except for the studies of Nookandeh et al. (Sprague Dawley rats received single dose of approx. 1000 mg XN/g b.w. by gavage) (Nookandeh et al. 2004) and Nozawa et al. (KK-A^y mice were fed with a XN enriched diet resulting in a daily XN uptake of approx. 1000 mg XN/g b.w. for 4 weeks) (Nozawa 2005). In none of these studies any adverse side effects of XN have been reported, but it has to be taken into account that these studies were not designed for identifying any adverse effects of XN.

2.6 Effects of xanthohumol on the liver

The liver is the largest gland in the human body and plays a major role in metabolism. It has a number of functions in the body, including regulation of carbohydrate and lipid metabolism, the production of bile, hormones and coagulation factors, production and decomposition of red blood cells, plasma protein synthesis, vitamin storage, detoxification and others.

The tissue of the liver consists of about 94% (v/v) parenchymal cells which are called hepatocytes and about 6% (v/v) non-parenchymal cells. Hepatocytes are the main functional cells of the liver. The non-parenchymal cell fraction can be subdivided into Kupffer cells (macrophages of the liver), liver sinusoidal endothelial cells (LSEC), liver-resident lymphocytes, cholangiocytes, hepatic stellate cells and some minor fractions. Hepatic stellate cells (HSC) account for about 10% of non-parenchymal cells and are the main storage site for retinoids (40-70% of the body reserves). They are located in the perisinusoidal space (space of Disse; see Figure 2.8), located between hepatocytes and sinusoidal endothelial cells (Pinzani 1995).

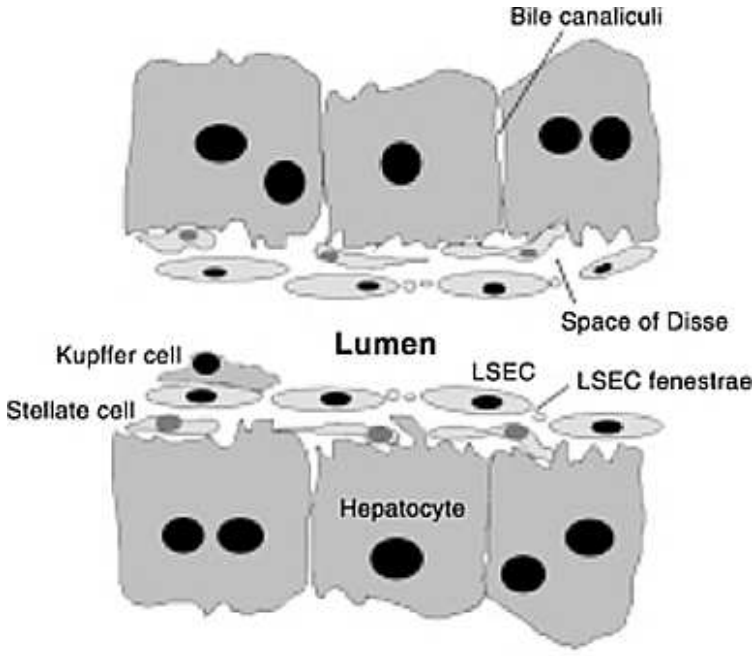

Figure 2.8 Schematic structure of the liver sinusoidal endothelium. Liver sinusoids are lined by liver sinusoidal endothelial cells (LSEC), which separate the sinusoid lumen from hepatocytes. Kupffer cells patrol the sinusoids and bind to LSEC and occasionally hepatocytes through the gaps of two adjacent LSEC. Hepatic stellate cells are located in the space of Disse. Figure from Bertolino *et al.*, 2002 (Bertolino et al. 2002).

2.6.1 Effects of oral administered xanthohumol on the liver

The only study which described *in vivo* effects of oral administered XN on liver relevant parameters is the study performed by Hussong *et al*. (Hussong et al. 2005), mentioned in chapter 2.5. The described decrease of the relative liver weights and glycogen content could be seen only after feeding very high amounts of XN (1000 mg/kg b.w. per day). At a 10-fold lower dose, no differences in relative liver weights could be detected. None of the other studies, in which XN was fed to either mice or rats mention any adverse effects of XN (Albini et al. 2006; Avula et al. 2004; Nookandeh et al. 2004; Nozawa 2005; Vanhoecke et al. 2005b). As described in chapter 2.4.7, Nozawa *et al*. detected lowered levels of hepatic triglycerides in XN treated obese mice (Nozawa 2005), which may be linked to the inhibitory effect of XN on diacylglycerol acyltransferase and microsomal triglyceride transfer protein described by Casachi *et al*. and Tabata *et al*. (see chapter 2.4.7) (Casaschi et al. 2004; Tabata et al. 1997).

2.6.2 Effects of xanthohumol on hepatocellular carcinoma cells

Despite the extensive research on anticancer functions of XN, very few studies have evaluated the inhibitory effects of XN on hepatocellular carcinoma (HCC), but it has been reported that several other flavonoids from plants, including apigenin, luteolin and isoliquiritigenin, have anti-HCC effects (Chiang et al. 2006; Hsu et al. 2005; Lee et al. 2005). Exposure of the human hepatoma cell line HepG2 to XN concentrations of up to 10 µM for 24 h did not affect cell viability, determined by Plazar *et al*. using the MTT assay (Plazar et al. 2007). Exposure to 50 µM or 100 µM XN, however, reduced the cell viability by almost 50 and 85%, respectively, compared to untreated control cells. Similar results were found by Dietz *et al*. (Dietz et al. 2005) with Hepa 1c1c7 cells, a mouse hepatoma cell line. In a crystal violet toxicity assay an IC_{50} of 30 µM (referred to cell survival) has been determined. Ho *et al*. studied the pro-apoptotic effects of XN on two human HCC cell lines and one nonmalignant murine hepatoma cell line *in vitro* (Ho et al. 2008). The human HCC cell lines HA22T/VGH and Hep3B were more sensitive to XN than the murine nonmalignant hepatoma cell line AML12, as indicated in their IC_{50} values assessed in a cell viability assay. The IC_{50} values for HA22T/VGH and Hep3B were 166 µM and 108 µM, respectively. For AML12 cells a significantly

higher IC_{50} of 211 µM has been determined. Further, treatment with 90 µM XN for 4 h resulted in 9.6 and 24.7% apoptotic cells in HA22T/VGH and Hep3B, respectively, determined by Annexin V-EGFP staining. No Annexin V-positive cells could be found in the AML12 cell line under the same conditions.

2.6.3 Effects of xanthohumol on hepatocytes

Only one study described the effects of XN on (nonmalignant) primary hepatocytes. Rodriguez *et al*. tested the effects of eight flavonoids (including XN) on *tert*-butyl hydroperoxide (TBH) treated primary cultures of rat hepatocytes (Rodriguez et al. 2001). XN and four other flavonoids reduced cytotoxic effects of 0.5 µM TBH, an inducer of lipid peroxidation, at concentrations of both 5 and 10 µM. Higher concentrations were not tested because some of the flavonoids revealed cytotoxic effects on primary rat hepatocytes at concentrations of 25 µM by themselves. Unfortunately, it remains unknown to the reader, which of the eight tested flavonoids exhibits the observed cytotoxicity.

Thus far, there existed no published data concerning the effects of XN on primary human hepatocytes (PHH).

2.6.4 Effects of xanthohumol on non-parenchymal liver cells

Up until now, studies describing the effects of XN on hepatic stellate cells, Kupffer cells, sinusoidal endothelial cells or other liver-specific non-parenchymal cells were missing.

2.7 Liver diseases

2.7.1 Definition and natural course of liver disease

Liver diseases can be divided into acute and chronic liver diseases. Intoxications or acute infections may lead to acute liver injury. Due to the high regeneration capacity of the liver such conditions rarely lead to complete liver failure. In these cases, liver transplantation is often the only therapeutic option. Fortunately, complete liver failure caused by acute injury is a rare condition. However, the main health problem and burden worldwide are chronic liver diseases. Here, regardless of the etiology, persistence of hepatic injury leads to chronic hepatic inflammation which can lead to liver fibrosis and ultimatively cirrhosis.

2.7.2 Liver fibrosis

Hepatic fibrosis can be looked upon as an exuberant wound healing process in which excessive connective tissue builds up in the liver (Bataller and Brenner 2005; Friedman 2003). The extracellular matrix (ECM), composed of collagen, elastin, structural glycoproteins, proteoglycans and some minor components, is either overproduced, degraded deficiently, or both. The trigger is chronic injury, especially, if there is an inflammatory component.

The main causes of liver fibrosis in industrialized countries include chronic HCV (see chapter 2.7.5.4.3) infection, alcohol abuse, and non-alcoholic steatohepatitis (NASH) (discussed later in chapter 2.7.5.5).

Fibrosis itself causes no symptoms but can lead to portal hypertension (the scarring distorts blood flow through the liver), cirrhosis and liver cancer. The main liver cells that produce ECM proteins are hepatic stellate cells (HSC), first described by von Kupffer in 1876 (Benyon and Arthur 1998; Burt 1993; Gabele et al. 2003). HSC are the central mediators of hepatic fibrosis in chronic liver disease (Bataller and Brenner 2005; Friedman 2008; Friedman 2004). HSC reside in the space of Disse and are the major storage sites of vitamin A (see also previous chapter 2.6). Following chronic liver injury, HSC proliferate, loose vitamin A and undergo a major phenotypical transformation to α-smooth muscle actin (α-sma) positive myofibroblasts (activated HSC) acquiring contractile, proinflammatory, and fibrogenic properties (Marra 1999; Milani et al. 1990) (Figure 2.9).

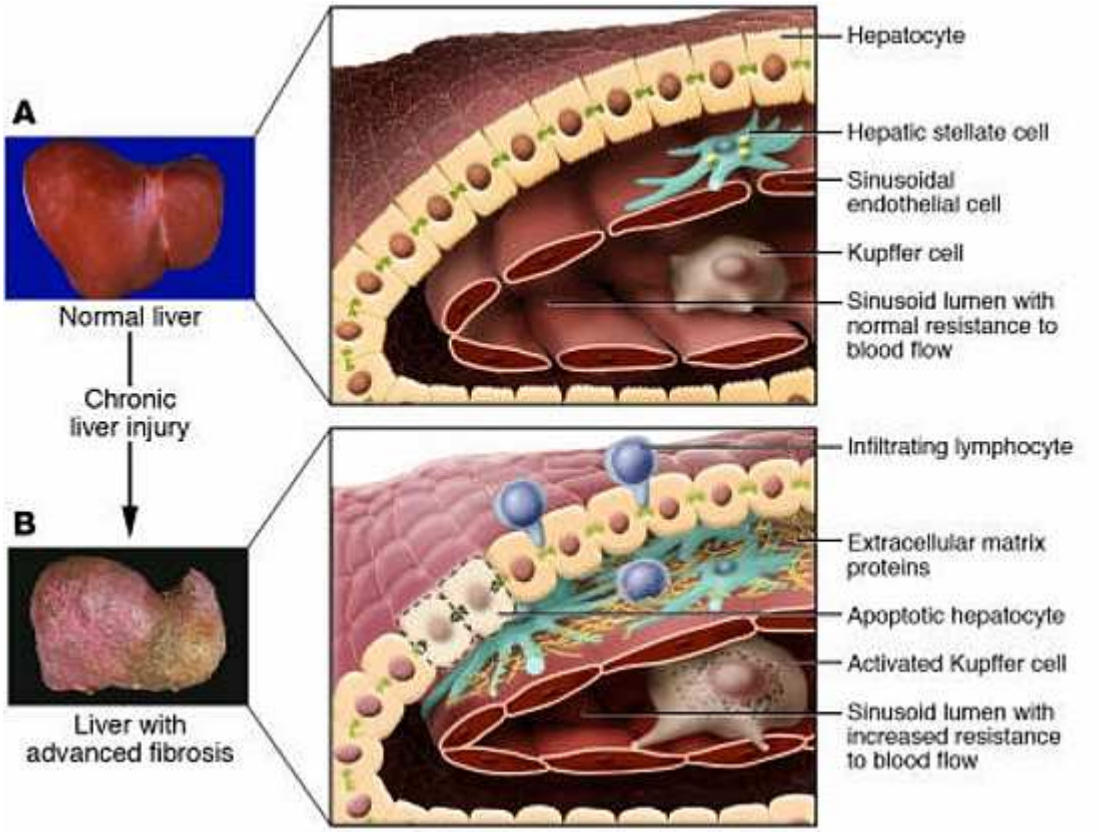

Figure 2.9 Changes in the hepatic architecture (A) associated with advanced hepatic fibrosis (B). Following chronic liver injury, inflammatory lymphocytes infiltrate the hepatic parenchyma. Some hepatocytes undergo apoptosis, and Kupffer cells get activated, releasing fibrogenic mediators. HSC proliferate and undergo a dramatic phenotypical activation, secreting large amounts of extracellular matrix proteins. Sinusoidal endothelial cells lose their fenestrations, and the tonic contraction of HSC causes increased resistance to blood flow in the hepatic sinusoid. Figure from Bataller and Brenner, 2005 (Bataller and Brenner 2005).

Activated HSCs migrate and accumulate at the sites of tissue repair, secreting large amounts of ECM and regulating ECM degradation. They produce a wide variety of collagenous and non-collagenous ECM proteins, building up fibrous scar tissue. Subsequently, this fibrous tissue can be remodeled through digestion by matrix metalloproteinases (MMPs). In turn, the digestion of matrix is controlled through the inhibition of MMPs by tissue inhibitors of matrix metalloproteinases (TIMPs) of which TIMP-1 is of major importance. In a healthy liver, the synthesis (fibrogenesis) and breakdown (fibrolysis) of matrix tissue are in balance. In chronic liver injury collagen types I, III, and IV are all increased. However, the increase of type I collagen is predominant, and therefore, its ratio to types III and IV is increased as well (Burt et al. 1990; Hahn et al. 1980; Rojkind et al. 1979; Seyer et al. 1977). Collagen synthesis in HSC is regulated at transcriptional and posttranscriptional levels (Lindquist et al. 2000). Increased collagen mRNA stability mediates the increased collagen synthesis in activated HSCs (Lindquist et

al. 2004; Stefanovic et al. 1997). Furthermore, activated HSC are characterized by increased proinflammatory gene expression and resistance to apoptosis (Bataller and Brenner 2005; Friedman 2004). It could be shown that NFκB plays a critical role in HSC activation (Elsharkawy et al. 2005; Hellerbrand et al. 1998a; Hellerbrand et al. 1998b). Increased hepatic NFκB activity is known to promote hepatic inflammation and fibrosis in chronic liver diseases (Elsharkawy and Mann 2007).

Liver fibrosis is now recognized to be a dynamic process that can progress or regress over periods as short as months (Friedman 2003; Hofmann and Zeuzem 2003; Soyer et al. 1976). The possibility of reversing the fibrosis is an essential issue for developing therapeutic approaches, since most liver diseases are not clinically present until reaching an advanced fibrotic stage.

As fibrotic liver diseases advance, disease progression from collagen bands to bridging fibrosis to frank cirrhosis occurs.

2.7.3 Liver cirrhosis

The accumulation of ECM proteins in progressive liver fibrosis distorts the hepatic architecture by forming a fibrous scar, and the subsequent development of nodules of regenerating hepatocytes defines cirrhosis. Cirrhosis produces hepatocellular dysfunction and increased intrahepatic resistance to blood flow, which both result in hepatic insufficiency and portal hypertension, respectively (Gines et al. 2004). This condition can cause further symptoms like fluid build-up in the abdomen (called ascites), build-up and bleeding of esophageal varices, muscle wasting, bleeding from the intestines, easy bruising, enlargement of the breasts in men (called gynaecomastia), and a number of other symptoms. Ultimatively, cirrhosis leads to a loss of liver function (decompensated cirrhosis), a condition with high morbidity and mortality.

Further, liver cirrhosis is the main risk factor for the development of hepatocellular carcinoma (HCC).

2.7.4 Liver cancer

Liver cancer implies all types of cancers located in the liver. Most of them are metastatic cancers (secondary liver cancers). Primary liver cancers (cancers that started in the liver) can be subdivided into different types of cancer, namely hepatocellular carcinoma (HCC), hepatoblastoma and cholangiocarcinoma (bile duct cancers). Tumors of the blood vessels located in liver are also known (angiosarcoma, hemangiosarcoma and hemangioendothelioma).

2.7.4.1 Hepatocellular cancer

2.7.4.1.1 Prevalence and incidence

Hepatocellular carcinoma (HCC) is a highly malignant disease with an extremely poor prognosis. It is the most common primary malignant tumor of the liver and accounts for approximately 90% of primary liver cancers (El-Serag et al. 2008; El-Serag and Rudolph 2007). Relative to other malignant diseases, HCC ranks fifth in overall frequency, causing almost one million deaths annually and its mortality is third among all cancers, behind only lung and colon cancer (Kubicka et al. 2000; Villanueva et al. 2007). In most countries, especially Western countries, the incidence of HCC is still rising (Deuffic et al. 1998; El-Serag and Mason 1999; El-Serag et al. 2001; Kubicka et al. 2000; Stroffolini et al. 1998; Taylor-Robinson et al. 1997). Furthermore, the distribution of patients with HCC has shifted toward relatively younger ages, with the greatest increases occurring between the ages of 45 and 60 years (Villanueva et al. 2007). In Germany, HCC ranks seventh to eighth in frequency, but it is the tumor with the highest increase of incidence (Kubicka et al. 2000).

2.7.4.1.2 Etiology

HCC pathogenesis is a multi-step process that involves genetic and epigenetic events occurring during initiation and progression of the disease. The genetic basis of hepatocarcinogenesis is still poorly understood. HCC develops in almost 80% of cases on a cirrhotic liver (Minguez et al. 2009), mostly caused by chronic HBV or HCV infection, chronic alcohol abuse or non-alcoholic steatohepatitis (NASH) (Villanueva et al. 2007). Further, exposure to aflatoxins is an important

contributor to the high incidence of liver cancer in tropical areas of the world, where contamination of food grains with the fungus *Aspergillus fumigatus* is common. There is a multiplicative interaction between aflatoxin exposure and chronic infection with HBV, suggesting that the carcinogenic mechanisms differ (Parkin 2001).

2.7.4.1.3 Therapy and prognosis

Despite some new promising drugs like multi-kinase inhibitors, HCC still has a very poor prognosis. Without specific treatment, the median survival time for patients with early and advanced tumors are 6-9 months and 1-2 months, respectively. (Bosch and Munoz 1989; Kew 2002; Lau and Lai 2008). Early diagnosis and treatment could significantly improve the prognosis, but HCC is frequently diagnosed at advanced stages, since early stages of HCC causes no or only little symptoms. Curative resection of HCC is possible (Hoofnagle 2004), however, the success of this approach is limited because in most cases the liver is cirrhotic, and there is a high rate of tumor recurrence or development of new tumors, respectively (Llovet et al. 2004). Liver transplantation has become a frequently used alternative, but it is not possible for all patients, and in a significant number of cases HCC reoccur in the transplanted liver (Schlitt et al. 1999), to some extent promoted by the post-transplantational immunosuppressive therapy (Buell et al. 2005). Local ablative therapies are increasingly being used to treat HCC, either as definitive therapy or as an intermediate step in patients awaiting liver transplantation. Transarterial chemoembolization (TACE) has been shown to increase survival in a randomized controlled trial (Llovet et al. 2002). Further, percutaneous ethanol injection (PEI) has been proven to be relatively easy to perform, and this procedure is inexpensive (Lencioni et al. 2004).

2.7.5 Causes for chronic liver diseases

Several mechanisms and diseases, respectively, may cause chronic hepatic inflammation, chronic liver damage and eventually liver failure, if fibrosis progresses, resulting in complete cirrhosis and loss of hepatic function.

2.7.5.1 Alcohol induced liver disease

Since the liver is responsible for metabolism of alcohol (ethanol), drugs and environmental toxins, prolonged exposure to any of these agents can cause hepatitis.

Thus, alcoholic liver disease (ALD) is still one of the most frequent causes for chronic liver disease, at least in Western countries (Barve et al. 2008; Bergheim et al. 2005). The quantity of alcohol consumed, the frequency with which it is consumed, and the pattern of consumption, respectively, determine the likelihood of developing ALD. There are no official guidelines for “sensible drinking” in Germany, but maximum doses of 3 standard drinks/day (men) and 2 standard drinks/day (women), respectively, are recommended as “low risk” alcohol consumption. In Germany, a standard drink is defined as a drink containing about 12 g of ethanol (AIM - Alcohol in Moderation 2009). Binge drinking, which is considered as being more harmful than frequent but moderate drinking due to the high peaks of blood alcohol concentration (BAC), is defined as consuming five or more drinks (men) or four or more drinks (women), respectively, in approximately 2 h (National Institute on Alcohol Abuse and Alcoholism 2004). This rate of drinking will elevate BAC to 0.08% on average (Li 2008). Even more harmful, heavy drinking is defined as frequent drinking of five or more drinks by men and four or more drinks by women per day. In addition to increasing the risk of developing alcohol-use disorders (AUD; alcohol abuse and alcohol dependence), excessive, long-term (chronic) alcohol consumption can cause a variety of adverse health effects, much of these derived from damage to inner organs, including alcoholic liver disease, alcoholic pancreatitis, impaired brain structure and function, and cardiomyopathy. Excessive drinking is also associated with an increased risk for cancers of the oropharynx, esophagus, and liver, and can exacerbate the health consequences of infection with hepatitis C, HIV and other infectious agents.

Even moderate alcohol consumption can promote development of a fatty liver. Although the alcoholic fatty liver is reversible with abstinence, the degree of steatosis, especially when associated with alcoholic hepatitis, predisposes to fibrosis and cirrhosis in subjects who continue to drink (Teli et al. 1995). The risk of cirrhosis increases proportionally with daily alcohol consumption above a daily threshold of 30 g (Bellentani et al. 1997). It is presumed that other factors such as

sex, genetic background, and environmental influences, including chronic viral infection, play a role in the genesis of ALD (Becker et al. 1996; Bode et al. 1995; Wilfred de Alwis and Day 2007). Approximately 10 to 35% of heavy drinkers develop alcoholic hepatitis, and 10 to 20% develop cirrhosis (National Institute on Alcohol Abuse and Alcoholism 1993).

2.7.5.2 Drug induced liver injury

Further, drug induced liver injury has emerged as a major cause of acute liver failure (ALF) and has become a leading reason for removal or restriction of approved drugs by regulatory agencies (Fontana 2008; Navarro and Senior 2006; Ostapowicz et al. 2002; Watkins 2005). Drug-induced ALF accounts for approximately 20% of ALF in children (Murray et al. 2008). The percentage is even higher in adults (Murray et al. 2008). Although most patients experience milder drug-induced hepatotoxic reactions such as moderate hepatitis, cholestasis, or asymptomatic enzyme elevation, it is important to recognize the potential for progression to ALF. Further, drug intake may exacerbate liver inflammation and/or fibrosis initially caused by other factors.

The most common cause of drug-induced ALF is acetaminophen, followed by antituberculotic, antiepileptic and antibiotic drugs. Most drugs cause liver injury infrequently. These reactions are considered idiosyncratic, occurring at therapeutic doses from 1 in every 1000 patients to 1 in every 100,000 patients, with a pattern that is consistent for each drug or drug class. However, a few drugs such as acetaminophen directly damage hepatocytes in a dose-dependent fashion (Lee 2003).

2.7.5.3 Autoimmune related mechanisms and genetic defects

Further, autoimmune related mechanisms and genetic defects may cause liver inflammation and chronic damage. For example, primary sclerosing cholangitis is an autoimmune disease affecting the bile ducts, while in primary biliary cirrhosis small bile ducts are affected. Gilbert's syndrome is a genetic disorder of the bilirubin metabolism, and there are genetically induced glycogen storage diseases. Wilson’s disease is a hereditary disorder leading to hepatic accumulation of copper. In hemochromatosis, a defect of the *HFE* gene leads to increased iron

uptake, and conseqently, increased hepatic iron accumulation. The latter is one of the most frequent monogenetic diseases in Caucasians.

However, besides hemochromatosis and alcoholic liver disease, the most frequent causes of chronic liver diseases are infections with hepatitis viruses and non-alcoholic stetaohepatitis.

2.7.5.4 Viral hepatitis

Hepatitis viruses have been named in the order of their discovery as hepatitis A, B, C, D, and E. Most relevant are hepatitis A, B and C.

2.7.5.4.1 Hepatitis A

Infection with the hepatitis A virus (HAV) occurs via faecal and oral transmission (*i.e.* by excrements) or by contaminated food. There is an effective vaccination against hepatitis A viruses that can prevent infection. In developing countries, and in regions with poor hygiene standards, the incidence of infection with this virus is high. In industrialized countries the infection is contracted primarily by susceptible young adults, most of whom are infected with the virus during trips to countries with a high incidence of the disease. Normally the infection processes without typical symptoms, and therefore, often remains unnoticed. In some cases an acute infection develops with symptoms like fatigue, nausea, absence of appetite, fever, vomiting, dark color of faeces and yellow color of the skin. In few cases (~1%), hepatitis A can take a severe course and may eventually lead to fulminant hepatic failure. The hepatitis A infection never takes a chronic course. Patient which have recovered from hepatitis A infection are protected against a new HAV infections.

2.7.5.4.2 Hepatitis B

The hepatitis B virus (HBV) can be transmitted by both sexual contact and blood. Furthermore, vertical transmission is the main route of transmission in regions with high HBV incidence. HBV is very infectious, but a safe vaccination is available and can efficiently prevent transmission. Acute hepatitis B infection occurs without specific symptoms in the majority of cases. Similar to hepatitis A, symptoms like fatigue, nausea, absence of appetite, fever, vomiting, dark colored faeces and

yellow color of the skin may occur. One third of patients develop an acute inflammation of the liver with more severe symptoms lasting several months (acute hepatitis B). In few cases (~1%), acute hepatitis B can take a severe course with fulminant hepatic failure. Complete cure of the infection leads to life long immunity. However, in 5% of adult patients the virus remains in the body and the infection takes a chronic course. Chronic hepatitis B also processes with unspecific symptoms in most cases. Fatigue and loss of motivation are frequent, but also symptoms of influenza, like aching muscles or joints, can appear. Approximately, one third of patients with chronic hepatitis B will develop liver cirrhosis, and eventually, liver cancer.

2.7.5.4.3 Hepatitis C

Main transmission route of hepatitis C virus (HCV) is direct blood contact (due to needle stick injury or intravenous drug consumption etc.), and in fewer cases also sexual contact. Further, vertical transmission may lead to infection. So far, there is no vaccination against hepatitis C. Acute hepatitis C normally processes without specific symptoms. Influenza like symptoms, fatigue, nausea, absence of appetite and pain in upper abdomen can appear. An acute HCV infection is diagnosed rarely. In most cases hepatitis C takes a chronic course, *i.e.* the virus remains in the body and causes a continuous inflammation of the liver. Mostly, chronic hepatitis C is mild and without clear disturbances. Main symptoms can be fatigue, loss of motivation and joint pain. Chronic forms of hepatitis C cause an enduring damage of the liver which leads to liver fibrosis, cirrhosis and liver cancer in a significant number of patients.

2.7.5.5 Non-alcoholic fatty liver disease (NAFLD)

Non-alcoholic fatty liver disease (NAFLD) plays a more and more important role, and is today considered as the most frequent liver disease in Western countries.

2.7.5.5.1 Definition

Non-alcoholic fatty liver disease (NAFLD) was first described by Ludwig *et al*. (Ludwig et al. 1980) and is defined as a spectrum of diseases ranging from hepatic

steatosis without inflammation to hepatic steatosis with an inflammatory component (non-alcoholic steatohepatitis; NASH) without or with progredient fibrosis. The latter may progress to cirrhosis and HCC (Figure 2.10).

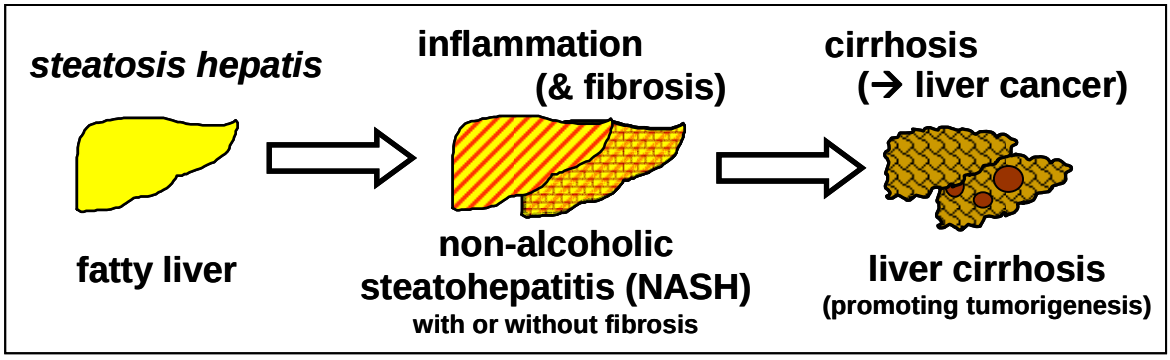

Figure 2.10 The spectrum of NAFLD: fatty liver (*steatosis hepatis*), non-alcoholic steatohepatitis (NASH) with or without fibrosis, and liver cirrhosis, which promotes development of liver cancers.

Overall, the histology as well as several other pathophysiological changes mimic alcoholic liver disease, although NAFLD and non-alcoholic steatohepatitis (NASH) develop *per definitionem* in the absence of chronic alcohol abuse (Anstee and Goldin 2006).

2.7.5.5.2 Prevalence of NAFLD/NASH

NAFLD is the most common cause of chronic liver disease in Western countries (Clark et al. 2002). Estimates of the prevalence of NAFLD in unselected populations from developed countries vary between 20 and 30% (Browning et al. 2004; Jimba et al. 2005; Marcos et al. 2000; Ruhl and Everhart 2004), and approximately 2-3% of the same population will have NASH (Neuschwander-Tetri and Caldwell 2003).

The prevalence of liver steatosis increases with increasing body weight (Andersen et al. 1984; Bellentani et al. 2000) and is estimated to be 65-75% in obese individuals (BMI > 30 kg/m²) (Angulo 2002; Bellentani et al. 2000) and even 85-90% in morbidly obese individuals (BMI > 35 kg/m²) (Andersen et al. 1984; Angulo 2002). In accordance, the vast majority of individuals with NAFLD are either overweight (BMI > 25 kg/m²) or obese (BMI > 30 kg/m²) (Bacon et al. 1994). Furthermore, in obese individuals, the prevalence of NASH increases disproportionately, and more than half of NASH patients have Type 2 diabetes mellitus and up to 80% reveal dyslipidaemia (Cortez-Pinto and Camilo 2004).

The overall prevalence of NAFLD in children is estimated at 3-10%, but it may be much higher in obese children (Shneider et al. 2006), and prevalence of obesity in children is rapidly increasing (Daniels et al. 2009; Ogden et al. 2006; Strauss and Pollack 2001).

NAFLD is strongly associated with insulin resistance (IR). Development of NAFLD is promoted by IR as well as NAFLD promotes IR. NAFLD is now believed to be the hepatic manifestation of the metabolic syndrome, which includes central obesity, insulin resistance, dyslipidemia, and hypertension (Powell et al. 1990; Sanyal 2002).

2.7.5.5.3 Etiology and pathogenesis

In recent years, there have been significant advances in the understanding of mechanisms that contribute to disease progression in NAFLD/NASH. The development of NAFLD/NASH is determined by the interaction of genetic and environmental factors (Day 2002).

In 1998 Day and James proposed the ‘two-hit’ hypothesis for the pathogenesis of NASH (Day and James 1998). The ‘first hit’ involves an imbalance in fatty acid metabolism that leads to hepatic lipid accumulation (steatosis) which sensitizes the liver to the induction of inflammation by a second pathogenic insult (‘second hit’) that promotes oxidative stress and dysregulated cytokine production and hence steatohepatitis. The ‘two-hit’ model has subsequently been revised in recognition that a combination of ‘second hits’ (both environmental and genetic) may lead to the development of steatohepatitis (Day 2002). The causes for progression to fibrosis or even cirrhosis in some NASH patients are subject of many studies and are often referred to as the ‘third hit’.

2.7.5.5.4 Prognosis and therapy

In general, the prognosis for simple steatosis is very good; however, NASH can progress to cirrhosis and hepatocellular carcinoma in 10-15% of patients. Once cirrhosis is present, it is estimated that 30-40% of these patients will progress to a liver-related death over a 10-year period (Bacon et al. 1994; Matteoni et al. 1999; Powell et al. 1990).

There is no established treatment for NAFLD except for weight loss and treating (each component of) the metabolic syndrome.

2.7.5.5.5 Experimental NASH models

Several mouse models are available to study the mechanisms involved in NALFD, which mimic the phenotypic abnormalities known from human liver diseases (Anstee and Goldin 2006). The use of genetic defects or targeted overexpression of specific genes to produce obesity or impaired hepatic lipid metabolism in rodents have been used as NAFLD models (Chen et al. 1996). Although these genetic manipulations can assess the biological importance of each gene *in vivo*, they might not reflect the natural etiology of NAFLD in patients and rarely lead to the pathology of NASH. Other models frequently used are based on nutritional manipulations, *e.g.* feeding of sucrose-rich and/or fat-rich diets (Surwit et al. 1995). However, in most of these models, rodents accumulate only minimal fat and develop merely subtile inflammation of the liver. A commonly used model to study the pathogenesis of NASH is feeding a methionine-choline deficient (MCD) diet to mice or rats. This treatment induces significant hepatic steatosis, inflammation and fibrosis similar as seen in human NASH. However, this diet leads to a rapid body weight loss, and therefore, does not reflect the situation mostly found in NASH patients, *i.e.* obesity and insulin resistance.

Recently, a new dietary based model was described (Matsuzawa et al. 2007): the so-called Paigen-diet contains 15% cocoa butter, 1.25% cholesterol and 0.5% sodium cholate and was originally designed to induce atherosclerosis in rodents by the group of Beverly Paigen in 1985 (Paigen et al. 1985). Interestingly, atherosclerosis and NASH share in large part the same pathogenetic causes, and there is a large overlap of NASH and atherosclerosis patients. In fact, NAFLD/NASH seems to promote development of atherosclerosis (Loria et al. 2008; Sookoian and Pirola 2008; Targher and Arcaro 2007). With regards to the liver, it could be observed that rodents fed with the Paigen-diet developed liver steatosis, and later on, liver inflammation and fibrosis (Jeong et al. 2005). Matsuzawa *et al*. systematically investigated the effects of the Paigen-diet on the liver and lipid/carbohydrate metabolism, respectively, in mice and demonstrated that the Paigen-diet is a suitable NASH model including progression of hepatic fibrosis (Matsuzawa et al. 2007).

2.8 Aim of the thesis

The aim of this thesis was to analyze the effects of XN on liver diseases with an emphasis on NASH and HCC. Here, once the Paigen-diet as a murine NASH model was used. Further, *in vitro* experiments with different primary liver cells and HCC cells were performed. Finally, the safety profile of orally applied XN was investigated in mice.

3 Materials and Methods

3.1 Chemicals and Reagents

Agarose SeaKem® LE	Biozym, Hess/Oldendorf, Germany
β-Mercaptoethanol	Sigma, Deisenhofen, Germany
Fatty acid free BSA	Sigma, Hamburg, Germany
Ciprobay	Bayer, Leverkusen, Germany
Collagenase type IV	Sigma, Hamburg, Germany
Diflucan	Pfizer, Karlsruhe
DMEM medium	PAA Laboratories, Cölbe, Germany
DMSO	Sigma, Deisenhofen, Germany
Edelstoff	Augustiner Bräu, Munich, Germany
FCS (fetal calf serum)	PAN-Biotech, Aidenbach, Germany
Milk powder	Carl Roth, Karlsruhe, Germany
Nonidet® P40	Roche Diagnostics, Mannheim, Germany
Palmitic acid	Sigma, Hamburg, Germany
Penicillin	Invitrogen, Karlsruhe, Germany
Propidium iodide	Sigma, Deisenhofen, Germany
Streptomycin	Invitrogen, Karlsruhe, Germany
TNF (human)	R&D, Wiesbaden-Nordenstadt, Germany
TNF (murine)	R&D, Wiesbaden-Nordenstadt, Germany
Trypsin/EDTA	PAA Laboratories, Cölbe, Germany
Xanthohumol	Alexis Biochemicals, Lausen, Switzerland

All chemicals not listed were purchased at VWR (Darmstadt, Germany).

3.2 Laboratory expendables

CryoTube vials	Nunc, Roskilde, Denmark
Pipet tips (10, 20, 100 und 1000 µl)	Eppendorf, Hamburg, Germany
Falcon tubes (50 ml)	Corning, New York, USA

glassware (various)	Schott, Mainz, Germany
Multiwell plates	Corning, New York, USA
Pipettes (stripettes®)	Corning, New York, USA
(5, 10, 25, 50 ml)	
Reaction vessels (1.5 and 2 ml)	Eppendorf, Hamburg, Germany
Scalpels (No. 11)	Pfm, Cologne, Germany
Strip tubes (0.2 ml)	Peqlab, Erlangen , Germany
Cell culture flasks T25, T75, T175	Corning, New York, USA

3.3 Laboratory instruments

Heating block:	
Thermomixer comfort	Eppendorf, Hamburg, Germany
PCR-cycler:	
GeneAmp® PCR System 9700	Applied Biosystems, Foster City, USA
Pipettes:	
Gilson (P2, P20, P200, P1000)	Gilson, Bad Camberg, Germany
Pipette controllers:	
Accu-jet®	Brand, Wertheim, Germany
Shaking devices:	
KS 260 Basic Orbital Shaker	IKA® Werke, Staufen, Germany
Power Supplies:	
Consort E145	Peqlab, Erlangen, Germany
Power Supply-EPS 301	Amersham Biosiences, Munich, Germany
Spectrophotometer:	
EMax® Microplate Reader	MWG Biotech, Ebersberg, Germany
SPECTRAFluor Plus	Tecan, Männedorf, Switzerland
Scale:	
MC1 Laboratory LC 620 D	Sartorius, Göttingen, Germany
Water bath:	
Haake W13/C10	Thermo Fisher Scientific, Karlsruhe, Germany
Centrifuge:	
Biofuge fresco	Heraeus, Hanau , Germany
Megafuge 1.0 R	Heraeus, Hanau, Germany

Microscope:

Olympus CKX41 with ALTRA20 soft imaging system	Olympus Hamburg, Germany

3.4 Buffers

PBS-Puffer	140 mM	NaCl	
	10 mM	KCl	
	6.4 mM	Na_2HPO_4	
	2 mM	KH_2PO_4	pH 7.4
TE-Puffer	10 mM	Tris/HCl	
	1 mM	EDTA	pH 8.0

3.5 Cell Culture

3.5.1 Cell culture medium

DMEM (high glucose/10%FCS)	4.5 g/l	Glucose
	300 µg/ml	L-Glutamine
	Supplemented with:	
	10% (v/v)	FCS
	400 U/ml	Penicillin
	50 µg/ml	Streptomycin
HSC medium	DMEM (high glucose/10%FCS)	
	Supplemented with:	
	10 µg/ml	Diflucan
	4 µg/ml	Ciprobay
Freezing medium	5 Vol	DMEM (highgluc./10%FCS)
	3 Vol	FCS
	2 Vol	DMSO

3.5.2 Cultivation of cell lines

All cell culture work was conducted within a laminar flow biosafety cabinet (Hera Safe, Heraeus, Osterode, Germany). The cells were cultivated in a Binder series CB incubator (Binder, Tuttlingen, Germany) in 10% CO_2 atmosphere at 37 °C. DMEM containing 4.5 g/l glucose and 300 µg/ml L-glutamine supplemented with 10% (v/v) FCS, 400 U/l penicillin and 50 µg/ml streptomycin was used as cell culture medium. For cell passaging adherent cells were washed with PBS and detached with trypsin (0.05%)/EDTA (0.02%) (PAA Laboratories, Cölbe, Germany) at 37 °C. Trypsination was stopped by addition of D MEM containing 10% FCS. Subsequently, cells were centrifuged at 500 g for 5 min and the obtained cell pellet was resuspended in fresh culture medium and distributed to new cell culture flasks achieving a cell density thinning factor of 5 to 10. Medium change took place every second day. Cell growth and morphology were controlled and documented with a microscope (Olympus CKX41 with ALTRA20 Soft Imaging System, Olympus, Hamburg, Germany). Cell culture waste was autoclaved before disposal with a Sanoclav autoclave (Wolf, Geislingen, Germany).

3.5.3 Human hepatocellular carcinoma cell lines

The hepatocellular carcinoma cell lines HepG2 (ATCC HB-8065) and Huh7 (JCR B0403) were obtained from the American Type Culture Collection (ATCC) and the Japanese Collection of Research Biosources (JCRB), respectively.

3.5.4 Isolation of primary human hepatocytes

Primary human hepatocytes (PHH) were isolated in co-operation with the Center for Liver Cell Research (Department of Surgery, University of Regensburg, Germany) from human liver resections using a modified two-step EGTA/collagenase perfusion procedure (Hellerbrand et al. 2008; Hellerbrand et al. 2007; Pahernik et al. 1996; Ryan et al. 1993; Weiss et al. 2002). The experimental procedures were performed according to the guidelines of the charitable state controlled foundation HTCR, with the informed patient's consent. For cell isolation only tissue which has been classified as not pathological after macroscopical and microscopical investigation was used. All used liver resections have been

negatively tested for HBV, HCV and HIV infection. Viability of the isolated hepatocytes was determined by trypan blue exclusion, and cells with a viability greater than 85% were used for further tests.

3.5.5 Isolation of primary murine hepatocytes

Primary murine hepatocytes (PMH) were isolated from mice by the two-step collagenase method of Seglen with minor modifications (Seglen 1976).

Used buffers:

Perfusion buffer	8 g/l	NaCl	
	0.4 g/l	KCl	
	90 mg/l	Na_2HPO_4 x $7H_2O$	
	60 mg/l	KH_2PO_4	
	1 g/l	Dextrose	
	0.19 g/l	EGTA	pH 7.3
Digestion buffer	Perfusion buffer		
	Supplemented with:		
	0.04%	Collagenase type IV Collagen digestion activity: 440 units/mg solid collagenase	
	1.5 mM	$CaCl_2$	

First, mice were anesthetized with ketamine/xylazine according to the guidelines of the Central Animal Facility (ZTL) of the University of Regensburg (Germany) (Central Animal Facility (ZTL) of the University of Regensburg 2009). Ketamine and xylazine was purchased from the Central Animal Facility (ZTL) of the University of Regensburg (Germany). The abdomen was opened by median incision 1-2 cm above the hind legs up to the *sternum*, followed by a horizontal incision on each side, ending at the rib cage (Figure 3.1 A,B).

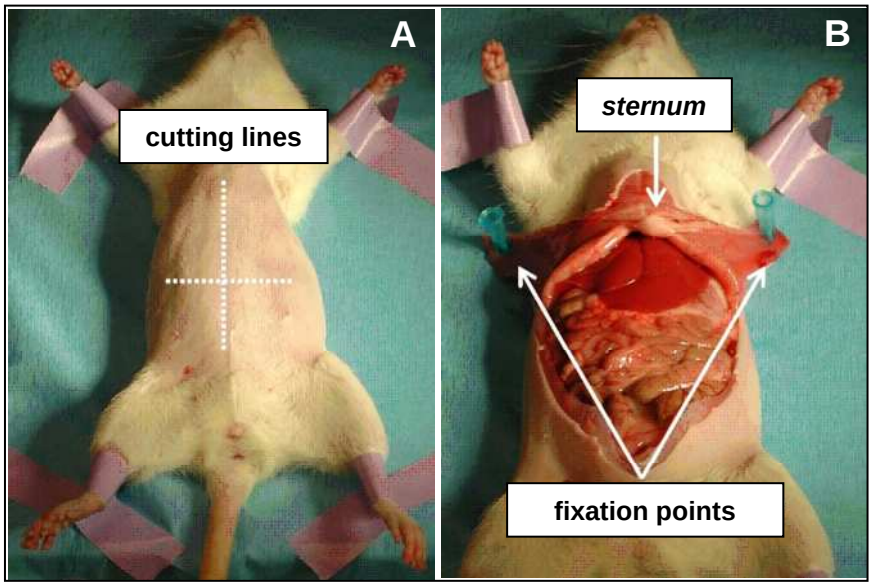

Figure 3.1 Anesthetized animal with (A) delineated cutting lines or (B) opened abdomen.

Vena cava inferior (IVC) and portal vein were ligated loosely with sterile threads (Figure 3.2 A,B). A 22 GA catheter (Optiva 2, Medex Medical, Klein-Winterheim, Germany) was inserted into the portal vein and fixed by tightening the portal vein ligation.

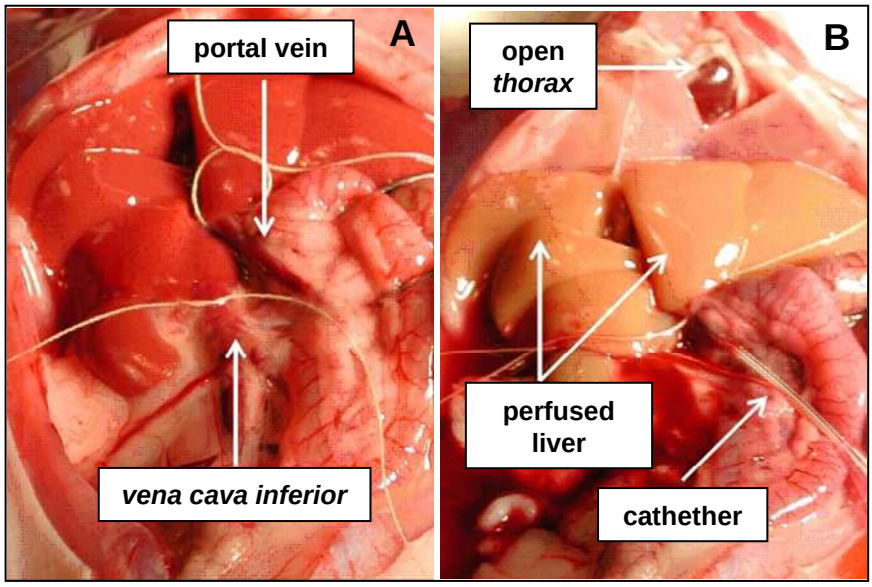

Figure 3.2 (A) Open abdomen with ligated portal vein and *vena cava inferior*. (B) Perfused liver with cathether connected to the portal vein.

Cathether was connected to the perfusion system composed of a water bath adjusted to 37℃ and an ISMATEC pump with appropria te flexible tubings (Novodirect, Kehl/Rhein, Germany). At first, the liver was perfused with perfusion buffer for 3 min at a flow rate of 8 ml/min. Immediately after starting the perfusion,

the IVC was cut below the ligation to prevent a pressure build-up in the liver. After 1 min of perfusion, thorax was opened, the heart was cut and the IVC ligation was tightened. After 3 min of perfusion liver was perfused for further 6 min with digestion buffer. Thereafter, liver was explanted, briefly washed with PBS and minced into small pieces. Gall bladder was removed prior to that. Minced liver was taken up in 45 ml cold perfusion buffer and filtered through nylon gaze (Sigma, Hamburg) to remove undigested and connective tissue, respectively. Liver cell suspension was transferred into 50 ml culture tubes and centrifuged at 30 g for 3 min (4 °C) to separate hepatocytes (pellet) from non-parenchymal cells (supernatant). Pelleted hepatocytes were washed two times by resuspending them in perfusion buffer and subsequent centrifugation (30 g, 3 min, 4 °C). Finally, the pellet was taken up in 30 ml of GIBCO HepatoZYME-SFM (Invitrogen, Carlsbad, CA). The viability of the final cell suspension was checked by trypan blue exclusion (see chapter 3.5.7); purity was analyzed by microscopical investigation. Cells with a viability greater than 80% and a non-parenchymal cell contamination less than 2% were used for further tests. PMH were seeded in 2 ml GIBCO HepatoZYME-SFM supplemented with 2 mmol/l L-glutamine, penicillin (100 IU/ml), and streptomycin (100 mg/ml) (all from PAA, Pasching, Austria) on type I collagen coated plastic dishes (BD Bioscience, Bedford, USA) with a density of 5.0×10^4 cells/cm^2. The first change of the medium was 1 h after seeding, and unattached PMH were washed off with GIBCO HepatoZYME-SFM medium. 24 h after seeding, cells were washed two times with warm PBS and subsequently used for further experiments.

3.5.6 Isolation of human hepatic stellate cells

Human hepatic stellate cells (HSC) were isolated in co-operation with the Center for Liver Cell Research (Department of Surgery, University of Regensburg, Germany). After perfusion and separation of hepatocytes by an initial centrifugation step at 50 g (5 min, 4 °C) the supernatant containing the non-parenchymal cells were centrifuged at 700 g for 7 min (4 °C). The obtained cell pellet was resuspended in HSC medium and cells were seeded into T75 flasks. Within the first week, the medium was replaced daily, from the second week on medium change took place every 2-3 days. Under these conditions only HSC

proliferate. Liver sinusoidal endothelial cells (LSEC) die within the first 24 h. By cultivation on uncoated plastic HSC activate within the first 2 weeks and transdifferentiate to myofibroblast-like cells. Liver disease mediated HSC activation can be simulated *in vitro* that way. After 2 weeks the cell culture was split 1:3 by incubating the cells with Trypsin (0.05%)/EDTA (0.02%) solution. Thereby, only HSC detach, whereas Kupffer cells remain adherent to the plastic surface. Therefore, after the first passage only activated HSC remain in the cell culture which was confirmed by previously done analysis (Mühlbauer et al. 2006).

3.5.7 Determination of cell number and viability

Cell number and viability was determined by trypan blue exclusion test. The cell suspension was diluted 1:2 with trypan blue solution (Sigma, Deisenhofen, Germany) and applied on a Neubauer hemocytometer (Marienfeld GmbH, Lauda-Königshofen, Germany). Cells with impaired cell membrane integrity are stained blue, and therefore, can be clearly distinguished from intact cells which appear white under microscopic inspection. The cell number could be calculated after counting cells in all four quadrants of the hemocytometer, each containing sixteen smaller squares, with the following equation:

$$\textit{Cell number/ml} = Z \times DF \times 10^4 \div 4$$

Z = counted cell number in all four quadrants

DF = dilution factor (in the described procedure the factor is 2)

The ratio of viable cells could be determined by setting the number of unstained cells in relation to the total cell number (blue und unstained cells).

3.5.8 Freezing cells for storage

To freeze cells for storage, cells were trypsinized, centrifuged and resuspended in 5 ml DMEM. Cells were counted, and 1 x 10^6 cells were pipetted in cryotube vials (Nunc, Roskilde, Denmark) and centrifuged again. The supernatant was discarded, and the obtained cell pellet was resuspended in 1 ml of freezing medium. To gently freeze the cell suspension the temperature was lowered

stepwise using a Nicool LM 10 freezing machine (Air Liquide, Düsseldorf, Germany) following the listed program:

Level 4:	30 min
Level 8:	30 min
Level 10:	30 min

Thereafter, the cryotube vials containing the frozen cell suspension were transferred to a liquid nitrogen storage tank.

Thawing of the frozen cell stocks was done quickly with a water bath adjusted to 37 °C. The defrosted cell suspension was transferred into 8 ml of warm DMEM and centrifuged at 300 g for 5 minutes. The obtained cell pellet was resuspended in 10 ml of warm DMEM and pipetted into a T25 cell culture flask.

3.6 Isolation and analysis of RNA

3.6.1 RNA isolation and determination of RNA concentration

RNA isolation was performed with the RNeasy® mini kit (Qiagen, Hilden, Germany) according to the manufacturer's instructions. The principle of RNA isolation is based on the adsorption of RNA to hydrophilic silicon-gel membranes in presence of suitable buffer systems. Biological samples were first lysed and homogenized in the presence of a highly denaturing guanidine isothiocyanate containing buffer, which immediately inactivates RNases to ensure isolation of intact RNA. To homogenize tissue samples a hand-held rotor-stator homogenizer (Xenox Motorhandstück 2.35 with a Roti®-Speed-Rührer Ø 7 mm, Carl Roth, Karlsruhe, Germany) has been used. After lysis, ethanol has been added to provide ideal conditions for the binding of RNA to the silica-gel membranes. Contaminants have been washed away with suitable buffers before RNA was eluted in water and stored at -80 °C. The concentration of RNA was measured with the NanoDrop® ND-1000 UV/VIS spectrophotometer (Peqlab, Erlangen, Germany).

3.6.2 Reverse transcription of RNA to cDNA

Transcription of RNA to complementary DNA (cDNA) was conducted with the Reverse Transcription System Kit (Promega, Mannheim, Germany) which uses avian myeloblastosis virus reverse transcriptase (AMV RT). The working solution was pipetted with contamination-free aerosol filter pipet tips after the following pipetting scheme:

0.5 µg	RNA
5 µl	$MgCl_2$ (25 mM)
2.5 µl	10x reverse transcription buffer
2.5 µl	dNTP mix (10 mM)
1.25 µl	random primer
0.625 µl	RNasin ribonuclease inhibitor
ad 25 µl	$H_2O_{dest.}$

For reverse transcription the samples have been incubated in a GeneAmp® PCR cycler (Applied Biosystems, Foster City, USA) for 30 min at 42 °C. For denaturation of the AMV RT the temperature has been raised to 99 °C for 5 min. After cooling down to 4 °C the obtained cDNA was diluted with 75 µl $H_2O_{dest.}$ and used immediately or stored at -20 °C.

3.6.3 Quantitative real time polymerase chain reaction

To quantify the expression of specific mRNA, quantitative real time polymerase chain reaction (qRT-PCR) has been performed with the LightCycler II system (Roche Diagnostics, Mannheim, Germany). The qRT-PCR is principally based on a conventional polymerase chain reaction (PCR), but offers the additional possibility of quantification, which is accomplished by fluorescence measurements at the end and/or during a PCR cycle. As fluorescent reagent SYBR® Green (QuantiTect SYBR® Green PCR Kit, Qiagen, Hilden, Germany) has been used. SYBR® Green intercalates with double-strand DNA whereby the fluorescence emission rises significantly. Therefore, the fluorescence signal increases proportionally with the amount of PCR products. To quantify the expression of a specific gene of interest, the results have been normalized to the housekeeper

gene β-actin for human samples and to 18s rRNA for murine samples, respectively. The results were evaluated with the LightCycler software version 3.5 (Roche Diagnostics, Mannheim, Germany) following the manufacturer's instructions. The qRT-PCR was performed according to the QuantiTect® SYBR® Green PCR Master Mix protocol (Qiagen, Hilden, Germany):

10 µl	QuantiTect® SYBR® Green PCR Master Mix
2 µl	cDNA
0.5 µl	forward primer (20 µM)
0.5 µl	reverse primer (20 µM)
7 µl	$H_2O_{dest.}$

Following standard scheme has been used and adapted to particular primer melting point temperature:

Initial denaturation:	20 ℃/s to 95 ℃, 900 s
Three step PCR:	20 ℃/s to 95 ℃, 15 s
	20 ℃/s to 55-65 ℃, 20 s, 40 cycles
	20 ℃/s to 72 ℃, 20 s
Analysis of melting curve:	20 ℃/s to 95 ℃, 0 s
	20 ℃/s to 65 ℃, 15 s
	0.1 ℃/s to 95 ℃, 0 s
	20 ℃/s to 40 ℃, 30 s

For validation, after qRT-PCR 5-10 µl of the PCR product has been mixed with loading buffer (Peqlab, Erlangen, Germany) and loaded on a agarose gel with ethidium bromide (50 µg/100 ml gel) to determine the PCR product length. Each experimental condition was performed in triplicates and experiments were repeated at least three times.

Table 3.1 Used forward and reverse primers for qRT-PCR, Species: mouse or human.

name	forward primer	reverse primer
human α-sma	5'-CGT GGC TAT TCC TTC GTT AC	5'-TGC CAG CAG ACT CCA TCC
human β-actin	5'-CTA CGT CGC CCT GGA CTT CGA GC	5'-GAT GGA GCC GCC GAT CCA CAC GG
human collagen I	5'-CGG CTC CTG CTC CTC TT	5'-GGG GCA GTT CTT GGT CTC
human IL8	5'-TCT GCA GCT CTG TGT GAA GGT GCA GTT	5'-AAC CCT CTG CAC CCA GTT TTC CT
human MCP-1	5'-CGC GAG CTA TAG AAG AAT CAC	5'-TTG GGT TGT GGA GTG AGT GT
murine 18s	5'-AAA CGG CTA CCA CAT CCA AG	5'-CCT CCA ATG GAT CCT CGT TA
murine collagen I	5'-CGG GCA GGA CTT GGG TA	5'-CGG AAT CTG AAT GGT CTG ACT
murine CYP2E1	QIAGEN QuantiTect Primer Assay	QIAGEN QuantiTect Primer Assay
murine ICAM-1	QIAGEN QuantiTect Primer Assay	QIAGEN QuantiTect Primer Assay
murine IL-1α	QIAGEN QuantiTect Primer Assay	QIAGEN QuantiTect Primer Assay
murine MCP-1	5'-TGG GCC TGC TGT TCA CA	5'-TCC GAT CCA GGT TTT TAA TGT A
murine p47phox	QIAGEN QuantiTect Primer Assay	QIAGEN QuantiTect Primer Assay
murine TGF-β	QIAGEN QuantiTect Primer Assay	QIAGEN QuantiTect Primer Assay
murine TIMP-1	QIAGEN QuantiTect Primer Assay	QIAGEN QuantiTect Primer Assay
murine TNF	QIAGEN QuantiTect Primer Assay	QIAGEN QuantiTect Primer Assay

Primers were synthesized by SIGMA Genosys (Hamburg, Germany) or purchased as QantiTect Primer Assays form Qiagen (Hilden, Germany). The lyophilized primers were solved in $H_2O_{dest.}$ (SIGMA Genosys primers) or TE buffer (QantiTect Primer Assays), respectively, and stored at -20 ℃.

3.7 Protein analysis

3.7.1 Preparation of whole cell protein extracts

Used buffer:

RIPA buffer	50 mM	Tris/HCl; pH 7.5
	150 mM	NaCl
	1% (v/v)	Nonidet® P40
	0.5% (w/v)	Sodium desoxycholate
	0.1% (w/v)	SDS

To extract whole cell protein from cell lines the cell culture medium was discarded and cells were washed once with PBS, then scraped off with a cell scraper (Corning, NewYork, USA) and taken up into 1 ml of cooled PBS. After centrifugation (1700 g, 5 min, 4 ℃) the cell pelle t was resuspended in 200 µl RIPA buffer and treated with an ultrasonoscope (Sonoplus hp 70, Bandelin electronics, Berlin, Germany) 10 x 3 s at an intensity of 40% for cell lysis. Subsequently, the solved proteins were separated from the non soluble cell components by centrifugation at 20,000 g (10 min, 4 ℃). The prot ein solution was transferred into new reaction tubes and stored at -20 ℃.

3.7.2 Preparation of nuclear protein extracts

Used buffers:

Buffer 1 (hypotonic buffer)	10 mM	Hepes; pH 7.9
	10 mM	KCl
	0.1 mM	EDTA
	0.1 mM	EGTA
Buffer 2 (lysis buffer)	20 mM	Hepes; pH 7.9
	0.4 mM	NaCl
	1 mM	EDTA
	1 mM	EGTA

Before use, the buffers were supplemented with 1 mM DTT and cooled on ice. Cells were detached from cell culture plates by trypsination and centrifuged at 700 g for 5 min (4 ℃). Subsequently, the cell pell et was resuspended in 400 µl of buffer 1 (hypotonic buffer) and incubated for 15 min on ice, resulting in cell swelling. This leads to fragile cell membranes. Addition of 25 µl of the detergent Nonidet-P40 (Roche Diagnostics, Mannheim, Germany) causes leakage of the cytoplasmatic protein into the supernatant. After centrifugation at 10,000 g for 5 min (4 ℃) the supernatant with the cytoplasmatic fraction has been discarded and the pelleted nuclei were resuspended in 50 µl of buffer 2 (lysis buffer) and incubated for 15 min (on ice) on a orbital shaker for lysis. Remaining cell debris were removed by centrifugation (16,000 g, 10 min, 4 ℃) and the supernatant, containing the solved nuclear proteins, was used immediatedly for further analysis or shock frosted in liquid nitrogen and stored at -80 ℃.

3.7.3 Determination of protein concentration

To determine the protein concentrations of protein solutions the BCA Protein Assay Kit (Pierce, Rockford, USA) was used. The assay combines the reduction of Cu^{2+} to Cu^{1+} by protein in an alkaline medium with the highly sensitive and selective colorimetric detection of the cuprous cation Cu^{1+} by bicinchoninic acid (BCA). The first step is the chelation of copper with protein in an alkaline environment to form a blue-colored complex. In this reaction, known as the biuret reaction, peptides containing three or more amino acid residues form a colored chelate complex with cupric ions in an alkaline environment. One cupric ion forms a colored coordination complex with four to six nearby peptides bonds. In the second step of the color development reaction, BCA, a highly sensitive and selective colorimetric detection reagent reacts with the cuprous cation Cu^{1+} that was formed in step 1. The purple-colored reaction product is formed by the chelation of two molecules of BCA with one cuprous ion. The BCA/copper complex is water-soluble and exhibits a strong linear absorbance at 562 nm with increasing protein concentrations. 200 µl of alkaline BCA/copper(II) solution (50 parts of solution A mixed with 1 part of solution B) was added to 2 µl of protein solution using a 96-well plate and have been incubated for 1 h at RT. Thereafter the purple color was measured at 562 nm with a spectrophotometer (EMax® Microplate

Reader, MWG Biotech, Ebersberg, Germany). The optical absorbance values could be translated into specific protein concentrations by parallel quantification of a BSA standard.

3.7.4 SDS polyacrylamid gel electrophoresis

Used buffers:

Laemmli buffer	62.5 mM	Tris/HCl; pH 6.8
	2% (w/v)	SDS
	10% (v/v)	Glycerine
	5% (v/v)	β-Mercaptoethanol
Running buffer	25 mM	Tris/HCl; pH 8.5
	200 mM	Glycine
	0.1% (w/v)	SDS
10% Resolving gel	7.9 ml	$H_2O_{dest.}$
	5.0 ml	1.5 M Tris/HCl; pH 8.8
	0.2 ml	10% (w/v) SDS
	6.7 ml	Acrylamide/Bisacrylamide 30%/0.8% (w/v)
	0.2 ml	Ammonium persulfate 10% (w/v)
	0.008 ml	TEMED
5% Stacking gel	2.7 ml	$H_2O_{dest.}$
	0.5 ml	1.0 M Tris/HCl; pH 6.8
	0.04 ml	10% (w/v) SDS
	0.67 ml	Acrylamide/Bisacrylamide (30%/0.8% w/v)
	0.04 ml	Ammonium persulfate 10% (w/v)
	0.004 ml	TEMED

The protein solutions were heated at 95 °C for 5 min in Laemmli buffer and applied on a SDS polyacrylamid gel for protein fractionation by size at 35 mA/150 V (XCell SureLock™ Mini-Cell, Invitrogen, Karlsruhe, Germany). As size marker the Full Range Rainbow Molecular Weight Marker (GE Healthcare, Freiburg, Germany) was used.

3.7.5 Western blotting

Used buffer:

Transfer buffer	10% (v/v)	Methanol
	25 mM	Tris
	190 mM	Glycine

To detect the proteins after SDS-PAGE by use of specific antibodies the proteins were transferred electrophoretically to a nitrocellulose membrane (Invitrogen, Karlsruhe, Germany) at 220 mA/300 V for 1.5 h (XCell II Blot Module, Invitrogen, Karlsruhe, Germany). To block unspecific binding sites, the membrane was bathed in PBS containing 3% BSA or 5% milk powder for 1 h at RT. Then, the membrane was incubated with a specific primary antibody (Table 3.2) over night at 4 °C. After washing, the membrane was incubated with a secondary horseradish peroxidase (HRP) conjugated antibody (Table 3.2) for 1 h at RT. Thereafter, the membrane was washed with PBS and incubated with the ECL Plus Western Blotting Detection System (GE Healthcare, Freiburg, Germany) for 1 min. This system utilizes chemiluminescence technology for the detection of proteins. It consists of the acridan substrate Lumigen PS-3, which is converted to an acridinium ester intermediate when catalyzed by HRP. The ester intermediate reacts with peroxide in alkaline conditions and emits light, which was detected by autoradiography using a Biomax film (Kodak, Stuttgart, Germany) and a Curix 60 automatic film developer (Agfa, Cologne, Germany). All incubation steps were done on a KS 260 Basic Orbital Shaker (IKA®; Staufen, Germany). Western blot experiments were repeated at least three times.

Table 3.2 Used primary and secondary antibodies for western blot analysis; used dilution; manufacturing company. Secondary antibodies are conjugated with horseradish peroxidase (HRP)

Primary Antibody	**Diluton**	**Manufactoring company**
Actin (mouse)	1:20,000	Sigma, Deisenhofen
IκB-α (mouse)	1:1,000	Santa Cruz, Heidelberg
Secondary Antibody	**Dilution**	**Manufactoring company**
anti-mouse HRP	1:3,000	Santa Cruz, Heidelberg

3.7.6 Quantification of NFκB activity

To quantify NFκB activity in nuclear extracts, the TransAM NFκB p65 Transcription Factor Assay Kit (Active Motif, Rixensart, Belgium) has been used. Analysis was performed according to manufacturer's instructions. The kit contains a 96-well plate on which an oligonucleotide containing the NFκB consensus site (5'-GGGACTTTCC-3') has been immobilized. The active form of NFκB specifically binds to this oligonucleotide. The primary p65 antibody used to detect NFκB recognize an epitope on the p65 NFκB subunit that is accessible only when NFκB is activated (*i.e.* after IκBα degradation; see chapter 2.4.1). Quantification was done by spectrophotometry after incubation with a HRP-conjugated secondary antibody. Each experimental condition was performed in triplicates and experiments were repeated at least twice.

3.7.7 Quantification of caspase-3/7 activity

Caspases, or cysteine-aspartic acid proteases, are a family of cysteine proteases, which play essential roles in apoptosis. There are two types of apoptotic caspases: initiator (apical) caspases and effector (executioner) caspases. Initiator caspases (*e.g.* caspase-2, -8, -9 and -10) cleave inactive pro-forms of effector caspases, thereby activating them. Effector caspases (*e.g.* caspase-3, -6 and -7) in turn cleave other protein substrates within the cell, to trigger the apoptotic process.

To analyze caspase-3/7 activity we used the Apo-One Homogeneous Caspase-3/7 Assay kit (Promega, Madison, WI, USA) according to the manufacturer's instructions. We used 6000 cells/well (96-well plate) and incubated

cells with the provided caspase substrate Z-DEVD-R110 for 1 h. Cleavage of the non-fluorescent caspase substrate Z-DEVD-R110 by caspase-3/7 liberates the fluorescent rhodamine 110, which was detected fluoro-spectrometrically with a SPECTRAFluor Plus microplate reader (Tecan, Männedorf, Switzerland) at wavelengths of 485 nm (excitation) and 520 nm (emission). Each experimental condition was performed in triplicates and experiments were repeated at least twice.

3.7.8 Analysis of cell culture supernatants

Analysis of cell culture supernatants were performed at the Department of Clinical Chemistry and Laboratory Medicine (University of Regensburg, Germany).

Effects on cell viability were assessed by lactate dehydrogenase (LDH), alanine aminotransferase (ALT) and aspartate aminotransferase (AST) leakage into the culture medium. Therefore, culture medium was centrifuged at 20,000 g for 5 min to pellet detached cells and cell debris. The clear supernatant was used for LDH, ALT and AST measurements. LDH was quantified indirectly by reduction of nicotinamide adenine dinucleotide (NAD^+) to NADH by lactate dehydrogenase catalyzed oxidation of L-lactate to pyruvate. ALT and AST were quantified in a three-step-reaction, which results in a decrease of NADH concentration. Increase or decrease of NADH concentration could be detected spectrophotometryly by measurement of absorbance at 340 nm. Lactate dehydrogenase L-P (LDLP) kit, alanine aminotransferase (ALTP5P) kit and aspartate aminotransferase (ASTP5P) kit (all from Bayer HealthCare, Leverkusen, Germany) were used according to manufacturer's instructions adapted to the Advia 1800 analyzer (Siemens Healthcare Diagnostics, Eschborn, Germany). Each experimental condition was performed (at least) in duplicates and experiments were repeated at least three times.

3.8 Flow cytometry

Suspensions of fluorescence labeled cells were analyzed by flow cytometry with a Coulter®EPICS®XL™ flow cytometer (Beckman Coulter, Krefeld, Germany) which uses an argon ion laser tuned to a wavelength of 488 nm. Cell types and their

physical and biochemical conditions can be characterized by detection of light scatter in forward and orthogonal directions together with the fluorescence signals. Measurements were evaluated with the Expo32 ADC Software version 1.1C (Beckman Coulter, Krefeld, Germany). Each experimental condition was performed in triplicates and experiments were repeated at least twice.

3.8.1 Annexin V / Propidium iodide double staining

In the early stages of apoptosis cells change the structure of their membrane, which leads to the exposure of phosphatidylserine on the membrane surface. In living cells, phosphatidylserine is transported to the inside of the lipid bilayer by the aminophospholipid translocase, a Mg^{2+} ATP dependent enzyme. At the onset of apoptosis, phosphatidylserine is translocated to the external membrane and serves as a recognition signal for phagocytes.

Annexins are ubiquitous homologous proteins that bind phospholipids in the presence of calcium. Since the redistribution of phosphatidylserine from the internal to the external membrane surface represents an early indicator of apoptosis, Annexin V and its conjugates can be used for the detection of apoptosis because they interact strongly and specifically with exposed phosphatidylserine.

The differentiation between apoptotic and necrotic cells can be performed by simultaneous staining with propidium iodide (PI), a dye that stains by intercalating into nucleic acid molecules. The cell membrane integrity excludes PI in viable cells, whereas necrotic cells are permeable to PI. Thus, dual parameter flow cytometric analysis allows for the discrimination between viable, early apoptotic and late apoptotic/necrotic cells.

To quantify apoptotic cells we used the ApoTarget Annexin-V FITC Apoptosis Kit (Invitrogen, Karlsruhe, Germany). Therefore, we resuspended 2 x 10^5 cells in 100 µl of the provided binding buffer and added 5 µl of the FITC-labeled Annexin V reagent and 10 µl of the PI solution. After incubation for 15 min at room temperature flow cytometric analysis was performed. The FITC-Annexin V signal was detected at a wavelength of 525 ± 12.5 nm, the PI signal at a wavelength of 620 ± 12.5 nm. The result of the dual parameter flow cytometric analysis were depicted as dotplot and evaluated by quadrant analysis. The y-axis of the dotplot shows the PI fluorescent signal intensity, the x-axis the FITC-Annexin V

fluorescent signal intensity. The discrimination of viable, early apoptotic and late apoptotic/necrotic cells were done by means of different intensities of the FITC-Annexin V or PI fluorescent signals. Viable cells show low FITC-Annexin V and PI fluorescence (lower left quadrant), early apoptotic cells show high FITC-Annexin V but low PI fluorescence (lower right quadrant) and late apoptotic/necrotic cells show both high FITC-Annexin V and PI fluorescence (upper right quadrant) (see Figure 3.3).

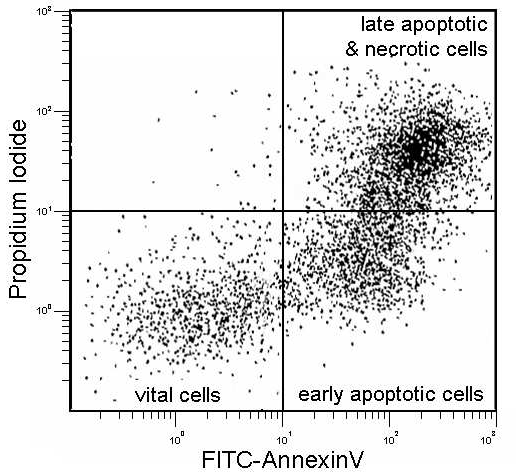

Figure 3.3 Annexin V / Propidium iodide staining dot plot.

To assess the effects of a specific apoptosis or necrosis inducing reagent the percental distribution of viable, early apoptotic and late apoptotic/necrotic cells related to the total of counted cell (10^4 cells) were calculated.

3.8.2 Cell viability analysis via propidium iodide staining

To differentiate between viable and non-viable cells only (disregarding early apoptotic cells), staining with PI alone is sufficient (see 3.8.1). Therefore, we resuspended 2 x 10^5 cells in 100 µl of PBS supplemented with 0.2% FCS and added 10 µl of PI solution. After incubation for 15 min at room temperature flow cytometric analysis was performed. Non-viable cells will be stained by PI and have been detected at a wavelength of 620 ± 12.5 nm. Resulting data (of 10^4 counted cells) were plotted on histograms as PI fluorescence intensity (x-axis) versus event counts (y-axis) as shown in Figure 3.4.

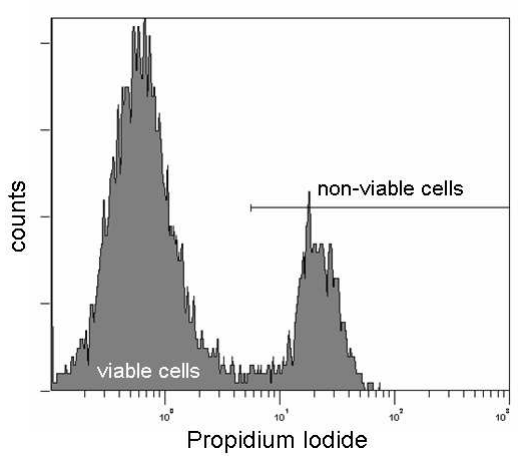

Figure 3.4 Histogram of flow cytometrical analysis of cell viability via propidium iodide staining.

3.8.3 Flow cytometrical analysis of caspase-3 activity

Caspase-3 activity (see also chapter 3.7.7) was quantified by flow cytometry using the CaspGLOW Fluorescein Active Caspase-3 Staining Kit (BioCat, Heidelberg, Germany) according to manufacturer's instructions. Briefly, cells were washed two times with PBS, suspended in DMEM supplemented with 10% FCS and incubated with the FITC-conjugated caspase-3 inhibitor (FITC-DEVD-FMK) for 30 min at room temperature. Thereafter, cells were washed with the provided washing buffer and analyzed by flow cytometry. The FITC signal was detected at a wavelength of 525 ± 12.5 nm. Percentages of FITC positive (active caspase-3) cells of 10^4 analyzed cells were evaluated (see Figure 3.5).

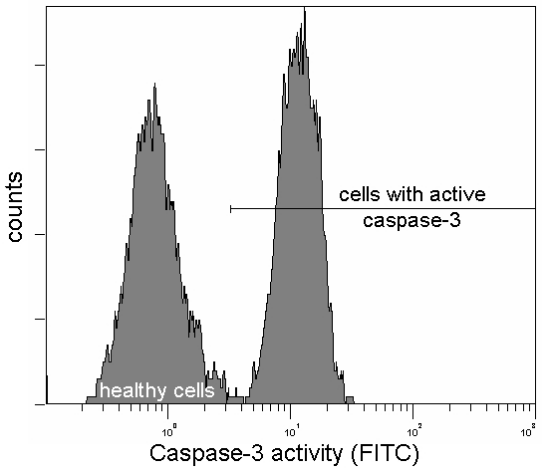

Figure 3.5 Histogram of flow cytometrical analysis of caspase-3 activity.

3.9 Functional assays

3.9.1 XTT-proliferation assay

Cell proliferation was quantified with the XTT kit (Roche Diagnostics, Mannheim, Germany). The assay is based on the ability of metabolic active cells to reduce the tetrazolium salt XTT (2,3-bis(2-methoxy-4-nitro-5-sulfophenyl)-5-[phenylamino)carbonyl]-2H-tetrazolium hydroxide) to orange colored compounds of formazan. The dye formed is water soluble and dye intensity can be read with a spectrophotometer at a wavelength of 450 nm and a reference absorbance wavelength of 650 nm. The intensity of the dye is proportional to the number of metabolic active cells.

To quantify the effects of certain reagents on cell proliferation, cells were seeded in 96-well tissue culture plates (4000 cells per well) and incubated for 4 h in medium containing 10% FCS. Thereafter, medium was taken off and cells were starved for 16 hours in FCS free medium. After a further medium change and addition of specific stimulatory reagents, cells were incubated for different time intervals (1-7 days). At the chosen time points XTT reagent was added and the intensity of the forming dye was measured two hours thereafter with an EMax Microplate Reader (MWG Biotech, Ebersberg, Germany). Values of optical density (OD) at individual time points were corrected for background by subtracting the OD value of a blank well without cells. Each experimental condition was performed in triplicate and experiments were repeated three times.

3.9.2 Migration assay

The migratory potential of cells was quantified using the Cultrex 96 Well Cell Migration Assay (Trevigen, Gaithersburg, USA) according to the manufacturer's instructions. This assay is based on two medium-filled compartments separated by a microporous membrane. In general, cells are placed in the upper compartment and are allowed to migrate through the pores of the membrane to the lower compartment, in which chemotactic agents are present. After an appropriate incubation time, migrated cells are detached from the lower side of the membrane by an appropriate detachment buffer and quantified using calcein acetoxymethylester (calcein AM). Calcein AM is internalized by the cells, and

intracellular esterases cleave the acetomethylester moiety to generate free calcein, which can be detected fluorometrically.

Briefly, cells were seeded into the upper compartment of the provided 96-well plate (4×10^4 cells/well) in DMEM. The lower compartment was filled with DMEM supplemented with conditioned medium from fibroblasts and 10% FCS as chemoattractants. After incubation at 37℃ for 5 h cell migration was quantified by fluorimetry using a SPECTRAFluor Plus microplate reader (Tecan, Männedorf, Switzerland). Each experimental condition was performed in triplicate and experiments were repeated twice.

3.10 Animal experiments

3.10.1 Animal treatment and sample asservation

Female BALB/c mice were purchased from Charles River Laboratories (Sulzfeld, Germany) at 6 weeks of age and housed in a 22℃ con trolled room under a 12 h light-dark cycle with free access to food and water. After 1 week of acclimatization mice were divided into experimental groups (5-6 mice) and fed with standard chow (Ssniff® R/M-H Cat.# V1534-0) as control diet or with experimental chows as indicated. All chows were prepared by Ssniff (Soest, Germany).

At the end of the experiments, mice were sacrificed by heart puncture under ketamine/xylazine anesthesia according to the guidelines of the Central Animal Facility (ZTL) of the University of Regensburg (Regensburg) (Central Animal Facility (ZTL) of the University of Regensburg 2009). Ketamine and xylazine was purchased from the Central Animal Facility (ZTL) of the University of Regensburg. Tissue sections for gene expression or glycogen analysis were frozen in liquid nitrogen immediately after organ explantation and stored at -80 ℃, whereas tissue for histological analysis was fixed for 24 hours in buffered formaldehyde solution (3.7% in PBS) at room temperature, dehydrated by graded ethanol and embedded in paraffin. For serum analysis murine blood was collected by heart puncture under deep anesthesia. After clotting (30 min on ice) blood was centrifuged at 2000 g to remove cellular components. Serum (supernatant) was used immediately for further analysis or stored at -80 °C.

3.10.2 Murine NASH model

Mice were divided into 3 groups (5-6 mice per group) and fed either with control diet or the NASH inducing Paigen-diet (see also chapter 2.7.5.5.5) with or without supplementation with 1.37% (w/w) XN rich hop extract, resulting in a final XN content of 1% (w/w), for 3 weeks. The XN rich hop extract that contains XN at 73% (w/w) was provided by Nateco (Wolnzach, Germany). The Paigen-diet was prepared according to Matsuzawa *et al*. and consisted of standard chow enriched with 15% fat (cocoa butter), cholesterol (1.25%) and sodium cholate (0.5%) (Matsuzawa et al. 2007).

3.10.3 Toxicity study

Mice were divided into 2 groups (6 mice per group) and fed either with control (standard) diet or standard diet supplemented with 0.5% (w/w) XN for 3 weeks. XN was obtained from Alexis Biochemicals (Lausen, Switzerland) with a purity ≥ 98% as determined by HPLC.

3.11 Histology and Immunohistochemistry

For histological and immunohistochemical analysis tissue was fixed for 24 hours in buffered formaldehyde solution (3.7% in PBS) at room temperature, dehydrated by graded ethanol and embedded in paraffin. Sections were cut at 5 µm and stuck on glass slides (Menzel-Gläser, Braunschweig, Germany) for further processing.

3.11.1 Hematoxylin/Eosin staining

Paraffin embedded tissue sections stuck on a glass slide were deparaffinized with xylene. Then, the tissue was rehydrated and dipped into an aqueous solution of hematoxylin. Hematoxylin binds to basophilic structures such as the anionic phosphate groups of nucleic acids. Following dehydration in alcohol, the tissue was dipped into an alcoholic solution of eosin. Eosin carries a negative charge and reacts with the cationic groups common to amino acids (eosinophilic structures). Once stained, the tissue was covered with a thin glass cover slip (Carl Roth, Karlsruhe, Germany) attached by mounting medium (Vector Laboratories,

Burlingame, USA). In general, the eosin imparts a pink to red color to proteins, and hematoxylin stains the basophilic structures, usually containing nucleic acids, such as ribosomes and the chromatin-rich cell nucleus, from blue to purple. Digital images were captured with an Olympus CKX41 microscope equipped with the ALTRA20 Soft Imaging System (Olympus, Hamburg, Germany).

3.11.2 Immunohistochemical analysis of α-smooth muscle actin

For visualization of α-sma positive cells the LSAB+ System-HRP Kit (Dako, Hamburg, Germany) was used according to the manufacturer's instructions. The technique used in this kit is based on the LSAB (labeled streptavidin biotin) method.

Used buffer:

TBS-T buffer	6.1 g/l	Tris	
	8.8 g/l	NaCl	
	37 ml	1 N HCl	
	ad 1 l	$H_2O_{dest.}$	pH 7.6
	0.05%	TWEEN 20	

First, paraffin embedded tissue sections stuck on a glass slide were deparaffinized with xylene. Then, endogenous peroxidase activity was quenched by incubating the tissue for 5 min in 3% H_2O_2. Subsequently, tissue was incubated with the primary antibody (monoclonal α-sma antibody (mouse) from Abcam, Cambridge, UK) for 30 min. For this purpose, the primary antibody was diluted 1:200 with TBS-T buffer. Thereafter, sequential incubations with the biotinylated link antibody (15 min) and peroxidase-labeled streptavidin (15 min) were performed. Staining is completed after incubation with the provided substrate-chromogen (3,3'-diaminobenzidine) solution (15 min). For counterstaining the tissue was dipped into an aqueous solution of hematoxylin for 1 min. Finally, tissue was rinsed with $H_2O_{dest.}$ and covered with a thin glass cover slip (Carl Roth, Karlsruhe, Germany) attached by mounting medium (Vector Laboratories, Burlingame, USA). Digital images were captured with an Olympus CKX41 microscope equipped with the ALTRA20 Soft Imaging System (Olympus, Hamburg, Germany).

3.12 Serology

Analysis of serological parameters were performed at the Department of Clinical Chemistry and Laboratory Medicine (University of Regensburg, Germany) using appropriate kits, namely Albumin (ALB)-, Alkaline Phosphatase (ALPAMP)-, Alanine Aminotransferase (ALTP5P)-, Aspartate Aminotransferase (ASTP5P)-, Enzymatic Creatinine_2 (ECRE_2)-, Glucose Hexokinase II (GLUH)-, Lipase (LIP)-, Potassium (K)-, Sodium (Na)-, Total Protein II (TP)- and Urea Nitrogen (UN)-kit (all from Bayer HealthCare, Leverkusen, Germany) according to manufacturer's instructions and adapted to the Advia 1800 analyzer (Siemens Healthcare Diagnostics, Eschborn, Germany). Murine serum samples were collected and prepared as described in chapter 3.10.1. Each experimental condition was performed (at least) in duplicates, experimental groups consisted of 5-6 murine serum samples and experiments were repeated two times.

3.13 Limulus Amebocyte Lysate assay

For quantification of endotoxin serum levels, blood was collected and processed under sterile and pyrogen-free conditions and the obtained serum was stored in endotoxin free cups. Endotoxin concentration was determined using the Limulus Amebocyte Lysate (LAL) assay from Hycult Biotechnology (Uden, The Netherlands) according to the manufacturer's instructions. Bacterial endotoxin, like lipopolysaccharide (LPS), is a fever-producing by-product of gram-negative bacteria commonly known as pyrogen. The principle of the used test is based on the fact that bacteria cause intravascular coagulation in the American horseshoe crab, *Limulus polyphemus*. The agent responsible for the clotting phenomena resides in the crab's amebocytes. Bacterial endotoxin triggers an enzymatic reaction resulting in turbidity and gelation of the Limulus amebocyte lysate (LAL), which is utilized in this assay. Briefly, samples and standards were incubated with the provided LAL reagent. The enzymatic reaction, triggered by endotoxin, will cause a yellow color to develop upon cleavage of the chromophore, p-nitroaniline. The enzymatic reaction is then stopped by the addition of acetic acid. Subsequently, the absorbance at 405 nm was measured with an EMax Microplate Reader (MWG Biotech, Ebersberg, Germany). A standard curve was obtained by plotting the absorbance versus the corresponding concentrations of the *E. coli*

standards. Each experimental condition was performed in triplicates, experimental groups consisted of 5-6 murine serum samples and experiments were repeated two times.

3.14 Glycogen assay

Hepatic glycogen content was quantified using the Glycogen Assay Kit from BioVision (Heidelberg, Germany) according to the manufacturer's instructions. Briefly, frozen liver tissue sections were weighed (approx. 50 mg) and homogenized in 1 ml $H_2O_{dest.}$ under cooling. Thereafter, enzymes were inactivated by boiling the homogenates for 5 min. After cooling samples down to 37 °C, glycogen was hydrolyzed to glucose applying the provided hydrolyses enzyme mix. Thereafter, the provided OxiRed development enzyme mix was added and glucose was quantified colorimetrically using an EMax Microplate Reader (MWG Biotech, Ebersberg, Germany). Standard curve was assessed by dilution and quantification of the provided glycogen standard. Each experimental condition was performed in triplicates, experimental groups consisted of 5-6 murine blood samples and experiments were repeated three times.

3.15 Cholesterol assay

To quantify the hepatic total cholesterol content, total lipids/cholesterol were extracted from liver tissue sections using the method of Bligh and Dyer with slight modifications (BLIGH and DYER 1959). In brief, liver sections (approx. 50 mg) were weighed into 1 ml of a chloroform/methanol mix (2:1 v/v) and incubated for 1 h at room temperature on an orbital shaker to extract the lipids. After addition of 200 µl $H_2O_{dest.}$, vortexing and centrifugation for 5 min at 3000 g, the lower lipid phase was collected and dried at room temperature. The lipid pellet was then re-dissolved in 60 µl *tert*-butanol and 40 µl of a Triton X-114/methanol mix (2:1 v/v), and total cholesterol content was quantified using the Cholesterol/Cholesteryl Ester Quantitation Kit from BioVision (Heidelberg, Germany) according to the manufacturer's instructions. The principle of this assay is based on enzymatic reactions which set free an easy detectable chromophore. First, cholesterol esterase hydrolyses esterified cholesterols into cholesterol. The free cholesterol is

then oxidized by cholesterol oxidase to yield H_2O_2, which interacts with a sensitive probe to produce resorufin. Quantification of resorufin was performed spectrophotometrically at 540 nm using an EMax Microplate Reader (MWG Biotech, Ebersberg, Germany). Each experimental condition was performed in triplicates, experimental groups consisted of 5-6 murine livers and experiments were repeated three times.

3.16 Reagent preparation for *in vitro* experiments

3.16.1 Palmitic acid preparation

Palmitic acid (C16:0) is the most prevalent long-chain saturated free fatty acid found in circulation. In human blood it is bound to albumin, with a physiologic ratio of fatty acid to albumin of approximately 2:1. In states of insulin resistance and obesity (as major risk factors for NAFLD/NASH), serum fatty acid levels are commonly elevated, yielding ratios as high as 7.5:1 (Kleinfeld et al. 1996). In order to simulate hepatic steatosis, we recently established a palmitic acid-induced *in vitro* fatty liver model (Wobser et al. 2009). Palmitic acid was complexated to BSA in a molar ratio of approx. 6.7:1, thereby mimicking hyperlipidemic conditions.

Preparation of the palmitic acid stock solution was carried out as described by Cousin *et al*. (Cousin et al. 2001). Briefly, a 100 mM palmitic acid stock solution was prepared in 0.1 mM NaOH by heating at 70 °C. A 10% (w/v) aqueous free fatty acid free BSA solution was prepared, and maintained at 55 °C in a water bath. 10 mM palmitic acid/1% BSA solution was obtained by complexation of the appropriate amount of palmitic acid stock solution with 10% BSA at 55 °C for another 30 min. The obtained solution was then cooled to 25 °C, filter sterilized and stored at −20 °C until use. For *in vitro* experiments the 10 mM palmitic acid/10% BSA stock solution was heated for 15 min at 55 °C and subsequently cooled down to working temperature (37 °C) before use. Samples indicated as controls received an appropriate amount of a vehicle control stock solution, which was prepared analogous to the palmitic acid/10% BSA stock solution, except for adding palmitic acid.

3.16.2 Xanthohumol preparation

For *in vitro* experiments XN was dissolved in DMSO and added to cell culture at the indicated concentrations. Samples indicated as controls contained vehicle (DMSO) only.

3.17 Statistical analysis

Values are presented as mean ± SEM or mean ± SD as indicated. All experiments were repeated at least three times. Comparison between groups was made using the Student's unpaired t-test. Welch's correction was performed when required. A p-value < 0.05 was considered statistically significant. All calculations were performed using the statistical computer package GraphPad Prism version 4.00 for Windows (GraphPad Software, San Diego, CA, USA).

4 Results

As described in the introduction xanthohumol (XN) exhibits several biological effects (see chapter 2.4), however, with regards to effects on liver cells or liver diseases respectively, only few data are available (see also chapter 2.6).The aim of this thesis was to address this issue.

In particular, the focus was placed on three aspects:
4.1 Effects of xanthohumol on hepatic inflammation and fibrosis
4.2 Effects of xanthohumol on hepatocellular carcinoma cells
4.3 Safety profile of orally applied xanthohumol

4.1 Effects of xanthohumol on hepatic inflammation and fibrosis

4.1.1 Motivation

Obesity and insulin resistance have reached epidemic proportions worldwide, and as one of the consequences non-alcoholic fatty liver disease (NAFLD) has emerged as a considerable public health concern. Previously, NAFLD was often considered a relatively benign condition, but today it is evident that a significant number of patients will progress to more severe stages of liver disease including NASH (non-alcoholic steatohepatitis). In addition to fatty infiltration of the liver, NASH is characterized by inflammation, hepatocellular damage and fibrosis (see also chapter 2.7.5.5) (Caldwell et al. 1999; Powell et al. 1990).
The development of fibrosis, and particularly cirrhosis, is associated with a significant morbidity and mortality (see also chapters 2.7.2 and 2.7.3). Thus, there is a considerable imperative to develop antifibrotic strategies that are applicable to liver fibrosis. Such an approach is attractive since it is aimed at the final common pathological pathway of chronic liver disease, regardless of etiology.
Here, we studied the effect of XN on primary human HSC and hepatocytes *in vitro*. Further, we tested the effects of XN on hepatic inflammation and fibrogenesis in a murine NASH model.

4.1.2 Effects of xanthohumol on HSC

As mentioned in the introduction (see chapter 2.7.2) current evidence indicates that hepatic stellate cells (HSC) are central mediators of hepatic fibrosis in chronic liver disease including NASH. However, studies investigating the effects of XN on HSC were missing so far.

4.1.2.1 Effects on HSC activation *in vitro*

The activation of HSC is one of the central pathophysiological mechanism of liver fibrogenesis (Bataller and Brenner 2005; Friedman 2008). First, we therefore aimed to analyze the effect of XN on the *in vitro* activation process of HSC. Two days after isolation human HSC were exposed to XN at two different doses (5 µM and 10 µM) for three days. Here, and in subsequent experiments control cells were treated with DMSO at the same concentration as used as solvent for XN. Subsequently, mRNA expression of two established markers of HSC activation, namely collagen type I and alpha-smooth muscle actin (α-sma), was determined by qRT-PCR analysis. Treatment with XN significantly reduced the expression of collagen type I (collagen I) and α-sma compared to control HSC (Figure 4.1).

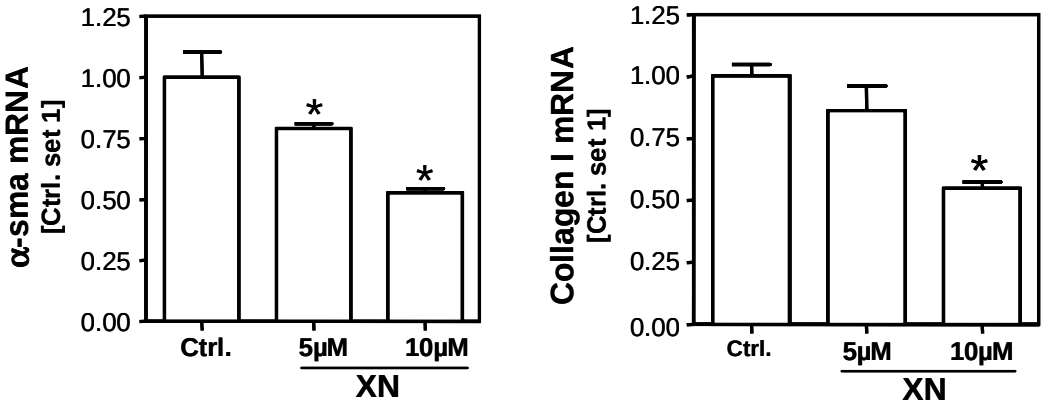

Figure 4.1 Two days after isolation HSC were incubated with xanthohumol (XN; 5 µM and 10 µM) for 72 h. Subsequently, α-sma and collagen I mRNA expression were analyzed by qRT-PCR analysis. *: $p<0.05$ compared to control.

4.1.2.2 Induction of apoptosis in activated HSC *in vitro*

Once they are activated HSC are characterized by high resistance to apoptosis, a mechanism that has therefore been proposed to play a key role in the progression of fibrosis in chronic liver disease. Incubation of *in vitro* activated HSC with XN for 6 h led to dose-dependent (0-20 µM) activation of caspase-3/7 (Figure 4.2).

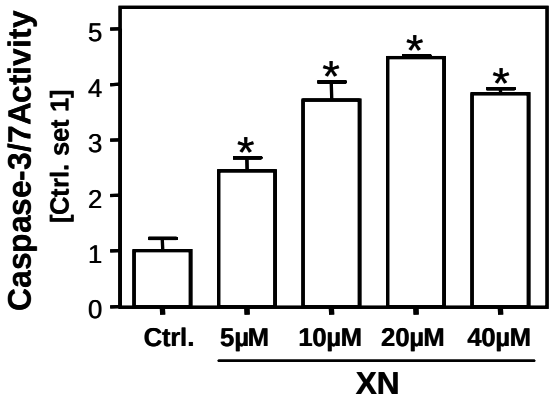

Figure 4.2 *In vitro* activated HSC were incubated with different doses of XN. Caspase-3/7 proteolytic activity was measured in cytosolic protein extracts by cleavage of the fluorigenic substrate Z-DEVD-rhodamine-110. Activities are represented as fold-increase of rhodamine-110 fluorescence over control. *: $p<0.05$ compared to control.

Incubation of HSC with higher doses of XN led to detachment of HSC. After 24 h incubation with 10 µM or 20 µM XN almost all cells appear positive for propidium iodide, indicating late apoptosis and necrosis (Figure 4.3).

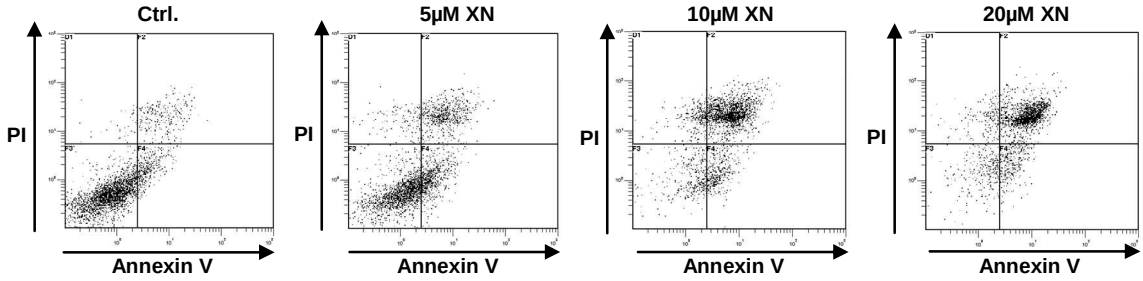

Figure 4.3 Apoptosis was analyzed by flow cytometry applying annexin V and propidium iodide staining. Annexin V+ and PI- cells reflect early apoptosis while annexin V+ and PI+ cells indicate late apoptosis / secondary necrosis.

In line with these data, secretion of LDH is dose-dependently increasing in XN treated HSC after 24 h and is reaching a plateau at 20 µM (Figure 4.4).

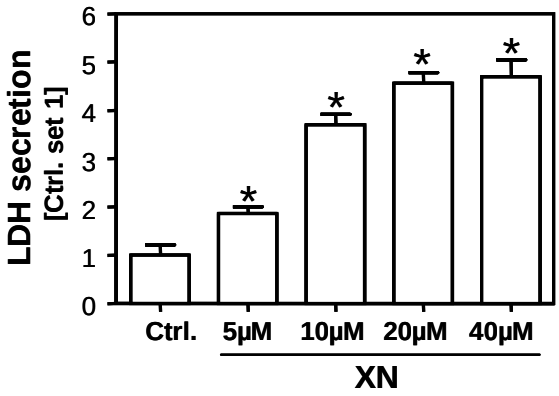

Figure 4.4 24 h after XN stimulation vitality was measured as cell membrane lysis and release of lactate dehydrogenase (LDH) into supernatants. *: p<0.05 compared to control.

4.1.2.3 Inhibition of NFκB activity and proinflammatory gene expression in HSC *in vitro*

XN is known to inhibit NFκB activity in tumorous cells (Albini et al. 2006), and it has been shown that NFκB activity is crucial for both HSC activation and resistance to apoptosis (Elsharkawy et al. 2005; Hellerbrand et al. 1998a). Here, we found that XN stimulation reduces both basal as well as TNF induced NFκB activity in nuclear extracts of activated HSC (Figure 4.5).

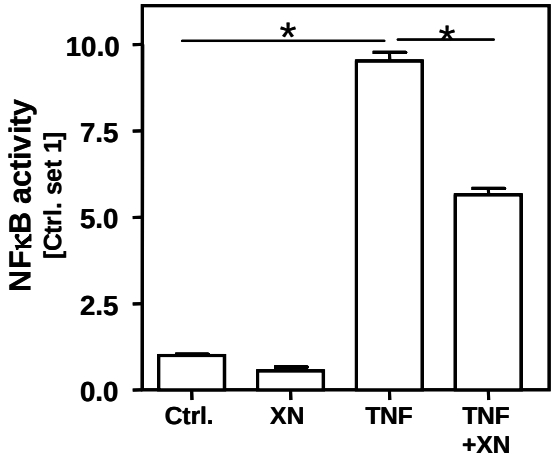

Figure 4.5 NFκB activity in nuclear extracts of TNF and/or xanthohumol (XN) treated cells and control cells by ELISA. After 24 h serum depletion activated human HSC were stimulated with XN (5 µM) for 3 h, and subsequently, with TNF (10 ng/ml) for 2 h in serum free medium. *: p<0.05

Furthermore, XN inhibits TNF mediated IκB-α degradation in activated HSC (Figure 4.6).

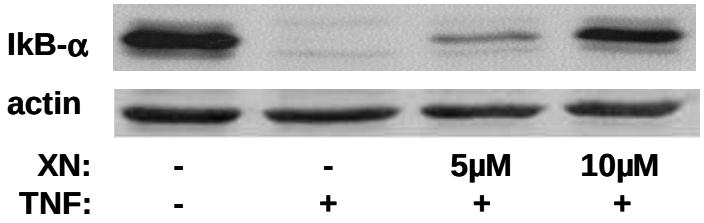

Figure 4.6 Analysis of IκBα in protein extracts of TNF and/or xanthohumol (XN) treated cells and control cells by Western blotting. After 24 h serum depletion activated human HSC were stimulated with 5 µM or 10 µM xanthohumol (XN) for 3 h, and subsequently, with TNF (10 ng/ml) for 30 min in serum free medium.

In accordance, XN inhibited TNF-induced MCP-1 expression, a proinflammatory chemokine that is *de novo* expressed during HSC activation and that is highly regulated via activation of the transcription factor NFκB in activated HSC (Hellerbrand et al. 1998b) (Figure 4.7).

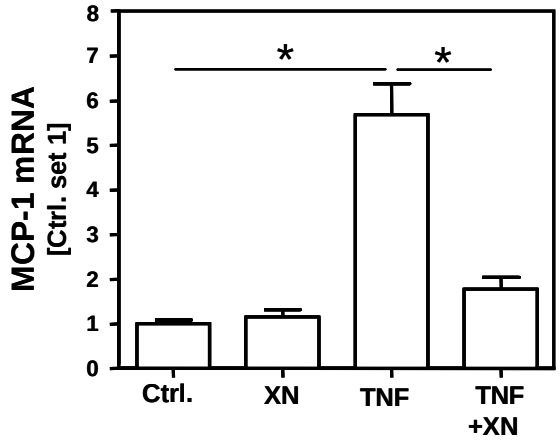

Figure 4.7 MCP-1 mRNA expression in TNF and/or xanthohumol (XN) treated cells and control cells analyzed by qRT-PCR. After 6 h serum depletion activated human HSC were stimulated with XN (5 µM) and/or TNF (10 ng/ml) for 24 h in serum free medium. *: $p<0.05$

4.1.3 Effects of xanthohumol on primary human hepatocytes

In vitro effects on HSC were achieved at the same or even lower concentrations as observed in human cancer cells of different origin (Colgate et al. 2007; Dell'Eva et al. 2007; Delmulle et al. 2006; Miranda et al. 1999). However, data regarding apoptotic or cytotoxic effects on primary human hepatocytes (PHH) were missing so far.

Noteworthy, XN did not affect LDH or ALT (Figure 4.8) levels in the supernatant of PHH incubated with XN doses as high as 50 µM for 24 h.

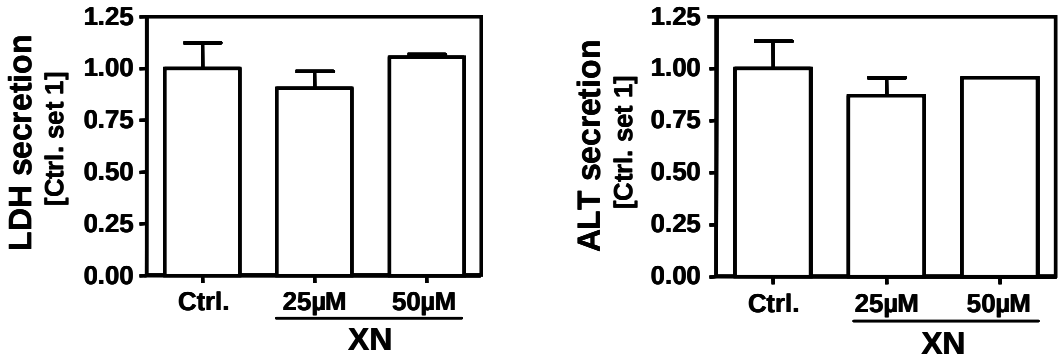

Figure 4.8 Primary human hepatocytes (PHH) were incubated with xanthohumol (XN) for 24 h at the concentrations indicated. Viability was assessed as release of LDH and ALT into the supernatants.

Flow cytometric analysis confirmed that there is no significant apoptosis or necrosis in PHH after 24 h stimulation with 25 µM or 50 µM XN (Figure 4.9).

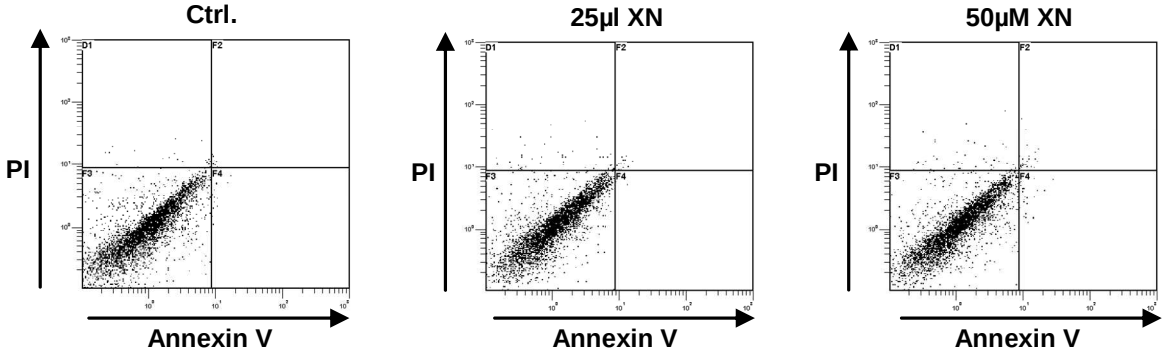

Figure 4.9 Analysis of apoptosis by flow cytometric analysis using annexin V/PI staining.

However, at the same concentrations a significant inhibition of IL-8 expression was observed (Figure 4.10), another chemokine known to be regulated by NFκB.

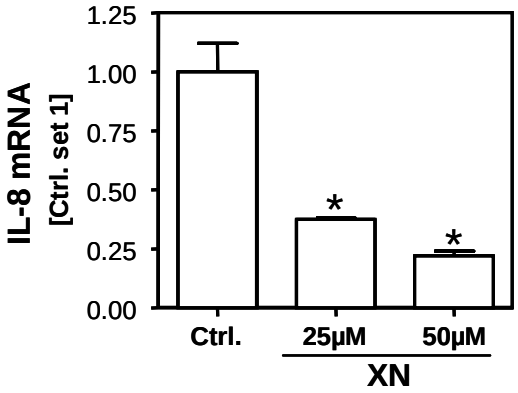

Figure 4.10 Analysis of IL-8 mRNA expression by qRT-PCR in xanthohumol (XN; 20 µM) stimulated and control PHH. *: p<0.05 compared to control.

Recent studies have shown that free fatty acids are capable of inducing NFκB and proinflammatory gene expression in hepatocytes (Joshi-Barve et al. 2007). Here, we confirmed significant induction of IL-8 expression in PHH following stimulation with 0.4 µM palmitic acid, and this induction was inhibited by simultaneous incubation with XN (Figure 4.11).

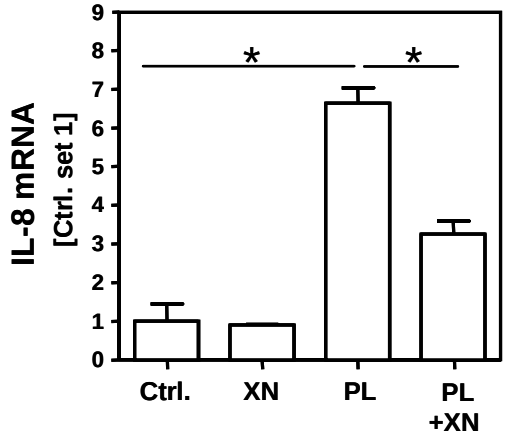

Figure 4.11 IL-8 mRNA expression in PHH stimulated with palmitic acid (PL; 0.4 µM) and/or xanthohumol (XN; 20 µM) for 24 h. PHH stimulated with the solvents DMSO and BSA served as control. *: p<0.05

4.1.4 *In vivo* effects of xanthohumol in a murine NASH model

4.1.4.1 No affection of hepatic steatosis in the murine NASH model

In vitro data indicate that XN exhibits antifibrogenic effects at concentrations that do not affect the viability of PHH but even suppress basal as well as free fatty acid induced expression of proinflammatory chemokines known to play a role in progression of NASH (Haukeland et al. 2006; Jarrar et al. 2008; Miranda et al. 1999). These *in vitro* findings encouraged us to test the effect of XN in a dietary NASH model, named Paigen-diet (Nishina et al. 1993; Nishina et al. 1990), in mice (see also chapters 2.7.5.5.5 and 3.10.2). We selected this model since recently Matsuzawa *et al*. described that feeding this diet rich in fat (15%) and supplemented with cholesterol and cholate induced severe hepatic inflammation and fibrogenesis within 6 or 24 weeks, respectively (Matsuzawa et al. 2007). Here, we applied the Paigen-diet either alone or supplemented with 1.37% (w/w) XN rich hop extract, resulting in a final XN content of 1% (w/w), for 3 weeks. Mice receiving standard chow served as control.

No significant differences were found between treatment groups regarding food and fluid intake or body weight throughout the study. However, liver body weight ratio was significantly lower in mice fed with Paigen+XN compared to mice receiving the pure Paigen-diet (Figure 4.12).

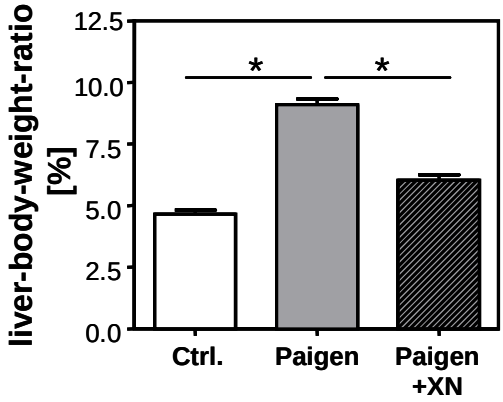

Figure 4.12 Liver-body-weigh-ratios of mice fed the NASH inducing Paigen-diet either alone or supplemented with xanthohumol (Paigen+XN) for 3 weeks. Mice receiving standard chow served as control. *: $p<0.05$

Despite the short feeding period the Paigen-diet induced macroscopically visible hepatic steatosis that appeared similar in the Paigen+XN group (Figure 4.13).

Figure 4.13 Representative macroscopic images of the livers of the three treatment groups.

Histological analysis revealed microvesicular steatosis in both mice fed the Paigen-diet alone or in combination with XN (Figure 4.14).

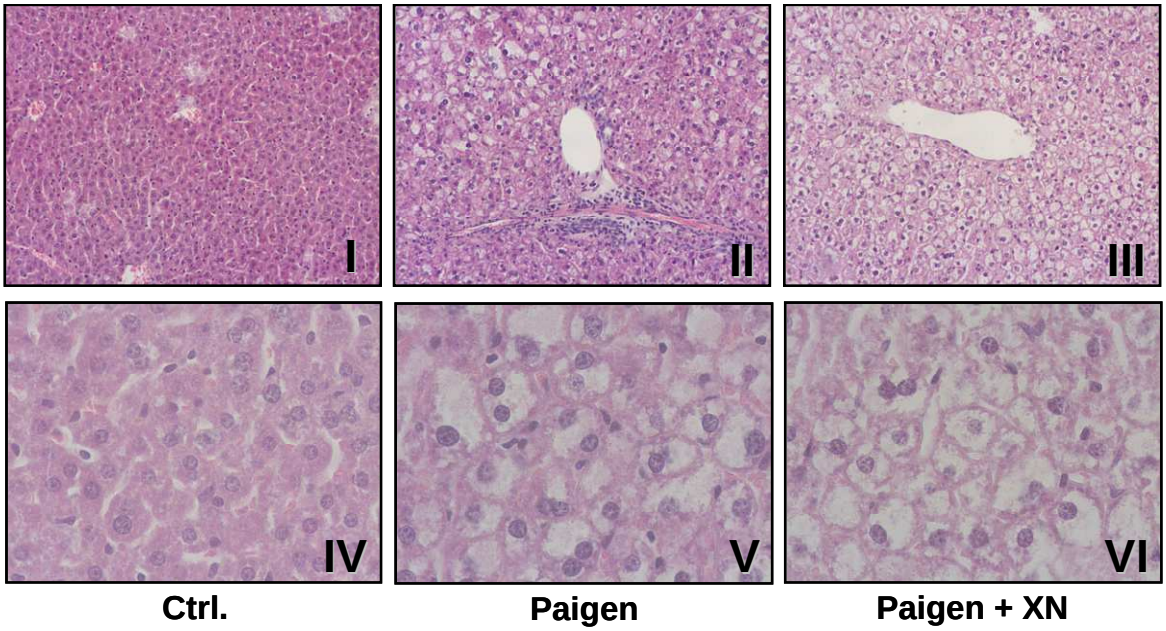

Figure 4.14 HE-staining of liver tissue from mice fed Paigen (II, IV), Paigen+XN (III,VI) or control mice (I,IV). Representative images at 2 different magnifications (I-III:100X; IV-VI:200X) are shown.

It has been shown that cholesterol is the predominant lipid accumulating in the liver after Paigen-feeding. Also here, we found a significant increase of hepatic cholesterol levels after 3 weeks feeding this diet, and cholesterol levels did not differ between the Paigen and the Paigen+XN group, respectively (Figure 4.15).

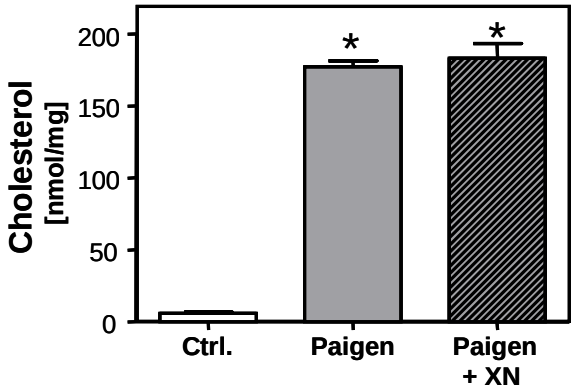

Figure 4.15 Intrahepatic cholesterol levels. *: p<0.05 compared to control.

4.1.4.2 Inhibition of hepatic inflammation in a murine NASH model

In addition to steatosis, histological analysis revealed significant inflammation and necrosis in mice fed with the Paigen-diet (Figure 4.14,II), but these histopathological changes were apparently less pronounced in the Paigen+XN group (Figure 4.14,III). In accordance, ALT and AST (Figure 4.16) serum levels were significantly increased in the Paigen-group but reduced to normal levels in mice fed Paigen+XN.

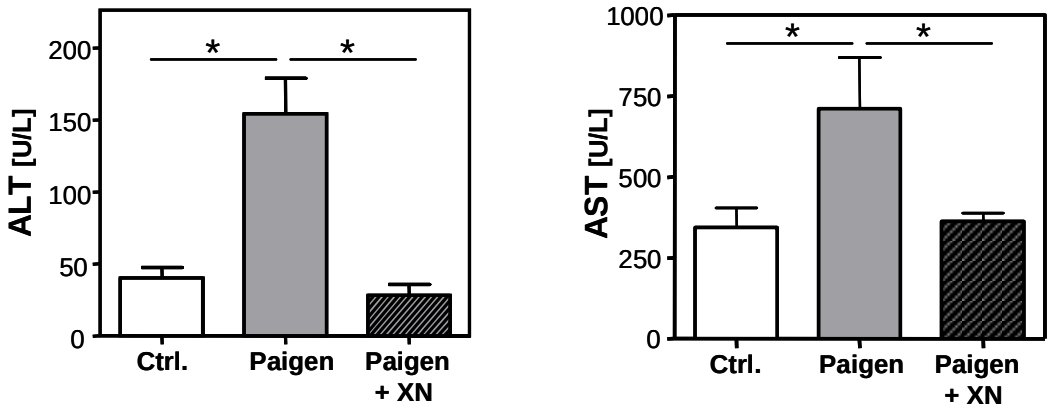

Figure 4.16 Analysis of ALT and AST serum levels. *: p<0.05

Further, both TNF and IL-1α expression were significantly increased in mice fed the Paigen-diet (Figure 4.17), but this increase was almost completely blunted in mice fed Paigen+XN.

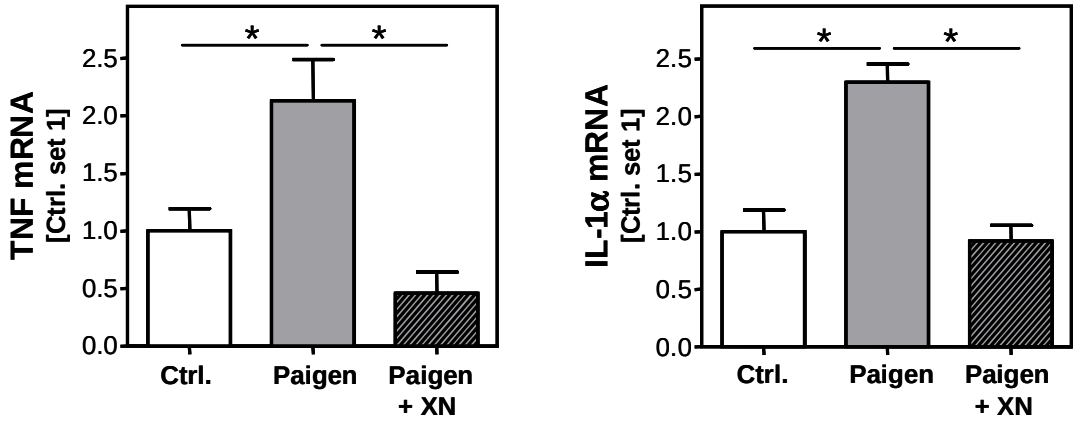

Figure 4.17 Analysis of hepatic TNF and IL1-α mRNA levels by qRT-PCR. *: p<0.05

Similarly, MCP-1 mRNA was significantly increased in mice fed the Paigen-diet compared to control fed mice, but the increase was diminished in the Paigen+XN group (Figure 4.18).

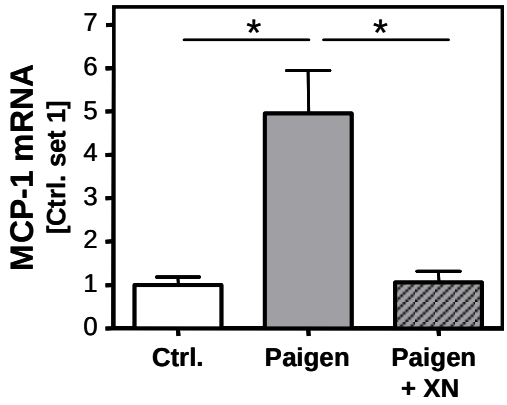

Figure 4.18 Analysis of hepatic MCP-1 mRNA levels by qRT-PCR. *: p<0.05

4.1.4.3 Inhibition of HCS activation and hepatic fibrosis *in vivo*

Besides inflammatory gene expression, a significant increase of the mRNA levels of the profibrogenic genes TGF-β and TIMP-1 was observed in mice fed the Paigen-diet (Figure 4.19).

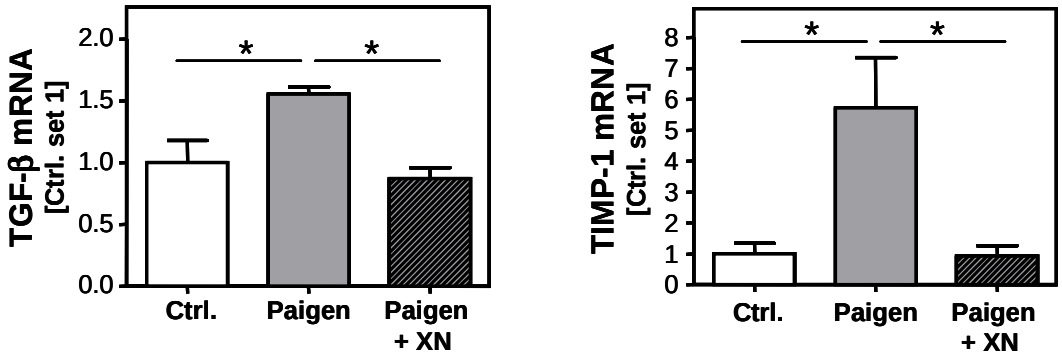

Figure 4.19 Analysis of hepatic TGF-β and TIMP-1 mRNA levels by qRT-PCR. *: p<0.05

In contrast, hepatic mRNA levels of both profibrogenic genes in Paigen-XN mice did not differ significantly from control mice. After 3 weeks feeding the Paigen-diet we did not yet observe hepatic fibrosis in histological analysis. However, collagen type I mRNA was significantly increased in Paigen-diet but not in Paigen+XN fed mice compared to mice fed control diet (Figure 4.20).

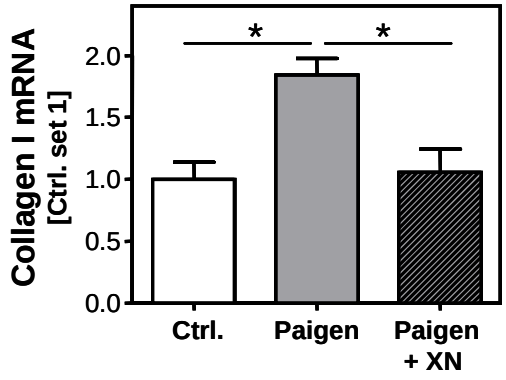

Figure 4.20 Analysis of hepatic collagen I mRNA levels by qRT-PCR. *: p<0.05

In line with these observations, immunohistochemical staining of liver tissue from the Paigen group revealed α-sma positive cells along the sinusoids (Figure 4.21). In contrast, in livers from mice fed Paigen+XN or control diet no α-sma immuno-signal was detected along the sinusoids indicating that the activation of HSC in response to the Paigen-diet was blunted by XN.

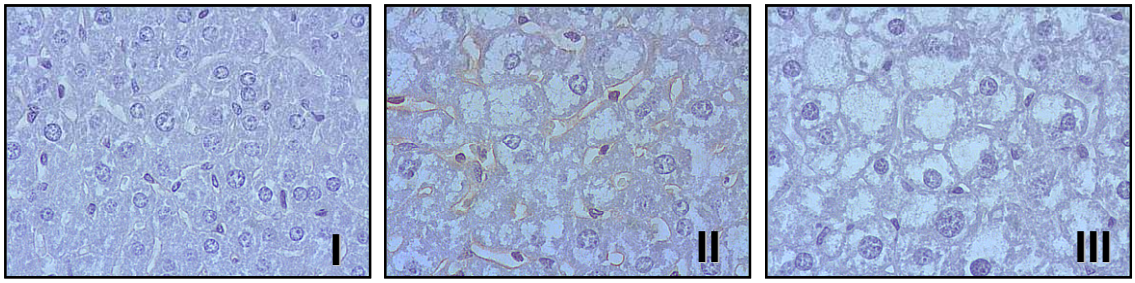

Figure 4.21 Immunohistochemical analysis of α-sma in liver tissue of mice fed Paigen (II), Paigen+XN (III) or control mice (I). α-sma positive HSC appear brownish.

4.1.5 Summary

Here, we could show that XN inhibits the activation of primary human HSC and induces apoptosis in activated HSC *in vitro* in a dose dependent manner (0-20 µM), but does not impair viability of primary human hepatocytes at even higher doses (50 µM). However, in both cell types XN inhibits NFκB activation and expression of NFκB dependent proinflammatory chemokines. *In vivo*, feeding of XN reduced levels of serum transaminases and hepatic expression of proinflammatory genes in a murine model of NASH. Moreover, XN treatment significantly inhibited hepatic expression of profibrogenic genes and activation of HSC *in vivo*. In conclusion, XN has the potential to ameliorate NASH induced liver injury, suggesting its potential use as functional nutrient to prevent progression of chronic liver disease.

4.2 Effects of xanthohumol on hepatocellular carcinoma cells

4.2.1 Motivation

Despite the extensive research on anticancer functions of XN, very few studies have evaluated the inhibitory effects of XN on hepatocellular carcinoma (HCC). More importantly, there exists no data concerning effects of XN on non-malignant primary human hepatocytes, which is a prerequisite for the use of XN as an anticancer agent. Here, we analyzed the effects of XN on two human HCC cell lines as well as on primary human hepatocytes (PHH).

4.2.2 Induction of cell death in HCC cells but not in PHH

First, we analyzed the effects of XN on the viability of the two human HCC cell lines HepG2 and Huh7. Microscopic observation revealed a marked decrease of the cell number after incubation with XN at a concentration of 25 µM for 24 h. Stimulation with higher XN concentrations led to an almost complete cell detachment (Figure 4.22).

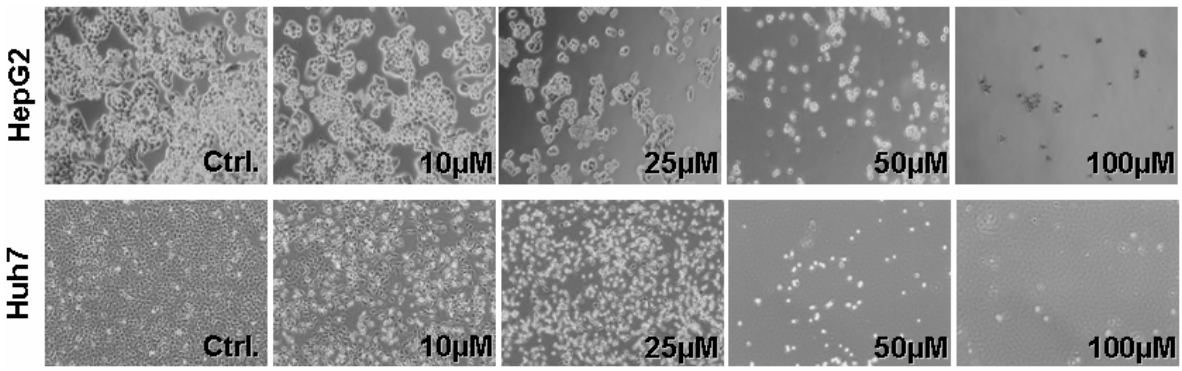

Figure 4.22 Representative phase-contrast images of HepG2 (upper row) and Huh7 (lower row) hepatocellular carcinoma cell line cultures after 24 h incubation with the indicated concentrations of xanthohumol (XN).

Consistently, a significant increase of LDH and AST levels were detected in the supernatants of HCC cells after incubation with 10, 25, 50 and 100 µM XN (Figure 4.23).

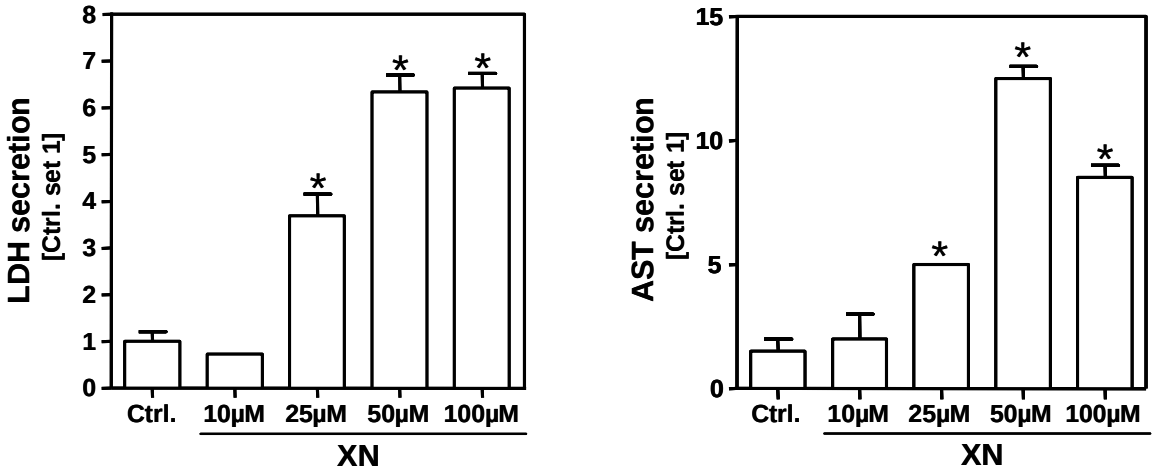

Figure 4.23 Hepatocellular carcinoma cells (Huh7) were incubated with xanthohumol (XN) for 24 h at the concentrations indicated. Viability was assessed as release of LDH and AST into the supernatants. *: $p<0.05$ compared to control.

In contrast, but in line with the findings described in the previous chapter 4.1.3, primary human hepatocytes (PHH) appeared completely unaffected after 24 h incubation with XN concentrations as high as 100 µM (Figure 4.24).

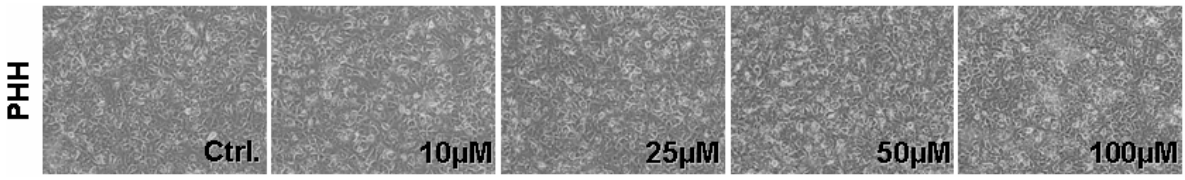

Figure 4.24 Representative phase-contrast images of primary human hepatocytes (PHH) after 24 h incubation with the indicated concentrations of xanthohumol (XN).

To further confirm this finding, PHH were detached by trypsination and stained with propidium iodide (PI), revealing no significant PI incorporation at any XN concentration up to 100 µM (Figure 4.25).

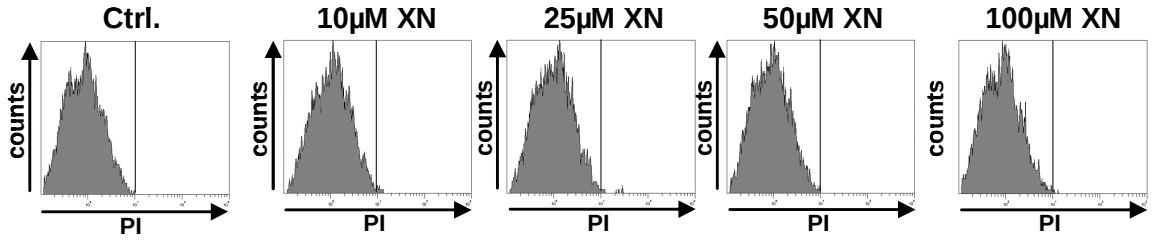

Figure 4.25 Flow cytometric analysis of propidium iodide (PI) stained PHH incubated with different XN concentrations for 24 h.

Further, no significant increase in LDH and AST levels were detected in the supernatants of PHH after incubation with XN at doses as high as 100 µM (Figure 4.26; see also chapter 4.1.3).

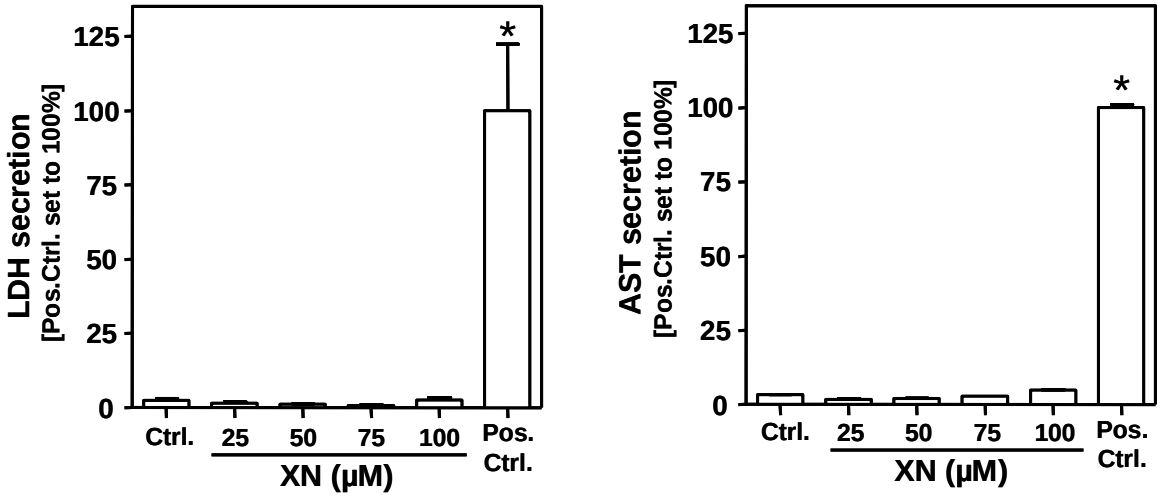

Figure 4.26 Primary human hepatocytes (PHH) were incubated with xanthohumol (XN) at the indicated concentrations for 24 h. Viability was assessed as release of LDH and AST into the supernatants. PHH treated with 5% (v/v) ethanol for 24 h served as positive control (Pos.Ctrl. set to 100%). *: $p<0.05$ compared to control.

4.2.3 Induction of apoptosis in HCC cells

To further study the underlying mechanisms leading to HCC cell death upon stimulation with XN we measured the time-dependent activation of caspase-3/7 in HepG2 cells incubated with 25 µM XN within 24 h. After 12 h incubation caspase-3/7 activity was unaltered, but 6 hours later a significant increase was observed remaining on this elevated level for at least the next 6 h (24 h stimulation time) (Figure 4.27). A similar time course of caspase-3/7 activation was observed in Huh7 cells.

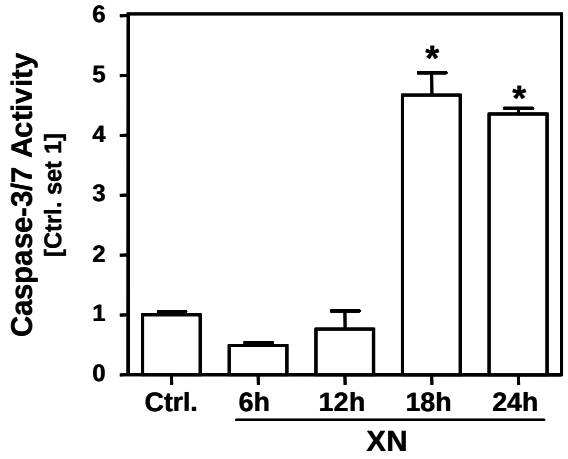

Figure 4.27 Caspase-3/7 activity in HepG2 cells stimulated with xanthohumol (XN) at a concentration of 25 µM for the time intervals indicated. *: p<0.05 compared to control.

Next, the effect of different XN concentrations on caspase-3/7 activity in Huh7 and HepG2 cells were analyzed revealing a concentration dependent increase of caspase-3/7 activity in both cell lines, reaching a maximum at 50 µM XN (Figure 4.28).

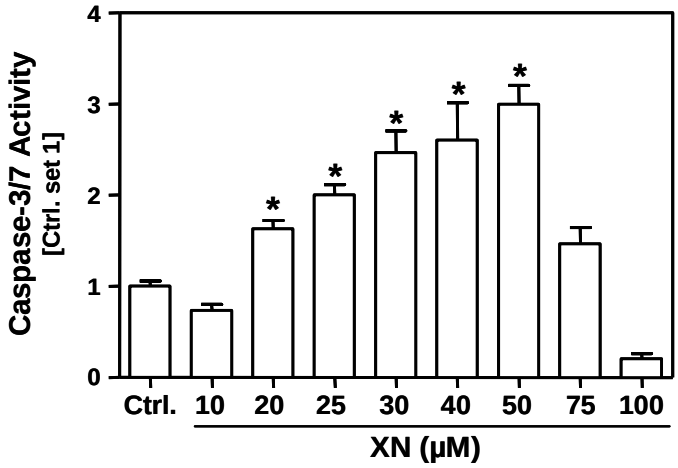

Figure 4.28 Caspase-3/7 activity in Huh7 cells stimulated for 24 h with different XN concentrations as indicated. *: p<0.05 compared to control.

At higher XN concentrations HCC cells detached, and accurate analysis of the caspase-3/7 was not possible with an ELISA based assay. To bypass this pitfall we additionally performed flow cytometric analysis, applying a FITC-labeled antibody against active caspase-3 (Figure 4.29).

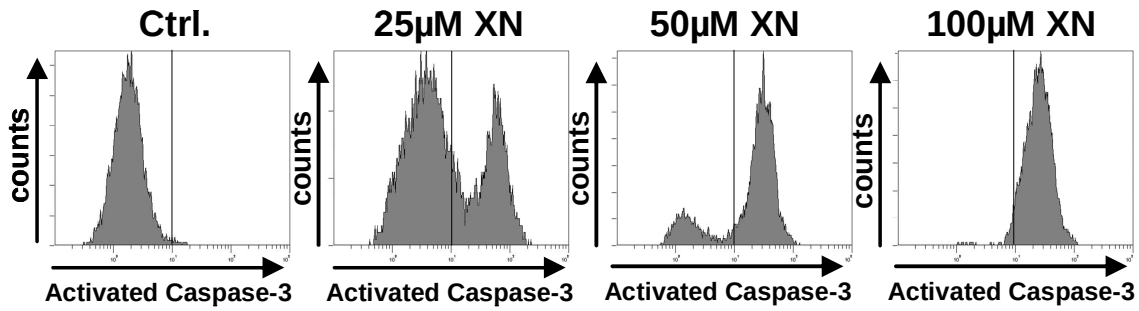

Figure 4.29 Flow cytometric analysis of caspase-3 activity in Huh7 cells after incubation with different XN concentrations for 24 h.

Here, basically all HCC cells revealed a positive signal for active caspase-3 after stimulation with 100 µM XN for 24 h (quantified in Figure 4.30).

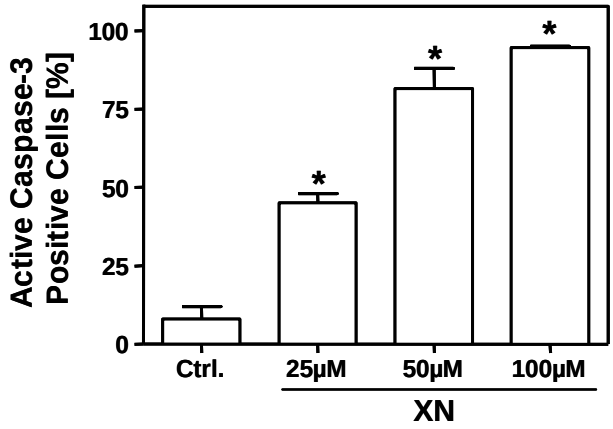

Figure 4.30 Percentage of Huh7 cells with active caspase-3 after treatment with XN at indicated concentrations for 24 h determined by flow cytometry. *: $p<0.05$ compared to control.

4.2.4 Inhibition of HCC cell proliferation and migration

To further characterize the effect of XN on HCC cells, we performed the XTT assay (see also chapter 3.9.1) with both cell lines using different XN concentrations. Proliferation was significantly inhibited after incubation with 15 µM XN, whereas concentrations higher than 30 µM completely abrogated cell proliferation in HepG2 and Huh7 (Figure 4.31) cells.

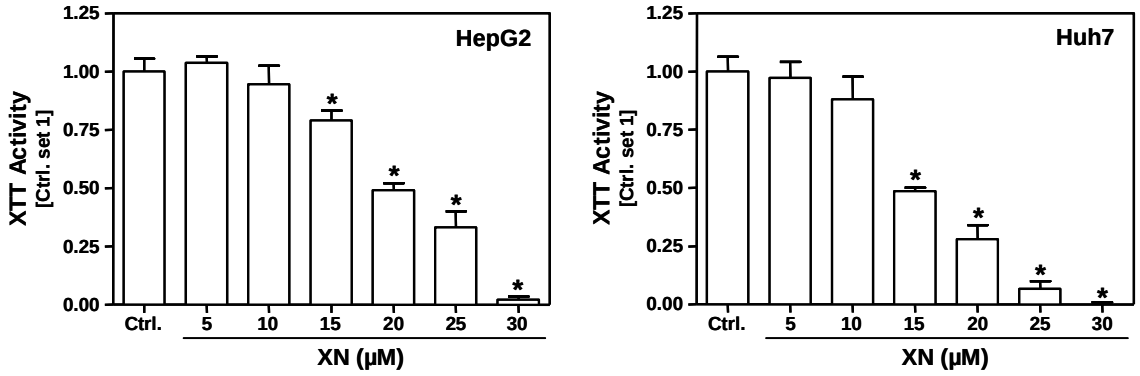

Figure 4.31 Proliferation of HepG2 and Huh7 cells 72 h after stimulation with different concentrations of xanthohumol (XN) relative to control cells (set to 1).*:p<0.05 compared to control.

Next, we analyzed whether XN affects the migration potential of HCC cells *in vitro*. For these experiments the Cultrex cell migration assay (see also chapter 3.9.2) was used and a short time span of 5 h was chosen to exclude pro-apoptotic or anti-proliferative effects of XN in the applied concentrations (10 µM or 25 µM). Noteworthy, we observed a significant inhibition of cell migration of HCC cells treated with 25 µM XN as compared to untreated control cells (Figure 4.32).

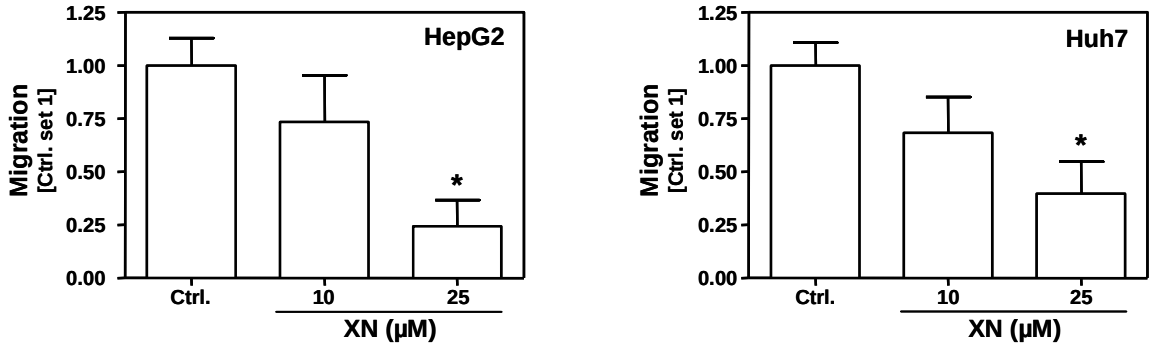

Figure 4.32 Quantification of migration of HepG2 and Huh7 cells incubated with XN (10 µM or 25 µM) in comparison to untreated control cells (set to 1). *: p<0.05 compared to control.

4.2.5 Inhibition of NFκB activation and IL-8 expression in HCC cells

XN has been shown to affect NFκB activity, and we and others have shown that NFκB plays an important role in hepatocarcinogenesis (Amann et al. 2009; Arsura and Cavin 2005; Pikarsky et al. 2004). Thus, we further analyzed the effect of XN on NFκB activity in HCC cells. To avoid potential paracrine side effects of dead HCC cells on NFκB activity we chose a not toxic XN concentration of 2.5 µM and

stimulated the cells for only 3 h. In this case, XN exhibited no effects on basal NFκB activity in both cell lines. However, TNF (10 ng/ml) induced NFκB activity was significantly blunted in XN treated Huh7 cells even at this low concentration (Figure 4.33).

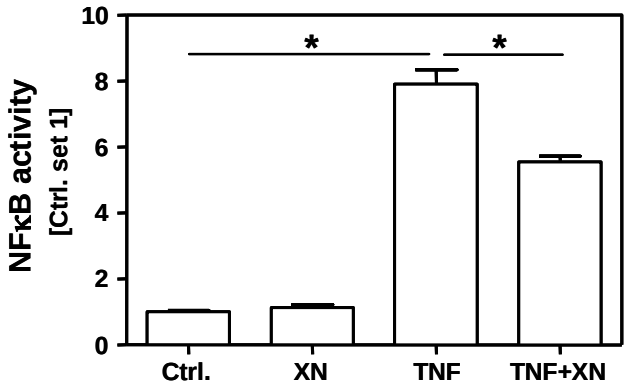

Figure 4.33 Basal and TNF induced (10 ng/ml; 15 min) NFκB activity in nuclear extracts of Huh7 cells, which were preincubated with xanthohumol (XN; 2.5 µM; 3 h), compared to control cells. *: p<0.05

Next, we analyzed the effect of XN on IL-8 expression in HCC cells, since IL-8 expression is known to be regulated by NFκB in HCC cells (Iguchi et al. 2000; Joshi-Barve et al. 2007; Kubo et al. 2005), and previous studies indicate that IL-8 is directly or indirectly involved in the progression of HCC (Kubo et al. 2005; Ren et al. 2003). In accordance with the effects on NFκB activity, basal IL-8 expression was not affected by stimulation with XN for 24 h, however, TNF induced IL-8 expression was significantly lower in Huh7 cells pre-incubated with XN as compared to controls (Figure 4.34).

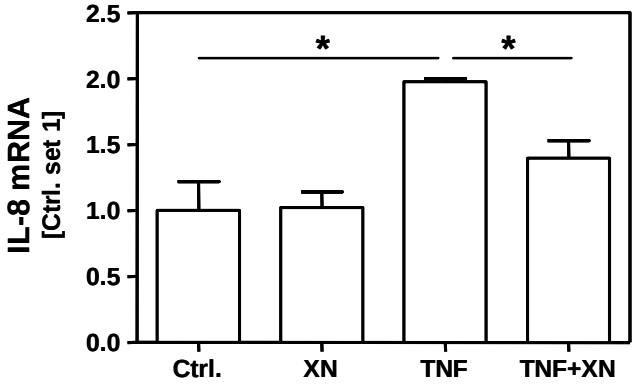

Figure 4.34 Analysis of basal and TNF (10 ng/ml for 1 h) induced IL-8 mRNA expression by qRT- PCR. *: p<0.05

4.2.6 Summary

Here, we showed that xanthohumol induced apoptosis at a concentration of 25 µM in two HCC cell lines (HepG2 and Huh7). Furthermore, xanthohumol repressed proliferation and migration, as well as TNF induced NFκB activity and interleukin-8 expression in both cell lines at even lower concentrations. In contrast, xanthohumol concentrations up to 100 µM did not affect viability of primary human hepatocytes *in vitro*, in accordance with the findings observed in chapter 4.1.

In summary, our data showed that xanthohumol can ameliorate different pro-tumorigenic mechanisms known to promote HCC progression, indicating its potential as promising therapeutic agent that selectively affects cancer cells.

4.3 Safety profile of orally applied xanthohumol

4.3.1 Motivation

So far, two long term safety studies of XN have been reported. Vanhoecke et al. applied a daily dose of approximately 35 mg XN/kg b.w. per day to mice for four weeks, and did not observe any noticeable signs of toxicity (Vanhoecke et al. 2005b). Particularly, there were no signs of hepatotoxicity and differences regarding lipid or carbohydrate metabolism. In a second study, Hussong at al. applied 1000 mg XN/kg b.w. per day by gavage to female Sprague Dawley rats for four weeks (Hussong et al. 2005). Also in this carefully performed study no remarkable treatment-related changes were observed in most organs, and importantly, there were no adverse effects on female reproduction or the development of offspring. However, in XN treated rats liver weight was reduced and histological investigation indicated a loss of hepatic glycogen, suggestive of mild hepatoxicity. Particularly with respect to long term application even weak hepatoxicity is a critical issue since it harbors the risk to progress to chronic hepatic inflammation and fibrosis (Ramachandran and Kakar 2009; Stravitz and Sanyal 2003).

However, total liver weight and glycogen content are only unspecific and vague signs of hepatotoxicity. Furthermore, based on the studies of Hussong *et al.* (Hussong et al. 2005) and Vanhoecke *et al.* (Vanhoecke et al. 2005b) it is not clear whether the different XN doses or species differences account for the differing results regarding potential hepatoxicity.

Thus, in the present study, we aimed to detect possible side effects of high dose XN (1000 mg/kg b.w. per day) chronically fed to mice with an emphasis on affection of liver function and homeostasis.

4.3.2 In-life parameters

To study potential toxic effects of orally applied xanthohumol (XN) *in vivo*, we fed mice with standard chow supplemented with 0.5% (m/m) XN for 3 weeks to achieve a daily dose of approximately 1000 mg/kg b.w. per day. Control mice received the same chow without XN supplementation. Monitoring of daily food intake (Figure 4.35**,** 3.2 ± 0.20g XN supplemented chow per mouse and day)

confirmed that we achieved this goal (average XN dose 998 ± 21 mg XN/kg b.w. per day), and daily food and herewith XN consumption, respectively, did not significantly change over time. Furthermore, food and water (Figure 4.35) intake as well as total body weight gain (Figure 4.36) did not significantly differ between XN fed and control mice.

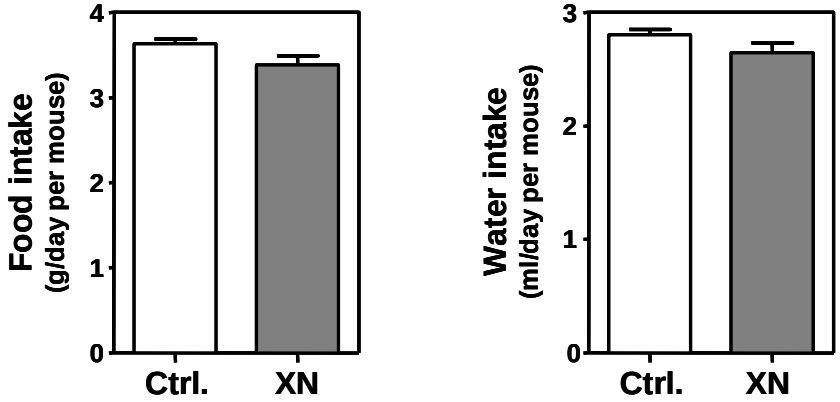

Figure 4.35 Analysis of in-life parameters during oral xanthohumol feeding. Mean daily food and water intake (per mouse) of xanthohumol treated (XN) and control (Ctrl.) mice.

Final body weights were 16.1 ± 0.7 g for control mice and 16.1 ± 1.1 g for XN fed mice.

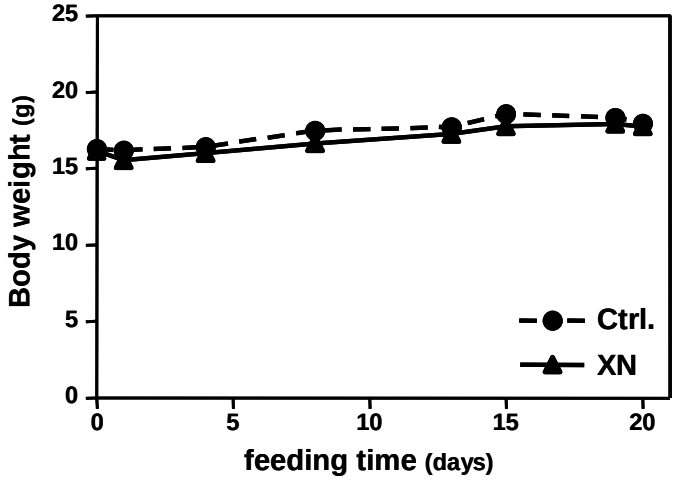

Figure 4.36 Mean total body weight during the experimental period (3 weeks) of xanthohumol treated (XN) and control (Ctrl.) mice.

Fecal excrements appeared normal in quantity, shape and consistency, solely color was more yellowish due to excreted XN. Throughout the experimental period no obvious clinical symptoms or deaths were observed.

4.3.3 Effects on function and homeostasis of inner organs

Mice were sacrificed after 3 weeks of feeding and investigated for anomalies. Blood was collected and inner organs were explanted for further investigation. Relative size of lung, heart, thymus, spleen, and kidney was not affected by XN, and neither macroscopical nor microscopical analysis revealed abnormalities or signs of toxicity caused by XN feeding (Figure 4.37).

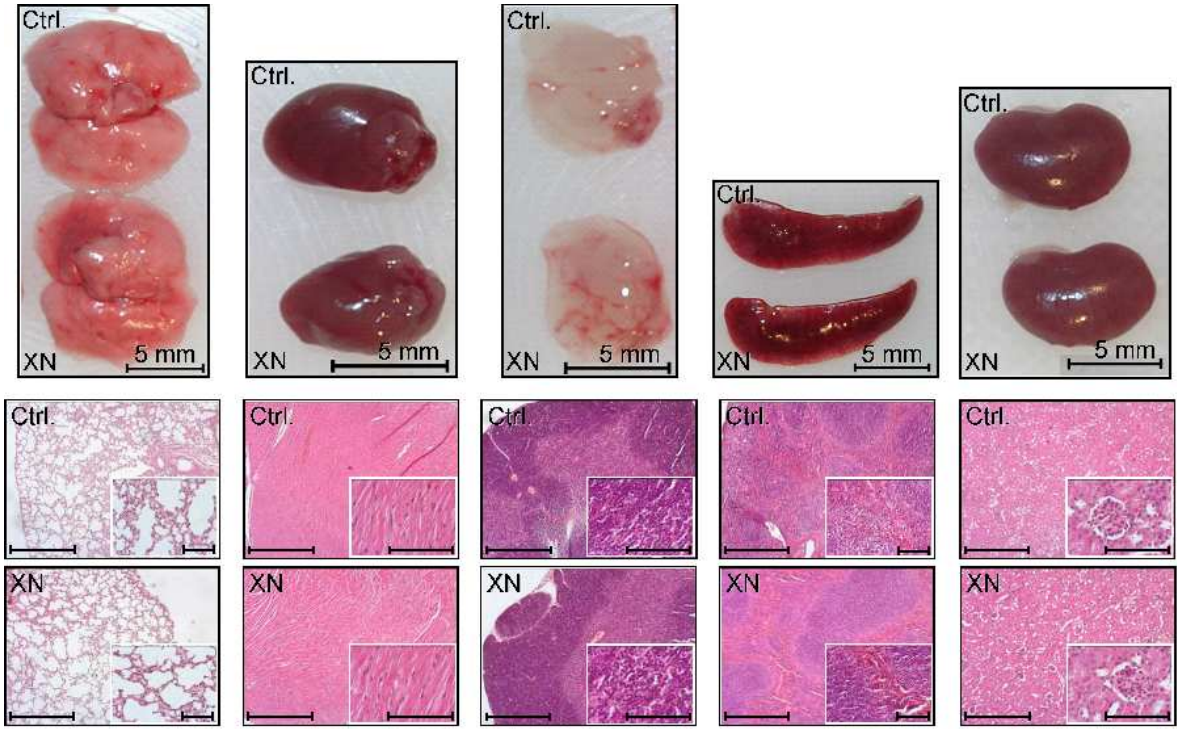

Figure 4.37 Representative photographs of lung, heart, thymus, spleen, kidney (from left to right) and corresponding histological pictures of sections of the according organs of xanthohumol treated (XN) and control (Ctrl.) mice (H&E Staining; bars indicate 500 µm and 100 µm in the insert, respectively).

Further, also the colon appeared normal (Figure 4.38), and colon length did not differ between groups (control: 9.3 ± 0.87 cm *vs.* XN: 8.53 ± 0.52 cm; p = 0.094).

Figure 4.38 Macroscopical and histological pictures of the colon of xanthohumol treated (XN) and control (Ctrl.) mice (H&E Staining; bars represent 100 µm).

To further detect potential intestinal toxicity of XN we measured bacterial endotoxin concentration in the serum as a marker for gut barrier dysfunction. Endotoxin levels in both groups were low and did not differ significantly between XN treated and control mice (Figure 4.39).

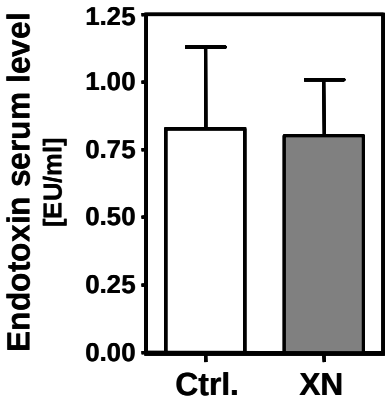

Figure 4.39 Endotoxin serum levels of xanthohumol treated (XN) and control (Ctrl.) mice assessed by limulus amebocyte lysate assay.

Due to the difficult explantation and histological processing of the pancreas, we decided to assess lipase activity in the serum as a marker for potential toxicity in the exocrine pancreas. Also here, no significant differences were found between groups (Table 4.1). Further, blood creatinine and urea nitrogen serum concentrations indicated an intact kidney function in both groups. Sodium and potassium as well as total protein concentrations in the serum were found to be unaffected by XN treatment as well (Table 4.1).

Table 4.1: Serum analysis of control and xanthohumol (XN) treated mice (mean ± stdv).

Parameter	control	XN	p-value
creatinine (mg/dL)	0.24 ± 0.04	0.26 ± 0.05	0.532
lipase (U/l)	44 ± 11	41 ± 14	0.732
potassium (mmol/l)	6.8 ± 2.0	5.6 ± 0.9	0.300
sodium (mmol/l)	154.4 ± 5.4	154 ± 5.2	0.913
total protein (g/l)	46.8 ± 4.1	43.5 ± 2.1	0.189
urea nitrogen (mg/dl)	26.5 ± 6.7	26.1 ± 5.5	0.931

4.3.4 Effects on liver function and homeostasis

Next to the gut the liver is generally exposed to highest doses of food derived compounds due to the direct blood transport from the gut via the portal vein. Furthermore, *in vitro* studies using liver microsomes indicate that the liver is a major site of XN biotransformation (Nikolic et al. 2005; Yilmazer et al. 2001a; Yilmazer et al. 2001b). Thus, we put emphasis on the identification of potential side effects of oral XN administration on the liver.

After 3 weeks neither absolute liver weight nor liver to body weight ratio differed significantly between XN treated and control mice (Figure 4.40).

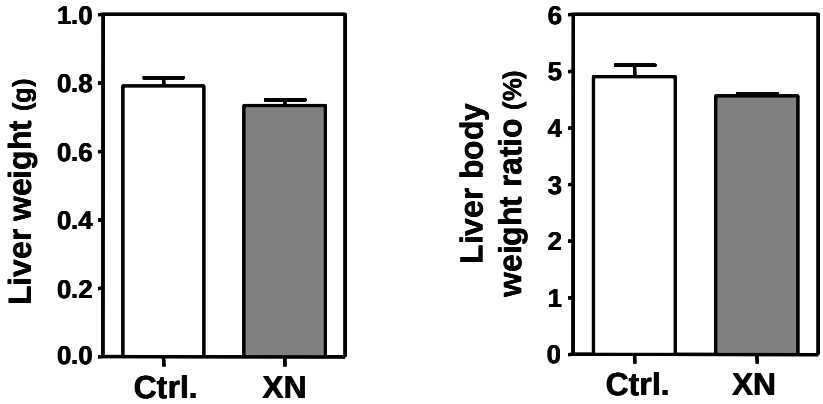

Figure 4.40 Absolute liver weight and liver-body-weight-ratio of xanthohumol treated (XN) and control (Ctrl.) mice after 3 weeks.

In line with these findings, macroscopical examination of the livers revealed no signs of hepatotoxicity (Figure 4.41).

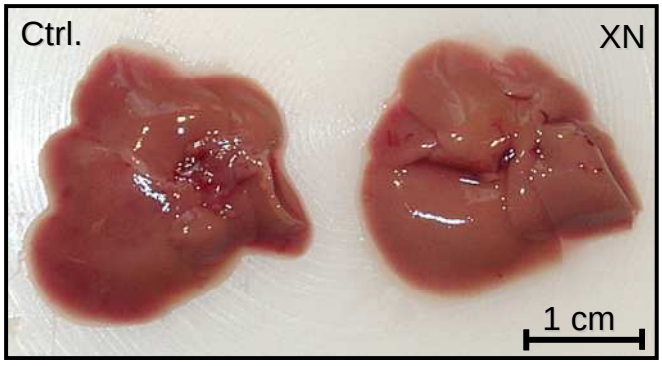

Figure 4.41 Representative photographs of the whole liver of xanthohumol treated (XN) and control (Ctrl.) mice.

Furthermore, no pathological changes were observed in histological investigation (Figure 4.42).

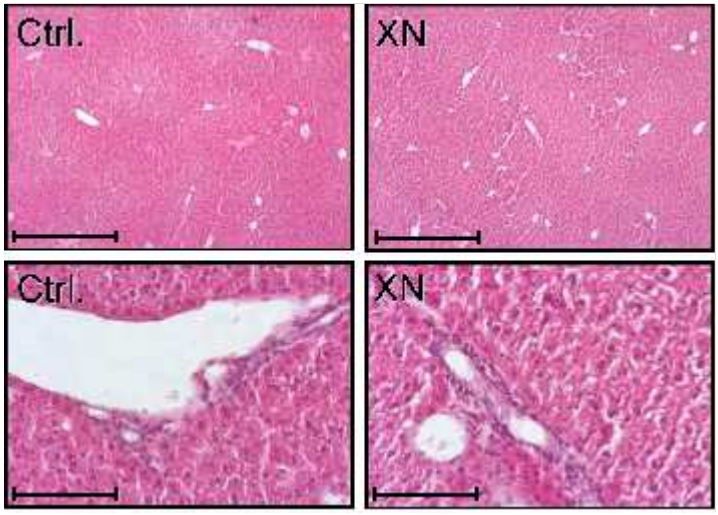

Figure 4.42 Histological analysis of hepatic tissue sections (H&E staining; bars represent 500 µm in the upper and 100 µm in the lower row) of xanthohumol treated (XN) and control (Ctrl.) mice.

Next, we performed biochemical analysis of serum parameters indicative of liver damage and hepatic synthesis capacity. Alanine and aspartate aminotransferase (ALT, AST) as well as albumin serum levels were similar in XN treated and control mice (Table 4.2).

Table 4.2: Liver relevant serum biochemistry of control and XN treated mice (mean ± stdv).

Parameter	control	XN	p-value
ALT (U/l)	43.2 ± 12.1	41.1 ± 11.5	0.790
AST (U/l)	222 ± 116	177 ± 62	0.507
albumin (g/l)	30.6 ± 2.9	27.5 ± 1.7	0.102
glucose (mg/dL)	230 ± 66	255 ± 50	0.613

Also glucose serum levels (Table 4.2) as well as hepatic glycogen content (Figure 4.43) revealed no differences between groups, further indicating an unimpaired liver function and carbohydrate metabolism, respectively, during XN treatment.

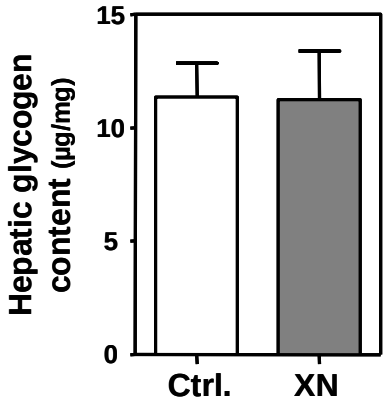

Figure 4.43 Analysis of hepatic glycogen content of xanthohumol treated (XN) and control (Ctrl.) mice.

In addition, we analyzed CYP2E1 mRNA expression since it is known to be regulated on the transcriptional level in response to xenobiotics as well as under conditions of hepatic inflammation or metabolic and endocrine disorders (Gonzalez 2007; Ioannides 2008). Consistent with our other findings, hepatic CYP2E1 mRNA expression was not affected in XN fed mice (Figure 4.44).

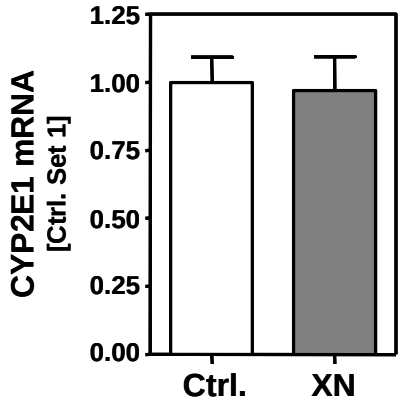

Figure 4.44 CYP2E1 mRNA expression of xanthohumol treated (XN) and control (Ctrl.) mice (control arbitrarily set to 1).

Furthermore, we analyzed the expression of genes known to be increased during liver inflammation. TNF and IL-1α are well-known markers for inflammation, the chemokine MCP-1 and the adhesion molecule ICAM-1 are responsible for infiltration of inflammatory cells into the liver, while p47phox is a subunit of neutrophil NADPH oxidase, which functions a generator of ROS in response to inflammatory stimuli. In addition, we measured hepatic collagen type I (coll-I) and TGF-β mRNA expression as early markers of liver fibrosis, a hallmark of chronic hepatic injury. None of these genes showed different mRNA expression levels in XN treated and control mice (Table 4.3).

Table 4.3: Hepatic mRNA expression levels of genes indicative for liver inflammation and fibrosis (mean ± stdv; control arbitrarily set to 1)

Gene	control	XN	p-value
TNF	1.0 ± 0.32	1.09 ± 0.60	0.771
IL-1α	1.0 ± 0.30	0.69 ± 0.36	0.142
MCP-1	1.0 ± 0.85	0.95 ± 0.41	0.903
ICAM-1	1.0 ± 0.29	1.12 ± 0.23	0.443
p47phox	1.0 ± 0.35	1.12 ± 0.07	0.421
coll-I	1.0 ± 0.20	0.97 ± 0.28	0.851
TGF-β	1.0 ± 0.23	1.04 ± 0.22	0.797

4.3.5 Comparison of cytotoxicity in murine and human hepatocytes *in vitro*

In preliminary analyses we compared the effect of XN on cell viability of murine and human primary hepatocytes (PMH and PHH, respectively*) in vitro*.

We found significantly increased LDH and AST levels in the supernatant of cultured PMH at concentrations as low as 50 µM XN (Figure 4.45), whereas PHH revealed no significant increase even at concentrations as high as 100 µM XN (see Figure 4.26 and see also results presented in the previous chapter 4.1.3).

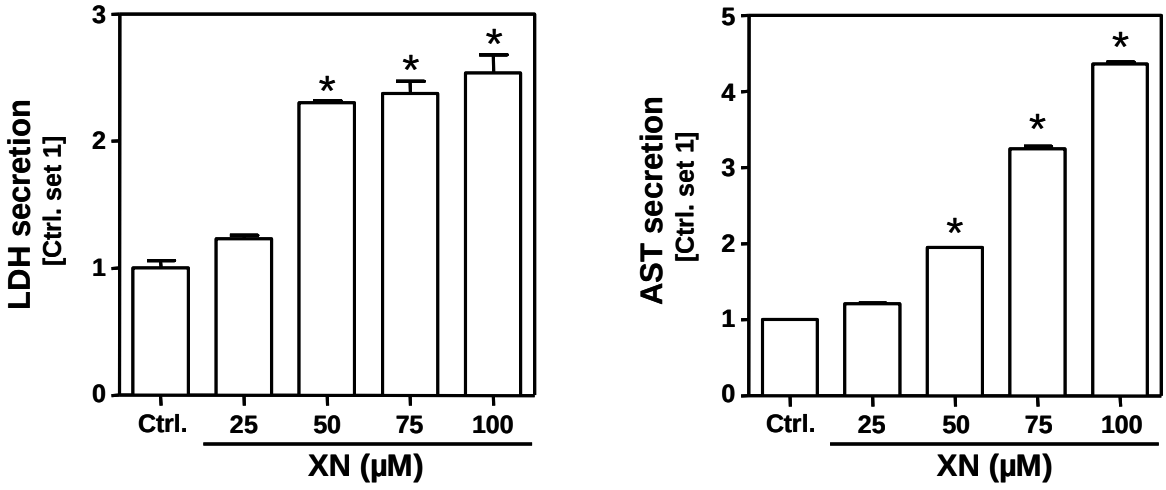

Figure 4.45 Primary murine hepatocytes (PMH) were incubated with xanthohumol (XN) at the indicated concentrations for 24 h. Viability was assessed as release of LDH and AST into the supernatants. *: $p<0.05$ compared to control.

4.3.6 Summary

Here, we fed female BALB/c mice with a standard diet supplemented with xanthohumol for three weeks and achieved a daily dose of approximately 1000 mg xanthohumol /kg body weight per day. There were no significant differences in body weight or food intake between xanthohumol-treated and control mice (that received pure standard diet). Macroscopical and histopathological examination of liver, kidney, colon, lung, heart, spleen and thymus revealed no signs of xanthohumol-toxicity, and biochemical serum analysis confirmed normal organ function. Further, serum glucose levels and hepatic glycogen content as well as hepatic CYP2E1 mRNA expression levels were unaffected by xanthohumol treatment. Also mRNA expression of several genes indicative of early hepatic inflammation and fibrosis, a hallmark of chronic liver injury, did not differ between xanthohumol treated and control mice. In summary, these results indicate that oral administration of xanthohumol exhibits no adverse effects on major organ function and homeostasis in mice. Particularly, hepatotoxic effects of xanthohumol could be ruled out confirming a good safety profile of xanthohumol as basis for further studies in humans.

Although *in vitro* data are only preliminary and *in vitro* data can not be fully transferred to the *in vivo* situation, the difference of murine and human hepatocytes regarding XN-mediated cytotoxic effects points to an at least 2-fold higher sensitivity of PMH compared to PHH. Thus, it may be speculated that the range of safe XN application with regards to hepatoxicity is even higher than 1000 mg XN/kg body weight per day in humans.

5 Discussion

Xanthohumol (XN) exhibits several biological effects (see chapter 2.4), however, with regards to effects on liver cells or liver diseases, respectively, only few data were available (see also chapter 2.6). The central aim of this thesis was to address this issue. In particular, we analyzed the effects of XN on hepatic inflammation and fibrosis (see chapter 4.1) as well as on hepatocellular carcinoma (HCC) cells (see chapter 4.2). Further, we assessed the safety profile of XN *in vivo* by feeding high doses of XN to BALB/c mice (see chapter 4.3).

In the following, the discussion is divided into three main chapters apposite to the arrangement of the results in chapter 4:

5.1 Xanthohumol and hepatic inflammation and fibrosis
5.2 Xanthohumol and hepatocellular carcinoma
5.3 Safety profile of xanthohumol

5.1 Xanthohumol and hepatic inflammation and fibrosis

The first aim of this thesis was to analyze the effects of XN on hepatic inflammation and fibrosis. After *in vitro* experiments with primary human liver cells we also assessed *in vivo* data using a murine NASH model.

5.1.1 *In vitro* effects of xanthohumol on primary human liver cells

Different pathophysiological mechanisms relevant for liver inflammation and fibrosis have been affected in HSC *in vitro*. Thus, HSC activation was inhibited while apoptosis of activated HSC was induced at XN concentrations as low as 5 µM. In contrast and importantly, 20-fold higher XN concentrations (100 µM) did not induce cytotoxic effects in primary human hepatocytes (PHH) *in vitro* (see also chapter 4.2.2). Moreover, XN inhibited MCP-1 and IL-8 expression in HSC and PHH, respectively. Both chemokines are regulated by NFκB and increased levels

are associated with more severe liver inflammation and fibrosis progression in NASH (Haukeland et al. 2006; Jarrar et al. 2008). Further, NFκB activation is a central pathophysiological mechanism during HSC activation (Elsharkawy et al. 2005; Hellerbrand et al. 1998a; Hellerbrand et al. 1998b), and importantly, XN inhibited basal as well as cytokine induced NFκB activity in HSC *in vitro*.

5.1.2 *In vivo* effects of xanthohumol in a murine NASH model

Based on these *in vitro* findings and the recently reported potential of XN to ameliorate metabolic disorders (Casaschi et al. 2004; Nozawa 2005; Tabata et al. 1997; Yang et al. 2007), we decided to apply an experimental NASH model to test the effect of XN on hepatic fibrogenesis *in vivo*. However, murine NASH models that do lead to hepatic fibrosis are limited (Anstee and Goldin 2006). To screen the therapeutic efficacy of XN *in vivo* we applied a dietary model (Paigen-diet, see also chapter 2.7.5.5.5) that has been recently shown to induce the pathology of steatohepatitis with HSC activation and finally caused precirrhotic steatohepatitis (Matsuzawa et al. 2007). Additional feeding of XN reduced levels of serum transaminases and hepatic expression of proinflammatory genes compared to mice fed only with the NASH inducing Paigen-diet. Moreover, XN treatment significantly inhibited hepatic expression of profibrogenic genes and activation of HSC *in vivo*. Finally, it has to be noted that the liver body weight ratio, a well known surrogate marker for hepatic steatosis and fibrosis, was almost completely normalized in XN-fed mice in comparison to mice fed with the NASH inducing Paigen-diet.

It is known that steatosis is mainly caused by cholesterol in this model (Matsuzawa et al. 2007; Vergnes et al. 2003) and that cholesterol induced oxidative stress is responsible for hepatic inflammation and NFκB activation (Matsuzawa et al. 2007; Vergnes et al. 2003; Wouters et al. 2008). In line with this, we found a significant increase of hepatic cholesterol levels in mice fed this diet but this increase was not affected by the addition of XN to the NASH diet. In a previous study hepatic cholesterol levels showed a lowered trend in XN-fed KK-A^y mice, a model for obesity and type 2 diabetes (Nozawa 2005). Further, feeding XN induced hepatic CYP7A1 expression (Nozawa 2005). CYP7A1 a.k.a. cholesterol-7α-hydroxylase catalyzes the initial step in cholesterol catabolism and bile acid synthesis.

However, the bile acid cholic acid, a main constituent of the Paigen-diet, strongly represses hepatic CYP7A1 expression (Watanabe et al. 2004), and it has been shown that cholic acid is necessary to induce profibrogenic gene expression in this model (Vergnes et al. 2003). Therefore, we speculate that the latter mechanism makes the effect of XN on hepatic cholesterol ineffective. However and strikingly, despite the fact that steatosis is not affected by XN in this model, hepatic inflammation, and even more importantly, HSC activation and profibrogenic gene expression were almost completely blunted in mice fed XN. Thus one may hypothesize that XN has therapeutic efficacy also in not steatosis-related liver injury.

5.1.3 Xanthohumol as a therapeutic agent for chronic liver diseases

Beer is the major dietary source of XN, but the average content of XN in beer is not high enough to produce a protective effect in humans. XN levels in beer are very low (approximately 0.1-1 mg/l) depending on the type of beer. Lager and pilsener beers have fairly low levels of this compound and highest levels are found in stout or porter (Stevens et al. 1999). Further, a brewing process has been developed that produces a beer that contains 10 times the amount of XN as traditional brews (Wunderlich et al. 2005). Still, a person would have to drink more than 10,000 liters of beer per day to consume the same amount of XN as applied in the present animal study. Regardless, there is certainly unanimous hesitancy among researchers to recommend drinking alcohol to avoid any kind of disease because of the fine line between moderate and binge drinking. Certainly, this is even more true in case of chronic liver disease. However, XN can be isolated from hops in large quantities and examined further for its use as a dietary supplement for prevention of NASH. Still, caution has to be taken that more research is needed before it is known whether the findings of the present study can be applied to humans. Our and other animal toxicity studies (see chapters 4.3 and 5.3) and our *in vitro* experiments using human liver cells (see chapters 4.1.3 and 4.2.2) provide evidence that XN may not be harmful to humans, but further safety and efficacy studies *in vivo* are required before XN can be recommended as a human dietary supplement for the treatment or the prevention of liver disease. However,

the present study indicates the potential of XN as a functional nutrition to ameliorate inflammation and fibrosis in chronic liver disease.

5.2 Xanthohumol and hepatocellular carcinoma

Hepatocellular cancer (HCC) develops in most cases on the basis of a fibrotic liver caused by chronic hepatic inflammation (see also chapter 2.7.4.1). Ameliorating hepatic inflammation and fibrosis *per se* may be beneficial for preventing development of HCC. However, considering the numerous reports of XN-mediated effects on various cancer cell types (Colgate et al. 2007; Delmulle et al. 2006; Goto et al. 2005; Miranda et al. 1999; Pan et al. 2005; Vanhoecke et al. 2005a), also direct effects of XN on HCC cells may be hypothesized, thus, indicating the potential to use this natural occurring chalcone for HCC prevention as well as for treatment of already established HCC.

The second aim of this thesis was to analyze the effects of XN on viability and function of HCC cells.

5.2.1 Effects of xanthohumol on HCC cell viability

We observed significant cell death in HCC cells (HepG2 and Huh7) upon stimulation with XN at a concentration of 25 µM, and analysis of the time course of caspase-3/7 activation indicated that XN induced cell death is caused by apoptosis rather than other cytotoxic effects at this concentration, while XN concentration higher than 50 µM led to a rapid and almost complete detachment of HCC cells *in vitro*. XN induced cell death has been described in cell lines derived from various cancers at similar concentrations as observed in the present study (Colgate et al. 2007; Lee et al. 2007; Lust et al. 2005; Miranda et al. 1999; Monteiro et al. 2007; Pan et al. 2005). Thus, stimulation of prostate cancer cells with 20 µM XN resulted in an approximately halved viability (Colgate et al. 2007), and a XN concentration of 100 µM induced 100% cell death in breast cancer cells (Miranda et al. 1999). Recently, Ho et al. reported that XN induced apoptosis in two HCC cell lines *in vitro* (Ho et al. 2008). However, in this study considerably higher XN concentrations (> 200 µM) were required to induce death of all HCC cells. One

reason for this discrepancy might be the different HCC cell lines used (HA22T and Hep3B in the study of Ho *et al.*, versus HepG2 and Huh7 cells in our experiments). Furthermore, Ho *et al.* used a hop extract containing 95.7% XN for their studies. Thus, confounding antagonizing effects of concomitant secondary hop constituents can not be excluded.

5.2.2 Functional effects of xanthohumol on HCC cells

In addition to viability, we analyzed functional effects of XN on HCC cells. Previous reports revealed an anti-proliferative effect of XN on prostate cancer, breast cancer, colon cancer and leukaemia cells (Dell'Eva et al. 2007; Delmulle et al. 2006; Pan et al. 2005; Vanhoecke et al. 2005a). However, we are the first reporting a growth inhibitory effect of XN on HCC cells at concentrations as low as 15 µM. Most likely the analysis of anti-proliferative effects of XN is overlapped by its pro-apoptotic and cytotoxic effects. However, our dose-response studies clearly indicate that the significant anti-proliferative effect of XN observed already in the low concentration range can not be exclusively explained by these confounding mechanisms of XN action.

Of note, we further revealed that XN inhibits the migratory potential of HCC cells *in vitro*. A higher migration potential in cancer cells is associated with an increased tendency for metastasis, and therefore, with higher malignancy. Also for migration studies we chose conditions excluding that the observed effects of XN are only explained by confounding mechanisms on cell viability. To the best of our knowledge, an effect of XN on the migratory potential of cancerous cells has not been described in previous reports.

5.2.3 Effects on NFκB activity and IL-8 expression in HCC cells

Furthermore, we demonstrated that XN inhibits TNF induced NFκB activity in HCC cells *in vitro*, a situation that reflects the *in vivo* situation since HCC almost exclusively develops and progresses on the basis of chronic liver inflammation (Pikarsky et al. 2004).

The transcriptional factor NFκB plays a key role in regulating immune responses and cell survival. Incorrect regulation of NFκB has been linked to cancer and inflammation. Increased NFκB activity is a common strategy of cancer cells to evade apoptosis, and further, has been shown to promote proliferation as well as migration of tumorous cells including HCC cells (Amann et al. 2009; Salvi et al. 2009; Shen and Tergaonkar 2009; Shirouzu et al. 2008; Zhang et al. 2009). Thus, potential NFκB inhibitors like XN may have beneficial effects in cancer treatment and prevention (Shen and Tergaonkar 2009). XN is known to decrease NFκB activity in various cancer cell types *in vitro* (Albini et al. 2006; Colgate et al. 2007), but until now, data concerning NFκB regulating effects of XN in HCC cells were missing.

In our experiments it was critical to exclude unspecific effects (e.g. paracrine effects caused by dying/dead cells), thus we applied XN at a very low dose (2.5 µM). XN exhibited no effects on basal NFκB activity, but significantly blunted TNF induced NFκB activity in XN treated HCC cells.

TNF and other members of the TNF superfamily are known to be capable of inducing cell death via death receptor mediated apoptosis pathways in tumor cells, and thus, appear attractive for cancer treatment (Van Horssen et al. 2006). However, one of the major obstacles regarding their therapeutic application is the adaptive resistance due to activation of the NFκB pathway (Bertazza and Mocellin 2008; Falschlehner et al. 2007). Therefore, suppression of NFκB appears as potential approach in overcoming the resistance to TNF induced apoptosis.

Furthermore, NFκB regulates the expression of the pro-inflammatory chemokine IL-8 in HCC cells (Dong et al. 2001; Joshi-Barve et al. 2007), and previous studies have shown that IL-8 promotes the progression of HCC (Kubo et al. 2005; Ren et al. 2003). Here, we could detect a significant attenuation of TNF induced increase of IL-8 mRNA expression by treatment with XN, which may be beneficial in HCC treatment.

Together, these data indicate the potential of XN as a therapeutic agent for HCC treatment. Moreover, the shown pro-apoptotic, anti-proliferative, anti-migrational and anti-inflammatory effects of XN in HCC cells may work together synergistically with other reported effects of XN, *e.g.* the reactive oxygen species (ROS)

scavenging properties of XN (Gerhäuser et al. 2002). ROS related signals may play important roles in the development of HCC (Tien and Savaraj 2006). In addition, ROS mediated induction of resistance gene expression, a major problem in cancer treatment, has been discussed (Tien and Savaraj 2006). ROS scavenging by XN could suppress these processes. Moreover, Lee et al. could demonstrate that XN clearly decreases the mRNA levels of the drug efflux genes ABCB1 (MDR1), ABCC1 (MRP1), ABCC2 (MRP2), and ABCC3 (MRP3) in lung cancer cells, which are known to be responsible for drug resistances (Lee et al. 2007). Hence, aside from the direct anti-cancerous effect of XN, a conjunction of XN with other anticancer chemotherapeutic agents could be a promising strategy to reduce drug resistances in cancer treatment.

Furthermore, inhibitory effects of XN on protein expression of the inducible nitric oxide synthase (iNOS), and suppression of cyclooxygenase (COX) activity were reported (Gerhäuser et al. 2002; Zhao et al. 2003). Both iNOS and COX are linked to inflammation as well as to carcinogenesis and angiogenesis. Interestingly, a study by Calvisi et al. indicates that the crosstalk between inducible nitric oxide synthase (iNOS) and NFκB cascades promotes HCC progression (Calvisi et al. 2008), and Amann et al. could demonstrate that suppression of iNOS signaling in HCC cells attenuates pro-migrational effects of factors derived from activated hepatic stellate cells (Amann et al. 2009).

5.2.4 Effects of xanthohumol on non-malignant cells

Very few studies have addressed the important question whether XN exhibits (unwanted) effects on healthy tissue or non-tumorous cells, respectively. Yang et al. described loss of viability in approximately 90% of 3T3-L1 cells, a murine adipocyte cell line, after 24 h treatment with 75 µM XN (Yang et al. 2007). In the (non-malignant) murine hepatoma cell line AML12 the maximal applied concentration of 225 µM XN (24 h) induced toxicity in approximately 50% of cells as reported by Ho et al. (Ho et al. 2008). However, to the best of our knowledge, no data have been reported concerning the effect of XN on primary human cells. In the present study we analyzed the effect of XN on the viability of primary human hepatocytes (PHH). Noteworthy, we found that viability of PHH was not affected after 24 h stimulation with a XN concentration as high as 100 µM.

5.2.5 Xanthohumol as therapeutic agent for HCC treatment

These data further promote the use of XN as anti-cancer therapeutic, and first insights regarding bioavailability and metabolism of flavonoids and polyphenols suggest that particularly HCC appears as predestined cancer for oral XN treatment. Metabolism of flavonoids is rather complex and depends on the structure, the dose and the matrix, but there is evidence that several congeners reach (to a certain extend) the small intestine unchanged (Spencer 2003), where absorption into the mesenteric circulation takes place. Accordingly, it can be presumed that upon oral administration of XN hepatocytes as well as HCC cells are exposed to intact XN reaching the liver via portal circulation after absorption. In general, metabolism of most xenobiotics takes place mainly in hepatocytes, and it has been already shown that XN is effectively metabolized by rat and human liver microsomes *in vitro* (Nikolic et al. 2005; Yilmazer et al. 2001a; Yilmazer et al. 2001b). These studies suggest that XN is probably completely metabolized in the liver, and therefore, it may be predicted that circulating plasma concentrations won't reach potentially effective levels for most other cancers if XN is administered orally.

In vivo studies in mice and rats (Hussong et al. 2005; Vanhoecke et al. 2005b) as well as our *in vitro* experiments using human hepatocytes indicate a very good safety profile of XN. Still, further safety and efficacy studies are required to evaluate the suitability of XN as a therapeutic agent for HCC (see next chapter).

However, the demonstrated pro-apoptotic, anti-proliferative, anti-migratory and anti-inflammatory effects of XN on HCC cells *in vitro* may act synergistically also *in vivo*, and herewith, XN appears as attractive and promising therapeutic agent for this highly aggressive tumor.

5.3 Safety profile of xanthohumol

There is a rising interest in the beneficial effects of natural compounds on various complaints and diseases. Especially the large group of polyphenols has received much attention. However, potential side effects of these compounds have to be identified before considering them as potential therapeutic agents.

The third aim of this thesis was to assess a safety profile of orally applied xanthohumol *in vivo*. For this purpose we fed BALB/c mice with high doses of xanthohumol for 3 weeks.

5.3.1 Previously performed safety studies

Xanthohumol (XN), the principle prenylflavonoid found in hops, has been shown to possess a variety of beneficial effects (Gerhäuser 2005a; Gerhäuser 2005b; Gerhäuser et al. 2002; Stevens and Page 2004; Zanoli and Zavatti 2008) (see also chapter 2.4), and previous studies revealed a maximal tolerable dose of more than 1000 mg XN/kg b.w. in rats. Two safety studies of chronic oral XN application in mice and rats, respectively, confirmed the absence of toxicity or remarkable treatment-related changes with one exception: In the study of Hussong et al. feeding of 1000 mg XN/kg b.w. per day for 4 weeks led to a reduction of total liver weight and a reduced hepatic glycogen content as assessed by histological investigation. The authors interpreted these findings as suggestive of mild hepatoxicity (Hussong et al. 2005). In contrast, the other safety study by Vanhoecke et al. did not reveal any signs of hepatoxicity but has been performed in mice and with a lower dose (approximately 35 mg/kg b.w. per day) (Vanhoecke et al. 2005b). Thus, in the present study we fed mice for three weeks with a XN enriched diet to achieve a daily XN dose of approximately 1000 mg/kg b.w., and studied possible side effects with a focus on the affection of liver function and homeostasis.

5.3.2 Effects of xanthohumol on inner organs

Macroscopical, histological and serum analysis revealed no toxic effects or abnormalities in inner organs including lung, heart, thymus, spleen, kidney and colon in XN treated animals. These findings are in line with all previous *in vivo* studies, but this report is the first that analyzed chronic application of such a high dose of XN in mice. Lipase activity as a marker for potential toxicity in the exocrine pancreas did not differ between XN fed mice and controls. Blood urea nitrogen and creatinine concentrations suggested an intact kidney function. Together with the unaltered albumin serum levels this data indicate an unchanged glomerular filtration rate. Normal sodium and potassium as well as total protein serum levels, respectively, further confirmed normal organ function after XN treatment.

Little is known about bioavailability and metabolism of XN *in vivo*. In general, the extent of dietary polyphenol absorption in the small intestine is rather limited (10-20%) (Kuhnle et al. 2000; Spencer et al. 1999), thereby implying that a large proportion reaches the colon. Here, we didn't find any signs of XN induced toxicity on the colon. Microscopic sections revealed normal colonic tissue structure, excrements appeared normal except for the yellowish color caused by excreted XN and colon length, a gross marker for colitis, did not differ between XN treated and control mice. Additionally, low serum endotoxin levels in both groups indicate an intact barrier function of the gut.

5.3.3 Effects of xanthohumol on liver function

Another organ which has to confront relatively high concentrations of orally applied XN is the liver. The part of ingested XN, which is absorbed in the small intestine, is pooled in the portal vein blood, which then reaches the liver unfiltered and undiluted. As already mentioned in chapter 5.2.5, it has been shown that XN is effectively metabolized by rat and human liver microsomes *in vitro* (Nikolic et al. 2005; Yilmazer et al. 2001a; Yilmazer et al. 2001b). Therefore, XN is probably completely metabolized in the liver and plasma concentrations presumably won't reach high levels, which is a well-known phenomenon for many other polyphenolic compounds (Scalbert and Williamson 2000). However, an accumulation of XN in hepatocytes could be speculated. For silibinin, a polyphenolic compound from the

milk thistle, known for its hepatoprotective effects, Singh et al. could show that after 5 weeks of feeding the highest concentration of silibinin were detected in the liver (Singh et al. 2002), thus confirming the rationality of the long-established application in this particular organ (Comelli et al. 2007).
Possible accumulation of XN in the liver, a high hepatic metabolism rate resulting in possibly active metabolites and potential therapeutic approaches to treat liver diseases with XN show the importance of identifying any adverse side effects of XN on the liver.

In the present study neither macroscopic, morphometric, histological nor biochemical analysis revealed any signs of hepatoxicity in XN treated mice. Albumin and glucose levels remained unaffected by XN feeding, and transaminase serum levels (ALT and AST) were not elevated. Further, mRNA expression levels of several genes known to be involved in early hepatic inflammation or fibrogenesis were not affected by XN application. TNF (tumor necrosis factor) and IL-1α (interleukin-1 *alpha*) are well-known markers for inflammation, the NFκB regulated proteins MCP-1 (monocyte chemoattractant protein-1) and ICAM-1 (inter-cellular adhesion molecule-1) are responsible for infiltration of inflammatory cells into the liver and p47phox is a subunit of neutrophil NADPH oxidase, which functions as a generator of ROS in response to inflammatory stimuli (*oxidative burst*). No changes in mRNA expression levels of any of these genes could be detected after XN treatment. Also coll-1 (collagen type 1) and TGF-β (transforming growth factor *beta*) mRNA expression levels, sensitive markers for beginning fibrogenesis, did not differ between XN treated and control mice. Keeping in mind that mRNA expression is a sensitive marker for even slight hepatic affection, hepatic injury appears very unlikely even after longer periods of XN intake.

Moreover, quantitative assessment of hepatic glycogen content as well as hepatic CYP2E1 mRNA expression revealed no difference between XN treated and control mice. CYP2E1 expression is known to be regulated on the transcriptional level in response to various xenobiotics, but also to inflammatory diseases and metabolic and nutritional disorders like diabetes, obesity and non alcoholic steatohepatitis (Cederbaum et al. 2009; Gonzalez 2007; Ioannides 2008; Raucy et al. 1991; Weltman et al. 1998; Woodcroft et al. 2002; Yun et al. 1992).

Furthermore, it is enhanced by starvation or low carbohydrate diets causing an increased rate of gluconeogenesis at the expense of emerging reactive oxygen species (ROS) (Hong et al. 1987; Jaeschke et al. 2002; Johansson et al. 1990; Lieber 1999; Lieber 2004; Lindros and Jarvelainen 1998; Teschke et al. 1981; Yoo et al. 1991).

These findings as well as the unaffected liver body weight ratios are in contrast to the previous study by Hussong et al. in rats (Hussong et al. 2005). Certainly, species differences may account in part for these discrepancies as shown for several other metabolic liver functions (Bun et al. 2005; Petersen et al. 1994). Further, histological analysis of glycogen content, as performed in the study of Hussong et al., is only a rough measurement, and both liver weight and hepatic glycogen content are only unspecific and vague indicators of hepatic injury. For example, also unspecific stress or fasting affects hepatic glycogen levels within hours (Aoki et al. 2009; Curi et al. 1990; Suh et al. 2007). Moreover, XN is a ligand of the farnesoid X receptor (FXR) and affects several genes involved in carbohydrate metabolism (Nozawa 2005) (see also chapter 2.4.7). Therefore and although not observed in the present study, reduced hepatic glycogen levels in response to XN treatment may be completely explained by direct effects of XN on carbohydrate metabolism rather than a potential hepatotoxic effect.

In conclusion, our study confirms the safety of oral XN administration to mice in a dose as high as 1000 mg/kg b.w per day. Especially, potential hepatotoxicity could be ruled out. Moreover, preliminary *in vitro* experiments with primary murine hepatocytes (PMH) (see chapter 4.3.5) point to an at least 3-fold higher sensitivity of PMH in comparison to primary human hepatocytes (PHH). Thus, although *in vitro* data can not be fully transferred to the *in vivo* situation, it may be speculated that range of safe XN application with regards to hepatoxicity is even higher than 1000 mg XN/kg b.w. in humans. However, the safety profile of XN surely has to be further studied in humans, but taken together our data indicate the safe use of XN as a therapeutic agent or functional nutrient.

5.4 Conclusion

As mentioned in the introduction XN exerts a variety of possibly beneficial effects. The reported anti-inflammatory, antioxidant and anti-infective effects of XN give rise to the presumption that this naturally occurring chalcone may also be useful for prevention or treatment of liver diseases, where chronic inflammation, oxidative stress and (mainly viral) infection play critical roles in most cases.

Additionally, the reported effects of XN on carbohydrate and lipid metabolism may be beneficial for patients with metabolic disorders like type 2 *diabetes mellitus* and/or insulin resistance. One of the major sites of carbohydrate and lipid metabolism and homeostasis is the liver, again identifying this specific organ as an interesting study object regarding XN-mediated effects.

Viral infections, chronic alcohol abuse and the metabolic syndrome are major risk factors for chronic liver disease. They lead to chronic hepatic inflammation, and if hepatitis continues, there is progression to liver fibrosis and subsequently to cirrhosis. The latter is the main risk factor for the development of hepatocellular cancer (HCC). Thus, regarding the known biological effects of XN liver disease appeared as attractive target for therapeutic XN application.

Considering bioavailability and metabolism of XN, the liver seems to be a predestined organ for XN-treatment, because the liver may be one of the few organs where oral application of this polyphenolic compound lead to therapeutically useful concentrations. In general, nutritional compounds have a higher concentration in the portal vein which directly connects the gut with the liver; distribution in the systemic circulation logically leads to a drop of the concentration. Additionally, a main function of the liver is to metabolize xenobiotics. Hepatocytes are specialized in confronting and taking up unmetabolized xenobiotics in high concentrations, and subsequently metabolize them. In many cases, the blood concentrations of xenobiotics or drugs are greatly reduced during the first liver passage, *i.e.* before the xenobiotic/drug reaches the systemic circulation (“first-pass effect”).

Taken together, the liver seems to be a promising target for XN treatment. However, up until now only very few studies have addressed this interesting point. Therefore, the major aim of this thesis was to evaluate the potential of XN as a therapeutic agent for liver diseases.

First, we analyzed the effects of XN on hepatic stellate cells (HSC), the central mediators of liver fibrogenesis and could detect significant induction of apoptosis *in vitro*. Furthermore, XN inhibits NFκB activation and expression of NFκB dependent proinflammatory chemokines in HCS. These data suggest that XN may suppress inflammation and fibrogenesis in injured livers. *In vivo*, feeding of XN reduced levels of serum transaminases and hepatic expression of proinflammatory genes in a murine model of non-alcoholic steatohepatitis (NASH), showing XN's hepatoprotective effect. Further, also *in vivo* XN treatment significantly inhibited hepatic expression of profibrogenic genes and activation of HSC.

Inhibition of inflammation and fibrosis may be beneficial in treatment of various liver diseases like non-alcoholic fatty liver diseases, alcohol induced liver diseases or chronic viral hepatitis. But also for prevention of HCC anti-inflammatory and anti-fibrotic agents may be useful. This aggressive cancer mostly develops and progresses, respectively, on the basis of a fibrotic liver caused by chronic hepatic inflammation.
Considering the numerous reports of anti-cancerous (and anti-angiogenic) effects of XN, evaluation of XN effects on HCC cells seemed to be promising. Indeed, XN showed significant cytotoxic and pro-apoptotic effects on HCC cells in doses where non-malignant primary human hepatocytes (PHH) were completely unaffected. Moreover, we could show for the first time that XN repressed HCC cell proliferation and migration *in vitro* as well as TNF induced NFκB activity and interleukin-8 expression in HCC cells at even lower concentrations. These data indicate, that XN may be used both for prevention and treatment of HCC. Surely, to evaluate these therapy options further studies are required.

However, potential adverse side effects of XN have to be identified before its therapeutic application. Especially the detection of even slight hepatotoxic effects, a frequent problem of novel therapeutics, is crucial. This is even more relevant if

intending to treat patients with impaired liver function or liver injury. Here, we detected no signs of XN-mediated toxicity after feeding XN in a dose of approximately 1000 mg XN/kg b.w. per day to female BALB/c mice for 3 weeks. Macroscopical and histopathological examination of liver, kidney, colon, lung, heart, spleen and thymus revealed no signs of XN-toxicity, and biochemical serum analysis confirmed normal organ function. Further, serum glucose levels and hepatic glycogen content as well as hepatic CYP2E1 mRNA expression levels were unaffected by xanthohumol treatment. Also mRNA expression of several genes indicative of early hepatic inflammation and fibrosis, a hallmark of chronic liver injury, did not differ between xanthohumol treated and control mice.

In conclusion, xanthohumol has the potential to ameliorate NASH induced liver injury as well as different pro-tumorigenic mechanisms known to promote HCC progression. Together with the good safety profile these data suggest the potential use of xanthohumol as functional nutrient or therapeutic agent to prevent or treat liver diseases like NASH or HCC.

6 References

AIM - Alcohol in Moderation. Online Source, URL: http://www.drinkingandyou.com /site/de/moder.htm, accessed at 8th Sept. 2009.

Airley, R.E. and Mobasheri, A. (2007) Hypoxic regulation of glucose transport, anaerobic metabolism and angiogenesis in cancer: novel pathways and targets for anticancer therapeutics. Chemotherapy 53, 233-256.

Albini, A., Dell'Eva, R., Vene, R., Ferrari, N., Buhler, D.R., Noonan, D.M. and Fassina, G. (2006) Mechanisms of the antiangiogenic activity by the hop flavonoid xanthohumol: NF-kappaB and Akt as targets. FASEB J. 20, 527-529.

Amann, T., Bataille, F., Spruss, T., Mühlbauer, M., Gabele, E., Scholmerich, J., Kiefer, P., Bosserhoff, A.K. and Hellerbrand, C. (2009) Activated hepatic stellate cells promote tumorigenicity of hepatocellular carcinoma. Cancer Sci. 100, 646-653.

Andersen, T., Christoffersen, P. and Gluud, C. (1984) The liver in consecutive patients with morbid obesity: a clinical, morphological, and biochemical study. Int. J. Obes. 8, 107-115.

Angulo, P. (2002) Nonalcoholic fatty liver disease. N. Engl. J. Med. 346, 1221-1231.

Anstee, Q.M. and Goldin, R.D. (2006) Mouse models in non-alcoholic fatty liver disease and steatohepatitis research. Int. J. Exp. Pathol. 87, 1-16.

Arimoto-Kobayashi, S., Sugiyama, C., Harada, N., Takeuchi, M., Takemura, M. and Hayatsu, H. (1999) Inhibitory effects of beer and other alcoholic beverages on mutagenesis and DNA adduct formation induced by several carcinogens. J. Agric. Food Chem. 47, 221-230.

Arsura, M. and Cavin, L.G. (2005) Nuclear factor-kappaB and liver carcinogenesis. Cancer Lett. 229, 157-169.

Avula, B., Ganzera, M., Warnick, J.E., Feltenstein, M.W., Sufka, K.J. and Khan, I.A. (2004) High-performance liquid chromatographic determination of xanthohumol in rat plasma, urine, and fecal samples. J. Chromatogr. Sci. 42, 378-382.

Bacon, B.R., Farahvash, M.J., Janney, C.G. and Neuschwander-Tetri, B.A. (1994) Nonalcoholic steatohepatitis: an expanded clinical entity. Gastroenterology 107, 1103-1109.

Barnes, J., Anderson, L. and Phillipson, J. (2002) Herbal Medicines: A Guide for Health Care Professionals. Pharmaceutical Press, London.

Barve, A., Khan, R., Marsano, L., Ravindra, K.V. and McClain, C. (2008) Treatment of alcoholic liver disease. Ann. Hepatol. 7, 5-15.

Bataller, R. and Brenner, D.A. (2005) Liver fibrosis. J. Clin. Invest 115, 209-218.

Becker, U., Deis, A., Sorensen, T.I., Gronbaek, M., Borch-Johnsen, K., Muller, C.F., Schnohr, P. and Jensen, G. (1996) Prediction of risk of liver disease by alcohol intake, sex, and age: a prospective population study. Hepatology 23, 1025-1029.

Bellentani, S., Saccoccio, G., Costa, G., Tiribelli, C., Manenti, F., Sodde, M., Saveria, C.L., Sasso, F., Pozzato, G., Cristianini, G. and Brandi, G. (1997) Drinking habits as cofactors of risk for alcohol induced liver damage. The Dionysos Study Group. Gut 41, 845-850.

Bellentani, S., Saccoccio, G., Masutti, F., Croce, L.S., Brandi, G., Sasso, F., Cristanini, G. and Tiribelli, C. (2000) Prevalence of and risk factors for hepatic steatosis in Northern Italy. Ann. Intern. Med. 132, 112-117.

Benyon, R.C. and Arthur, M.J. (1998) Mechanisms of hepatic fibrosis. J. Pediatr. Gastroenterol. Nutr. 27, 75-85.

Berasain, C., Castillo, J., Perugorria, M.J., Latasa, M.U., Prieto, J. and Avila, M.A. (2009) Inflammation and liver cancer: new molecular links. Ann. N. Y. Acad. Sci. 1155, 206-221.

Bergheim, I., McClain, C.J. and Arteel, G.E. (2005) Treatment of alcoholic liver disease. Dig. Dis. 23, 275-284.

Bertazza, L. and Mocellin, S. (2008) Tumor necrosis factor (TNF) biology and cell death. Front Biosci. 13, 2736-2743.

Bertl, E. (2005) Inhibition of angiogenesis by potential cancer chemopreventive agents -Establishment of a human in vitro anti-angiogenesis assay and mechanistic evaluation of potent inhibitors. Thesis, University of Heidelberg, URL: http://www.ub.uni-heidelberg.de/archiv/5760.

Bertl, E., Becker, H., Eicher, T., Herhaus, C., Kapadia, G., Bartsch, H. and Gerhäuser, C. (2004) Inhibition of endothelial cell functions by novel potential cancer chemopreventive agents. Biochem. Biophys. Res. Commun. 325, 287-295.

Bertolino, P., McCaughan, G.W. and Bowen, D.G. (2002) Role of primary intrahepatic T-cell activation in the 'liver tolerance effect'. Immunol. Cell Biol. 80, 84-92.

Bhattacharya, S., Virani, S., Zavro, M. and Haas, G.J. (2003) Inhibition of *Streptococcus mutans* and other oral streptococci by hop (*Humulus lupulus* L.) Constituents. Economic Botany 57, 118-125.

Bligh, E.G. and Dyer, W.J. (1959) A rapid method of total lipid extraction and purification. Can. J. Biochem. Physiol 37, 911-917.

Blumenthal, M. (1998) The Complete German Commission E Monograph: TherapeuticGuide to Herbal Medicines. In: TherapeuticGuide to Herbal Medicines, p. 147.

Blumenthal, M., Goldberg, A. and Brinckmann, J. (2000) Herbal Medicine: Expanded Commission E Monographs. In: Integrative Medicine Communications, pp. 297-303.

Bode, J.C., Alscher, D.M., Wisser, H. and Bode, C. (1995) Detection of hepatitis C virus antibodies and hepatitis C virus RNA in patients with alcoholic liver disease. Alcohol 30, 97-103.

Bosch, F.X. and Munoz, N. (1989) Epidemiology of hepatocellular cancer. Kluwer Academics.

Bown, D. (2001) The Herb Society of America New Encyclopedia of Herbs and Their Uses. Dorling Kindersley Ltd., London.

Boyde, A., Ali, N.N. and Jones, S.J. (1984) Resorption of dentine by isolated osteoclasts in vitro. Br. Dent. J. 156, 216-220.

Bremer, B., Bremer, K., Chase, M.W., Reveal, J.L., Soltis, D.E., Soltis, P.S., Stevens, P.F., Anderberg, A.A., Fay, M.F., Goldblatt, P., Judd, W.S., Kallersjo, M., Karehed, J., Kron, K.A., Lundberg, J., Nickrent, D.L., Olmstead, R.G., Oxelman, B., Pires, J.C., Rodman, J.E., Rudall, P.J., Savolainen, V., Sytsma, K.J., van der Bank, M., Wurdack, K., Xiang, J.Q. Y. and Zmarzty, S. (2003) An update of the Angiosperm Phylogeny Group classification for the orders and families of flowering plants: APG II. Bot. J. Linn. Soc. 141, 399– 436.

Browning, J.D., Szczepaniak, L.S., Dobbins, R., Nuremberg, P., Horton, J.D., Cohen, J.C., Grundy, S.M. and Hobbs, H.H. (2004) Prevalence of hepatic steatosis in an urban population in the United States: impact of ethnicity. Hepatology 40, 1387-1395.

Buckwold, V.E., Wilson, R.J., Nalca, A., Beer, B.B., Voss, T.G., Turpin, J.A., Buckheit, R.W., III, Wei, J., Wenzel-Mathers, M., Walton, E.M., Smith, R.J., Pallansch, M., Ward, P., Wells, J., Chuvala, L., Sloane, S., Paulman, R., Russell, J., Hartman, T. and Ptak, R. (2004) Antiviral activity of hop constituents against a series of DNA and RNA viruses. Antiviral Res. 61, 57-62.

Buell, J.F., Gross, T.G. and Woodle, E.S. (2005) Malignancy after transplantation. Transplantation 80, S254-S264.

Burt, A.D. (1993) C. L. Oakley Lecture (1993). Cellular and molecular aspects of hepatic fibrosis. J. Pathol. 170, 105-114.

Burt, A.D., Griffiths, M.R., Schuppan, D., Voss, B. and MacSween, R.N. (1990) Ultrastructural localization of extracellular matrix proteins in liver biopsies using ultracryomicrotomy and immuno-gold labelling. Histopathology 16, 53-58.

Caldwell, S.H., Oelsner, D.H., Iezzoni, J.C., Hespenheide, E.E., Battle, E.H. and Driscoll, C.J. (1999) Cryptogenic cirrhosis: clinical characterization and risk factors for underlying disease. Hepatology 29, 664-669.

Calvisi, D.F., Pinna, F., Ladu, S., Pellegrino, R., Muroni, M.R., Simile, M.M., Frau, M., Tomasi, M.L., De Miglio, M.R., Seddaiu, M.A., Daino, L., Sanna, V., Feo, F. and Pascale, R.M. (2008) Aberrant iNOS signaling is under genetic control in rodent liver cancer and potentially prognostic for the human disease. Carcinogenesis 29, 1639-1647.

Carr, L.G. and Westey, C. (1945) Surviving folktales and herbal lore among the Shinnecock Indians. Journal of American Folklore 58, 113-123.

Casaschi, A., Maiyoh, G.K., Rubio, B.K., Li, R.W., Adeli, K. and Theriault, A.G. (2004) The chalcone xanthohumol inhibits triglyceride and apolipoprotein B secretion in HepG2 cells. J. Nutr. 134, 1340-1346.

Central Animal Facility (ZTL) of the University of Regensburg. Anaesthesie - Empfehlungen: Maus / Ratte. Online Source, URL: http://www.uni-regensburg.de/Einrichtungen/ZTL/ztl/d/narkose.pdf, accessed at 8th Sept. 2009.

Chadwick, L.R., Pauli, G.F. and Farnsworth, N.R. (2006) The pharmacognosy of *Humulus lupulus* L. (hops) with an emphasis on estrogenic properties. Phytomedicine. 13, 119-131.

Chen, H., Charlat, O., Tartaglia, L.A., Woolf, E.A., Weng, X., Ellis, S.J., Lakey, N.D., Culpepper, J., Moore, K.J., Breitbart, R.E., Duyk, G.M., Tepper, R.I. and Morgenstern, J.P. (1996) Evidence that the diabetes gene encodes the leptin receptor: identification of a mutation in the leptin receptor gene in db/db mice. Cell 84, 491-495.

Chiang, L.C., Ng, L.T., Lin, I.C., Kuo, P.L. and Lin, C.C. (2006) Anti-proliferative effect of apigenin and its apoptotic induction in human Hep G2 cells. Cancer Lett. 237, 207-214.

Clark, J.M., Brancati, F.L. and Diehl, A.M. (2002) Nonalcoholic fatty liver disease. Gastroenterology 122, 1649-1657.

Colgate, E.C., Miranda, C.L., Stevens, J.F., Bray, T.M. and Ho, E. (2007) Xanthohumol, a prenylflavonoid derived from hops induces apoptosis and inhibits NF-kappaB activation in prostate epithelial cells. Cancer Lett. 246, 201-209.

Comelli, M.C., Mengs, U., Schneider, C. and Prosdocimi, M. (2007) Toward the definition of the mechanism of action of silymarin: activities related to cellular protection from toxic damage induced by chemotherapy. Integr. Cancer Ther. 6, 120-129.

Cortez-Pinto, H. and Camilo, M.E. (2004) Non-alcoholic fatty liver disease/non-alcoholic steatohepatitis (NAFLD/NASH): diagnosis and clinical course. Best. Pract. Res. Clin. Gastroenterol. 18, 1089-1104.

Cousin, S.P., Hugl, S.R., Wrede, C.E., Kajio, H., Myers, M.G., Jr. and Rhodes, C.J. (2001) Free fatty acid-induced inhibition of glucose and insulin-like growth factor I-induced deoxyribonucleic acid synthesis in the pancreatic beta-cell line INS-1. Endocrinology 142, 229-240.

Daniels, S.R., Jacobson, M.S., McCrindle, B.W., Eckel, R.H. and Sanner, B.M. (2009) American Heart Association Childhood Obesity Research Summit Report. Circulation 119, e489-e517.

Davalos, A., Gomez-Cordoves, C. and Bartolome, B. (2004) Extending applicability of the oxygen radical absorbance capacity (ORAC-fluorescein) assay. J. Agric. Food Chem. 52, 48-54.

Day, C.P. (2002) Pathogenesis of steatohepatitis. Best. Pract. Res. Clin. Gastroenterol. 16, 663-678.

Day, C.P. and James, O.F. (1998) Steatohepatitis: a tale of two "hits"? Gastroenterology 114, 842-845.

Dell'Eva, R., Ambrosini, C., Vannini, N., Piaggio, G., Albini, A. and Ferrari, N. (2007) AKT/NF-kappaB inhibitor xanthohumol targets cell growth and angiogenesis in hematologic malignancies. Cancer 110, 2007-2011.

Delmulle, L., Bellahcene, A., Dhooge, W., Comhaire, F., Roelens, F., Huvaere, K., Heyerick, A., Castronovo, V. and De Keukeleire, D. (2006) Anti-proliferative properties of prenylated flavonoids from hops (*Humulus lupulus* L.) in human prostate cancer cell lines. Phytomedicine. 13, 732-734.

Delmulle, L., Berghe, T.V., De Keukeleire, D. and Vandenabeele, P. (2008) Treatment of PC-3 and DU145 prostate cancer cells by prenylflavonoids from hop (*Humulus lupulus* L.) induces a caspase-independent form of cell death. Phytother. Res. 22, 197-203.

Deuffic, S., Poynard, T., Buffat, L. and Valleron, A.J. (1998) Trends in primary liver cancer. Lancet 351, 214-215.

Dietz, B.M., Kang, Y.H., Liu, G., Eggler, A.L., Yao, P., Chadwick, L.R., Pauli, G.F., Farnsworth, N.R., Mesecar, A.D., van Breemen, R.B. and Bolton, J.L. (2005) Xanthohumol isolated from *Humulus lupulus* Inhibits menadione-induced DNA damage through induction of quinone reductase. Chem. Res. Toxicol. 18, 1296-1305.

Dong, G., Chen, Z., Li, Z.Y., Yeh, N.T., Bancroft, C.C. and Van, W.C. (2001) Hepatocyte growth factor/scatter factor-induced activation of MEK and PI3K signal pathways contributes to expression of proangiogenic cytokines interleukin-8 and vascular endothelial growth factor in head and neck squamous cell carcinoma. Cancer Res. 61, 5911-5918.

Duke, J.A. (1985) Handbook of Medicinal Herbs. CRC Press, Boca Raton.

El-Serag, H.B., Marrero, J.A., Rudolph, L. and Reddy, K.R. (2008) Diagnosis and treatment of hepatocellular carcinoma. Gastroenterology 134, 1752-1763.

El-Serag, H.B. and Mason, A.C. (1999) Rising incidence of hepatocellular carcinoma in the United States. N. Engl. J. Med. 340, 745-750.

El-Serag, H.B., Richardson, P.A. and Everhart, J.E. (2001) The role of diabetes in hepatocellular carcinoma: a case-control study among United States Veterans. Am. J. Gastroenterol. 96, 2462-2467.

El-Serag, H.B. and Rudolph, K.L. (2007) Hepatocellular carcinoma: epidemiology and molecular carcinogenesis. Gastroenterology 132, 2557-2576.

Elsharkawy, A.M. and Mann, D.A. (2007) Nuclear factor-kappaB and the hepatic inflammation-fibrosis-cancer axis. Hepatology 46, 590-597.

Elsharkawy, A.M., Oakley, F. and Mann, D.A. (2005) The role and regulation of hepatic stellate cell apoptosis in reversal of liver fibrosis. Apoptosis 10, 927-939.

Eri, S., Khoo, B.K., Lech, J. and Hartman, T.G. (2000) Direct thermal desorption-gas chromatography and gas chromatography-mass spectrometry profiling of hop (*Humulus lupulus* L.) essential oils in support of varietal characterization. J. Agric. Food Chem. 48, 1140-1149.

Falschlehner, C., Emmerich, C.H., Gerlach, B. and Walczak, H. (2007) TRAIL signalling: decisions between life and death. Int. J. Biochem. Cell Biol. 39, 1462-1475.

Fontana, R.J. (2008) Acute liver failure due to drugs. Semin. Liver Dis. 28, 175-187.

Forster, A., Gahr, A., Ketterer, M., Beck, B. and Massinger, S. (2002) Xanthohumol in Bier – Möglichkeiten und Grenzen einer Anreicherung. In: Monatsschrift für Brauwissenschaft. 9/10, 184-194.

Friedman, S.L. (2003) Liver fibrosis -- from bench to bedside. J. Hepatol. 38 Suppl 1, S38-S53.

Friedman, S.L. (2004) Mechanisms of disease: Mechanisms of hepatic fibrosis and therapeutic implications. Nat. Clin. Pract. Gastroenterol. Hepatol. 1, 98-105.

Friedman, S.L. (2008) Mechanisms of hepatic fibrogenesis. Gastroenterology 134, 1655-1669.

Frölich, S., Schubert, C., Bienzle, U. and Jenett-Siems, K. (2005) In vitro antiplasmodial activity of prenylated chalcone derivatives of hops (*Humulus lupulus*) and their interaction with haemin. J. Antimicrob. Chemother. 55, 883-887.

Gabele, E., Brenner, D.A. and Rippe, R.A. (2003) Liver fibrosis: signals leading to the amplification of the fibrogenic hepatic stellate cell. Front Biosci. 8, d69-d77.

Gao, X., Deeb, D., Liu, Y., Gautam, S., Dulchavsky, S.A. and Gautam, S.C. (2009) Immunomodulatory activity of xanthohumol: inhibition of T cell proliferation, cell-mediated cytotoxicity and Th1 cytokine production through suppression of NF-kappaB. Immunopharmacol. Immunotoxicol. 31, 477-484.

Gerhäuser, C. (2005a) Beer constituents as potential cancer chemopreventive agents. Eur. J. Cancer 41, 1941-1954.

Gerhäuser, C. (2005b) Broad spectrum anti-infective potential of xanthohumol from hop (*Humulus lupulus* L.) in comparison with activities of other hop constituents and xanthohumol metabolites. Mol. Nutr. Food Res. 49, 827-831.

Gerhäuser, C., Alt, A., Heiss, E., Gamal-Eldeen, A., Klimo, K., Knauft, J., Neumann, I., Scherf, H.R., Frank, N., Bartsch, H. and Becker, H. (2002) Cancer chemopreventive activity of Xanthohumol, a natural product derived from hop. Mol. Cancer Ther. 1, 959-969.

Gines, P., Cardenas, A., Arroyo, V. and Rodes, J. (2004) Management of cirrhosis and ascites. N. Engl. J. Med. 350, 1646-1654.

Gonzalez, F.J. (2007) The 2006 Bernard B. Brodie Award Lecture. Cyp2e1. Drug Metab Dispos. 35, 1-8.

Gorissen, H., Bellink, C., Vancraenenbroeck, R. and Lontie, R. (1968) Separation and identification of (+)-gallocatechine in hops. Arch Int Physiol Biochim. 76, 932-934.

Goto, K., Asai, T., Hara, S., Namatame, I., Tomoda, H., Ikemoto, M. and Oku, N. (2005) Enhanced antitumor activity of xanthohumol, a diacylglycerol acyltransferase inhibitor, under hypoxia. Cancer Lett. 219, 215-222.

Grieve, M. (1971) A Modern Herbal. Dover Publications, Inc., New York.

Hahn, E., Wick, G., Pencev, D. and Timpl, R. (1980) Distribution of basement membrane proteins in normal and fibrotic human liver: collagen type IV, laminin, and fibronectin. Gut 21, 63-71.

Hamel, P.B. and Chiltoskey, M.U. (1975) Cherokee Plants and Their Uses. A 400-years History. Herald Publishing Co., Sylva, NC.

Hanske, L., Hussong, R., Frank, N., Gerhäuser, C., Blaut, M. and Braune, A. (2005) Xanthohumol does not affect the composition of rat intestinal microbiota. Mol. Nutr. Food Res. 49, 868-873.

Harborne, J.B. (1986) Nature, distribution and function of plant flavonoids. Prog. Clin. Biol. Res. 213, 15-24.

Haukeland, J.W., Damas, J.K., Konopski, Z., Loberg, E.M., Haaland, T., Goverud, I., Torjesen, P.A., Birkeland, K., Bjoro, K. and Aukrust, P. (2006) Systemic inflammation in nonalcoholic fatty liver disease is characterized by elevated levels of CCL2. J. Hepatol. 44, 1167-1174.

Hellerbrand, C., Amann, T., Schlegel, J., Wild, P., Bataille, F., Spruss, T., Hartmann, A. and Bosserhoff, A.K. (2008) The novel gene MIA2 acts as a tumour suppressor in hepatocellular carcinoma. Gut 57, 243-251.

Hellerbrand, C., Bumes, E., Bataille, F., Dietmaier, W., Massoumi, R. and Bosserhoff, A.K. (2007) Reduced expression of CYLD in human colon and hepatocellular carcinomas. Carcinogenesis 28, 21-27.

Hellerbrand, C., Jobin, C., Iimuro, Y., Licato, L., Sartor, R.B. and Brenner, D.A. (1998a) Inhibition of NFkappaB in activated rat hepatic stellate cells by proteasome inhibitors and an IkappaB super-repressor. Hepatology 27, 1285-1295.

Hellerbrand, C., Jobin, C., Licato, L.L., Sartor, R.B. and Brenner, D.A. (1998b) Cytokines induce NF-kappaB in activated but not in quiescent rat hepatic stellate cells. Am. J. Physiol 275, G269-G278.

Henderson, M.C., Miranda, C.L., Stevens, J.F., Deinzer, M.L. and Buhler, D.R. (2000) In vitro inhibition of human P450 enzymes by prenylated flavonoids from hops, Humulus lupulus. Xenobiotica 30, 235-251.

Herath, W., Ferreira, D., Khan, S.I. and Khan, I.A. (2003) Identification and biological activity of microbial metabolites of xanthohumol. *Chem. Pharm. Bull.* 51, 1237-1240.

Ho, Y.C., Liu, C.H., Chen, C.N., Duan, K.J. and Lin, M.T. (2008) Inhibitory effects of xanthohumol from hops (*Humulus lupulus* L.) on human hepatocellular carcinoma cell lines. Phytother. Res. 22, 1465-1468.

Hofmann, W.P. and Zeuzem, S. (2003) [Is liver fibrosis a reversible event? Effect of pegylated interferon and ribavirin in patients with chronic hepatitis C]. Z. Gastroenterol. 41, 271-274.

Holinka, C.F., Hata, H., Gravanis, A., Kuramoto, H. and Gurpide, E. (1986a) Effects of estradiol on proliferation of endometrial adenocarcinoma cells (Ishikawa line). J. Steroid Biochem. 25, 781-786.

Holinka, C.F., Hata, H., Kuramoto, H. and Gurpide, E. (1986b) Effects of steroid hormones and antisteroids on alkaline phosphatase activity in human endometrial cancer cells (Ishikawa line). Cancer Res. 46, 2771-2774.

Holinka, C.F., Hata, H., Kuramoto, H. and Gurpide, E. (1986c) Responses to estradiol in a human endometrial adenocarcinoma cell line (Ishikawa). J. Steroid Biochem. 24, 85-89.

Hoofnagle, J.H. (2004) Hepatocellular carcinoma: summary and recommendations. Gastroenterology 127, S319-S323.

Hsu, Y.L., Kuo, P.L. and Lin, C.C. (2005) Isoliquiritigenin induces apoptosis and cell cycle arrest through p53-dependent pathway in Hep G2 cells. Life Sci. 77, 279-292.

Hussong, R., Frank, N., Knauft, J., Ittrich, C., Owen, R., Becker, H. and Gerhäuser, C. (2005) A safety study of oral xanthohumol administration and its influence on fertility in Sprague Dawley rats. Mol. Nutr. Food Res. 49, 861-867.

Iguchi, A., Kitajima, I., Yamakuchi, M., Ueno, S., Aikou, T., Kubo, T., Matsushima, K., Mukaida, N. and Maruyama, I. (2000) PEA3 and AP-1 are required for constitutive IL-8 gene expression in hepatoma cells. Biochem. Biophys. Res. Commun. 279, 166-171.

Ioannides, C. (2008) Cytochromes P450: Role in the Metabolism and Toxicity of Drugs and Other Xenobiotics. Royal Soc of Chemistry, Cambridge, UK.

Iwatsuka, H., Shino, A. and Suzuoki, Z. (1970) General survey of diabetic features of yellow KK mice. Endocrinol. Jpn. 17, 23-35.

Jarrar, M.H., Baranova, A., Collantes, R., Ranard, B., Stepanova, M., Bennett, C., Fang, Y., Elariny, H., Goodman, Z., Chandhoke, V. and Younossi, Z.M. (2008) Adipokines and cytokines in non-alcoholic fatty liver disease. Aliment. Pharmacol. Ther. 27, 412-421.

Jeong, W.I., Jeong, D.H., Do, S.H., Kim, Y.K., Park, H.Y., Kwon, O.D., Kim, T.H. and Jeong, K.S. (2005) Mild hepatic fibrosis in cholesterol and sodium cholate diet-fed rats. J. Vet. Med. Sci. 67, 235-242.

Jimba, S., Nakagami, T., Takahashi, M., Wakamatsu, T., Hirota, Y., Iwamoto, Y. and Wasada, T. (2005) Prevalence of non-alcoholic fatty liver disease and its association with impaired glucose metabolism in Japanese adults. Diabet. Med. 22, 1141-1145.

Joshi-Barve, S., Barve, S.S., Amancherla, K., Gobejishvili, L., Hill, D., Cave, M., Hote, P. and McClain, C.J. (2007) Palmitic acid induces production of proinflammatory cytokine interleukin-8 from hepatocytes. Hepatology 46, 823-830.

Kac, J., Plazar, J., Mlinaric, A., Zegura, B., Lah, T.T. and Filipic, M. (2008) Antimutagenicity of hops (*Humulus lupulus* L.): bioassay-directed fractionation and isolation of xanthohumol. Phytomedicine. 15, 216-220.

Karnick, C.R. (1994) Pharmacopoeial Standards of Herbal Plants. Sri Satguru Publications, Delhi.

Kew, M.C. (2002) Epidemiology of hepatocellular carcinoma. Toxicology 181-182, 35-38.

Kim, S.F., Huri, D.A. and Snyder, S.H. (2005) Inducible nitric oxide synthase binds, S-nitrosylates, and activates cyclooxygenase-2. Science 310, 1966-1970.

Kleinfeld, A.M., Prothro, D., Brown, D.L., Davis, R.C., Richieri, G.V. and DeMaria, A. (1996) Increases in serum unbound free fatty acid levels following coronary angioplasty. Am. J. Cardiol. 78, 1350-1354.

Kubicka, S., Rudolph, K.L., Hanke, M., Tietze, M.K., Tillmann, H.L., Trautwein, C. and Manns, M. (2000) Hepatocellular carcinoma in Germany: a retrospective epidemiological study from a low-endemic area. Liver 20, 312-318.

Kubo, F., Ueno, S., Hiwatashi, K., Sakoda, M., Kawaida, K., Nuruki, K. and Aikou, T. (2005) Interleukin 8 in human hepatocellular carcinoma correlates with cancer cell invasion of vessels but not with tumor angiogenesis. Ann. Surg. Oncol. 12, 800-807.

Kuhnle, G., Spencer, J.P., Chowrimootoo, G., Schroeter, H., Debnam, E.S., Srai, S.K., Rice-Evans, C. and Hahn, U. (2000) Resveratrol is absorbed in the small intestine as resveratrol glucuronide. Biochem. Biophys. Res. Commun. 272, 212-217.

Lau, W.Y. and Lai, E.C. (2008) Hepatocellular carcinoma: current management and recent advances. Hepatobiliary. Pancreat. Dis. Int. 7, 237-257.

Lawless, J. (1995) The Illustrated Encyclopedia of Essential Oils: The Complete Guide to the Use of Oils in Aromatherapy and Herbalism. Element Books, Ltd., Dorset, UK.

Lee, H.J., Wang, C.J., Kuo, H.C., Chou, F.P., Jean, L.F. and Tseng, T.H. (2005) Induction apoptosis of luteolin in human hepatoma HepG2 cells involving mitochondria translocation of Bax/Bak and activation of JNK. Toxicol. Appl. Pharmacol. 203, 124-131.

Lee, S.H., Kim, H.J., Lee, J.S., Lee, I.S. and Kang, B.Y. (2007) Inhibition of topoisomerase I activity and efflux drug transporters' expression by xanthohumol from hops. Arch. Pharm. Res. 30, 1435-1439.

Lee, W.M. (2003) Drug-induced hepatotoxicity. N. Engl. J. Med. 349, 474-485.

Lencioni, R., Cioni, D., Crocetti, L. and Bartolozzi, C. (2004) Percutaneous ablation of hepatocellular carcinoma: state-of-the-art. Liver Transpl. 10, 91-97.

Li, R., Kenyon, G.L., Cohen, F.E., Chen, X., Gong, B., Dominguez, J.N., Davidson, E., Kurzban, G., Miller, R.E., Nuzum, E.O., Rosenthal P.J. and McKerrow J.H. (1995) In vitro antimalarial activity of chalcones and their derivatives. J. Med. Chem. 38, 5031-5037.

Li, T.K. (2008) Quantifying the risk for alcohol-use and alcohol-attributable health disorders: present findings and future research needs. J. Gastroenterol. Hepatol. 23 Suppl 1, S2-S8.

Lindquist, J.N., Marzluff, W.F. and Stefanovic, B. (2000) Fibrogenesis. III. Posttranscriptional regulation of type I collagen. Am. J. Physiol Gastrointest. Liver Physiol 279, G471-G476.

Lindquist, J.N., Parsons, C.J., Stefanovic, B. and Brenner, D.A. (2004) Regulation of alpha1(I) collagen messenger RNA decay by interactions with alphaCP at the 3'-untranslated region. J. Biol. Chem. 279, 23822-23829.

Liu, M., Wilairat, P. and Go, M.L. (2001) Antimalarial alkoxylated and hydroxylated chalcones [corrected]: structure-activity relationship analysis. J. Med. Chem. 44, 4443-4452.

Llovet, J.M., Fuster, J. and Bruix, J. (2004) The Barcelona approach: diagnosis, staging, and treatment of hepatocellular carcinoma. Liver Transpl. 10, S115-S120.

Llovet, J.M., Real, M.I., Montana, X., Planas, R., Coll, S., Aponte, J., Ayuso, C., Sala, M., Muchart, J., Sola, R., Rodes, J. and Bruix, J. (2002) Arterial embolisation or chemoembolisation versus symptomatic treatment in patients with unresectable hepatocellular carcinoma: a randomised controlled trial. Lancet 359, 1734-1739.

Loria, P., Lonardo, A. and Targher, G. (2008) Is liver fat detrimental to vessels?: intersections in the pathogenesis of NAFLD and atherosclerosis. Clin. Sci. (Lond) 115, 1-12.

Lotito, S.B. and Frei, B. (2004) The increase in human plasma antioxidant capacity after apple consumption is due to the metabolic effect of fructose on urate, not apple-derived antioxidant flavonoids. Free Radic. Biol. Med. 37, 251-258.

Lotito, S.B. and Frei, B. (2006) Consumption of flavonoid-rich foods and increased plasma antioxidant capacity in humans: cause, consequence, or epiphenomenon? Free Radic. Biol. Med. 41, 1727-1746.

Ludwig, J., Viggiano, T.R., McGill, D.B. and Oh, B.J. (1980) Nonalcoholic steatohepatitis: Mayo Clinic experiences with a hitherto unnamed disease. Mayo Clin. Proc. 55, 434-438.

Lust, S., Vanhoecke, B., Janssens, A., Philippe, J., Bracke, M. and Offner, F. (2005) Xanthohumol kills B-chronic lymphocytic leukemia cells by an apoptotic mechanism. Mol. Nutr. Food Res. 49, 844-850.

Malizia, R.A., Molli, J.S., Cardell, D.A. and Grau, R.J.A. (1999) Essential oil of hop cones (*Humulus lupulus* L.). Journal of Essential Oil Research 11, 13-15.

Marcos, A., Fisher, R.A., Ham, J.M., Olzinski, A.T., Shiffman, M.L., Sanyal, A.J., Luketic, V.A., Sterling, R.K., Olbrisch, M.E. and Posner, M.P. (2000) Selection and outcome of living donors for adult to adult right lobe transplantation. Transplantation 69, 2410-2415.

Marra, F. (1999) Hepatic stellate cells and the regulation of liver inflammation. J. Hepatol. 31, 1120-1130.

Matsuzawa, N., Takamura, T., Kurita, S., Misu, H., Ota, T., Ando, H., Yokoyama, M., Honda, M., Zen, Y., Nakanuma, Y., Miyamoto, K. and Kaneko, S. (2007) Lipid-induced oxidative stress causes steatohepatitis in mice fed an atherogenic diet. Hepatology 46, 1392-1403.

Matteoni, C.A., Younossi, Z.M., Gramlich, T., Boparai, N., Liu, Y.C. and McCullough, A.J. (1999) Nonalcoholic fatty liver disease: a spectrum of clinical and pathological severity. Gastroenterology 116, 1413-1419.

Mendes, V., Monteiro, R., Pestana, D., Teixeira, D., Calhau, C. and Azevedo, I. (2008) Xanthohumol influences preadipocyte differentiation: implication of antiproliferative and apoptotic effects. J. Agric. Food Chem. 56, 11631-11637.

Milani, S., Herbst, H., Schuppan, D., Kim, K.Y., Riecken, E.O. and Stein, H. (1990) Procollagen expression by nonparenchymal rat liver cells in experimental biliary fibrosis. Gastroenterology 98, 175-184.

Milligan, S., Kalita, J., Pocock, V., Heyerick, A., De Keukeleire, C.L., Rong, H. and De Keukeleire, D. (2002) Oestrogenic activity of the hop phyto-oestrogen, 8-prenylnaringenin. Reproduction. 123, 235-242.

Milligan, S.R., Kalita, J.C., Heyerick, A., Rong, H., De Keukeleire, L. and De Keukeleire, D. (1999) Identification of a potent phytoestrogen in hops (*Humulus lupulus* L.) and beer. J. Clin. Endocrinol. Metab 84, 2249-2252.

Milligan, S.R., Kalita, J.C., Pocock, V., Van, D.K., V, Stevens, J.F., Deinzer, M.L., Rong, H. and De, K.D. (2000) The endocrine activities of 8-prenylnaringenin and related hop (*Humulus lupulus* L.) flavonoids. J. Clin. Endocrinol. Metab 85, 4912-4915.

Minguez, B., Tovar, V., Chiang, D., Villanueva, A. and Llovet, J.M. (2009) Pathogenesis of hepatocellular carcinoma and molecular therapies. Curr. Opin. Gastroenterol. 25, 186-194.

Miranda, C.L., Aponso, G.L., Stevens, J.F., Deinzer, M.L. and Buhler, D.R. (2000a) Prenylated chalcones and flavanones as inducers of quinone reductase in mouse Hepa 1c1c7 cells. Cancer Lett. 149, 21-29.

Miranda, C.L., Stevens, J.F., Helmrich, A., Henderson, M.C., Rodriguez, R.J., Yang, Y.H., Deinzer, M.L., Barnes, D.W. and Buhler, D.R. (1999) Antiproliferative and cytotoxic effects of prenylated flavonoids from hops (*Humulus lupulus*) in human cancer cell lines. Food Chem. Toxicol. 37, 271-285.

Miranda, C.L., Stevens, J.F., Ivanov, V., McCall, M., Frei, B., Deinzer, M.L. and Buhler, D.R. (2000b) Antioxidant and prooxidant actions of prenylated and nonprenylated chalcones and flavanones in vitro. J. Agric. Food Chem. 48, 3876-3884.

Miranda, C.L., Yang, Y.H., Henderson, M.C., Stevens, J.F., Santana-Rios, G., Deinzer, M.L. and Buhler, D.R. (2000c) Prenylflavonoids from hops inhibit the metabolic activation of the carcinogenic heterocyclic amine 2-amino-3-methylimidazo[4, 5-f]quinoline, mediated by cDNA-expressed human CYP1A2. Drug Metab Dispos. 28, 1297-1302.

Mizobuchi, S. and Sato, Y. (1984) A new flavanone with antifungal activity isolated from hops. Agricultural and Biological Chemistry 48, 2771-2775.

Monteiro, R., Calhau, C., Silva, A.O., Pinheiro-Silva, S., Guerreiro, S., Gartner, F., Azevedo, I. and Soares, R. (2008) Xanthohumol inhibits inflammatory factor production and angiogenesis in breast cancer xenografts. J. Cell Biochem. 104, 1699-1707.

Monteiro, R., Faria, A., Azevedo, I. and Calhau, C. (2007) Modulation of breast cancer cell survival by aromatase inhibiting hop (*Humulus lupulus* L.) flavonoids. J. Steroid Biochem. Mol. Biol. 105, 124-130.

Mühlbauer, M., Fleck, M., Schutz, C., Weiss, T., Froh, M., Blank, C., Scholmerich, J. and Hellerbrand, C. (2006) PD-L1 is induced in hepatocytes by viral infection and by interferon-alpha and -gamma and mediates T cell apoptosis. J. Hepatol. 45, 520-528.

Murray, K.F., Hadzic, N., Wirth, S., Bassett, M. and Kelly, D. (2008) Drug-related hepatotoxicity and acute liver failure. J. Pediatr. Gastroenterol. Nutr. 47, 395-405.

Nagel, J. (2009) EST-Analyse von *Humulus lupulus* L.-Trichomen – Identifizierung einer O-Methyltransferase, welche die Biosynthese von Xanthohumol katalysiert. Thesis, Martin-Luther-University, Halle-Wittenberg. URL: http://sundoc.bibliothek.uni-halle.de/diss-online/09/09H051/prom.pdf.

National Institute on Alcohol Abuse and Alcoholism. (1993) Sensible Drinking Guidelines. Alcohol Alert No. 19: Alcohol and the Liver. In.

National Institute on Alcohol Abuse and Alcoholism. (2004) National Advisory Council on Alcohol Abuse and Alcoholism; Summary of the 105th Meeting. In.

Navarro, V.J. and Senior, J.R. (2006) Drug-related hepatotoxicity. N. Engl. J. Med. 354, 731-739.

Neuschwander-Tetri, B.A. and Caldwell, S.H. (2003) Nonalcoholic steatohepatitis: summary of an AASLD Single Topic Conference. Hepatology 37, 1202-1219.

Nikolic, D., Li, Y., Chadwick, L.R., Pauli, G.F. and van Breemen, R.B. (2005) Metabolism of xanthohumol and isoxanthohumol, prenylated flavonoids from hops (*Humulus lupulus* L.), by human liver microsomes. J. Mass Spectrom. 40, 289-299.

Nishina, P.M., Lowe, S., Verstuyft, J., Naggert, J.K., Kuypers, F.A. and Paigen, B. (1993) Effects of dietary fats from animal and plant sources on diet-induced fatty streak lesions in C57BL/6J mice. J. Lipid Res. 34, 1413-1422.

Nishina, P.M., Verstuyft, J. and Paigen, B. (1990) Synthetic low and high fat diets for the study of atherosclerosis in the mouse. J. Lipid Res. 31, 859-869.

Nookandeh, A., Frank, N., Steiner, F., Ellinger, R., Schneider, B., Gerhäuser, C. and Becker, H. (2004) Xanthohumol metabolites in faeces of rats. Phytochemistry 65, 561-570.

Nozawa, H. (2005) Xanthohumol, the chalcone from beer hops (*Humulus lupulus* L.), is the ligand for farnesoid X receptor and ameliorates lipid and glucose metabolism in KK-A(y) mice. Biochem. Biophys. Res. Commun. 336, 754-761.

Ogden, C.L., Carroll, M.D., Curtin, L.R., McDowell, M.A., Tabak, C.J. and Flegal, K.M. (2006) Prevalence of overweight and obesity in the United States, 1999-2004. JAMA 295, 1549-1555.

Ostapowicz, G., Fontana, R.J., Schiodt, F.V., Larson, A., Davern, T.J., Han, S.H., McCashland, T.M., Shakil, A.O., Hay, J.E., Hynan, L., Crippin, J.S., Blei, A.T., Samuel, G., Reisch, J. and Lee, W.M. (2002) Results of a prospective study of acute liver failure at 17 tertiary care centers in the United States. Ann. Intern. Med. 137, 947-954.

Pahernik, S.A., Thasler, W.E., Mueller-Hoecker, J., Schildberg, F.W. and Koebe, H.G. (1996) Hypothernic storage of pig hepatocytes: influence of different storage solutions and cell density. Cryobiology 33, 552-566.

Paigen, B., Morrow, A., Brandon, C., Mitchell, D. and Holmes, P. (1985) Variation in susceptibility to atherosclerosis among inbred strains of mice. Atherosclerosis 57, 65-73.

Pan, L., Becker, H. and Gerhäuser, C. (2005) Xanthohumol induces apoptosis in cultured 40-16 human colon cancer cells by activation of the death receptor- and mitochondrial pathway. Mol. Nutr. Food Res. 49, 837-843.

Parkin, D.M. (2001) Global cancer statistics in the year 2000. Lancet Oncol. 2, 533-543.

Pietta, P.G. (2000) Flavonoids as antioxidants. J. Nat. Prod. 63, 1035-1042.

Pikarsky, E., Porat, R.M., Stein, I., Abramovitch, R., Amit, S., Kasem, S., Gutkovich-Pyest, E., Urieli-Shoval, S., Galun, E. and Ben-Neriah, Y. (2004) NF-kappaB functions as a tumour promoter in inflammation-associated cancer. Nature 431, 461-466.

Pinzani, M. (1995) Novel insights into the biology and physiology of the Ito cell. Pharmacol. Ther. 66, 387-412.

Plazar, J., Filipic, M. and Groothuis, G.M. (2008) Antigenotoxic effect of Xanthohumol in rat liver slices. Toxicol. In Vitro 22, 318-327.

Plazar, J., Zegura, B., Lah, T.T. and Filipic, M. (2007) Protective effects of xanthohumol against the genotoxicity of benzo(a)pyrene (BaP), 2-amino-3-methylimidazo[4,5-f]quinoline (IQ) and tert-butyl hydroperoxide (t-BOOH) in HepG2 human hepatoma cells. Mutat. Res. 632, 1-8.

Possemiers, S., Bolca, S., Grootaert, C., Heyerick, A., Decroos, K., Dhooge, W., De Keukeleire, D., Rabot, S., Verstraete, W. and Van de Wiele, T. (2006) The prenylflavonoid isoxanthohumol from hops (*Humulus lupulus* L.) is activated into the potent phytoestrogen 8-prenylnaringenin in vitro and in the human intestine. J. Nutr. 136, 1862-1867.

Possemiers, S., Heyerick, A., Robbens, V., De Keukeleire, D. and Verstraete, W. (2005) Activation of proestrogens from hops (*Humulus lupulus* L.) by intestinal microbiota; conversion of isoxanthohumol into 8-prenylnaringenin. J. Agric. Food Chem. 53, 6281-6288.

Possemiers, S., Rabot, S., Espin, J.C., Bruneau, A., Philippe, C., Gonzalez-Sarrias, A., Heyerick, A., Tomas-Barberan, F.A., De Keukeleire, D. and Verstraete, W. (2008) *Eubacterium limosum* activates isoxanthohumol from hops (*Humulus lupulus* L.) into the potent phytoestrogen 8-prenylnaringenin in vitro and in rat intestine. J. Nutr. 138, 1310-1316.

Powell, E.E., Cooksley, W.G., Hanson, R., Searle, J., Halliday, J.W. and Powell, L.W. (1990) The natural history of nonalcoholic steatohepatitis: a follow-up study of forty-two patients for up to 21 years. Hepatology 11, 74-80.

Power, F.B., Tutin, F. and Rogerson, H. (1913) The Constituents of hops. J. Chem. Soc. 103, 1267-1292.

Rademakers, S.E., Span, P.N., Kaanders, J.H., Sweep, F.C., van der Kogel, A.J. and Bussink, J. (2008) Molecular aspects of tumour hypoxia. Mol. Oncol. 2, 41-53.

Ramachandran, R. and Kakar, S. (2009) Histological patterns in drug-induced liver disease. J. Clin. Pathol. 62, 481-492.

Ren, Y., Poon, R.T., Tsui, H.T., Chen, W.H., Li, Z., Lau, C., Yu, W.C. and Fan, S.T. (2003) Interleukin-8 serum levels in patients with hepatocellular carcinoma: correlations with clinicopathological features and prognosis. Clin. Cancer Res. 9, 5996-6001.

Rodriguez, R.J., Miranda, C.L., Stevens, J.F., Deinzer, M.L. and Buhler, D.R. (2001) Influence of prenylated and non-prenylated flavonoids on liver microsomal lipid peroxidation and oxidative injury in rat hepatocytes. Food Chem. Toxicol. 39, 437-445.

Rojkind, M., Giambrone, M.A. and Biempica, L. (1979) Collagen types in normal and cirrhotic liver. Gastroenterology 76, 710-719.

Ruhl, C.E. and Everhart, J.E. (2004) Epidemiology of nonalcoholic fatty liver. Clin. Liver Dis. 8, 501-19, vii.

Ryan, C.M., Carter, E.A., Jenkins, R.L., Sterling, L.M., Yarmush, M.L., Malt, R.A. and Tompkins, R.G. (1993) Isolation and long-term culture of human hepatocytes. Surgery 113, 48-54.

Sagesser, M. and Deinzer, M. (1996) HPLC-ion spray-tandem mass spectrometry of flavonol glycosides in hops. Journal of the American Society of Brewing Chemists 54, 129-134.

Salvi, A., Sabelli, C., Moncini, S., Venturin, M., Arici, B., Riva, P., Portolani, N., Giulini, S.M., De, P.G. and Barlati, S. (2009) MicroRNA-23b mediates urokinase and c-met downmodulation and a decreased migration of human hepatocellular carcinoma cells. FEBS J. 276, 2966-2982.

Sanyal, A.J. (2002) AGA technical review on nonalcoholic fatty liver disease. Gastroenterology 123, 1705-1725.

Scalbert, A. and Williamson, G. (2000) Dietary intake and bioavailability of polyphenols. J. Nutr. 130, 2073S-2085S.

Schlitt, H.J., Neipp, M., Weimann, A., Oldhafer, K.J., Schmoll, E., Boeker, K., Nashan, B., Kubicka, S., Maschek, H., Tusch, G., Raab, R., Ringe, B., Manns, M.P. and Pichlmayr, R. (1999) Recurrence patterns of hepatocellular and fibrolamellar carcinoma after liver transplantation. J. Clin. Oncol. 17, 324-331.

Seglen, P.O. (1976) Preparation of isolated rat liver cells. Methods Cell Biol. 13, 29-83.

Seyer, J.M., Hutcheson, E.T. and Kang, A.H. (1977) Collagen polymorphism in normal and cirrhotic human liver. J. Clin. Invest 59, 241-248.

Shen, H.M. and Tergaonkar, V. (2009) NFkappaB signaling in carcinogenesis and as a potential molecular target for cancer therapy. Apoptosis. 14, 348-363.

Shirouzu, Y., Ryschich, E., Salnikova, O., Kerkadze, V., Schmidt, J. and Engelmann, G. (2008) Rapamycin inhibits proliferation and migration of hepatoma cells in vitro. J. Surg. Res. [Epub ahead of print] doi:10.1016/j.jss.2008.07.035.

Shneider, B.L., Gonzalez-Peralta, R. and Roberts, E.A. (2006) Controversies in the management of pediatric liver disease: Hepatitis B, C and NAFLD: Summary of a single topic conference. Hepatology 44, 1344-1354.

Singh, R.P., Tyagi, A.K., Zhao, J. and Agarwal, R. (2002) Silymarin inhibits growth and causes regression of established skin tumors in SENCAR mice via modulation of mitogen-activated protein kinases and induction of apoptosis. Carcinogenesis 23, 499-510.

Sookoian, S. and Pirola, C.J. (2008) Non-alcoholic fatty liver disease is strongly associated with carotid atherosclerosis: a systematic review. J. Hepatol. 49, 600-607.

Sooriakumaran, P. and Kaba, R. (2005) Angiogenesis and the tumour hypoxia response in prostate cancer: a review. Int. J. Surg. 3, 61-67.

Soyer, M.T., Ceballos, R. and Aldrete, J.S. (1976) Reversibility of severe hepatic damage caused by jejunoileal bypass after re-establishment of normal intestinal continuity. Surgery 79, 601-604.

Spencer, J.P. (2003) Metabolism of tea flavonoids in the gastrointestinal tract. J. Nutr. 133, 3255S-3261S.

Spencer, J.P., Chowrimootoo, G., Choudhury, R., Debnam, E.S., Srai, S.K. and Rice-Evans, C. (1999) The small intestine can both absorb and glucuronidate luminal flavonoids. FEBS Lett. 458, 224-230.

Steele, J.C., Phelps, R.J., Simmonds, M.S., Warhurst, D.C. and Meyer, D.J. (2002) Two novel assays for the detection of haemin-binding properties of antimalarials evaluated with compounds isolated from medicinal plants. J. Antimicrob. Chemother. 50, 25-31.

Stefanovic, B., Hellerbrand, C., Holcik, M., Briendl, M., Aliebhaber, S. and Brenner, D.A. (1997) Posttranscriptional regulation of collagen alpha1(I) mRNA in hepatic stellate cells. Mol. Cell Biol. 17, 5201-5209.

Stevens, J.F., Miranda, C.L., Frei, B. and Buhler, D.R. (2003) Inhibition of peroxynitrite-mediated LDL oxidation by prenylated flavonoids: the alpha,beta-unsaturated keto functionality of 2'-hydroxychalcones as a novel antioxidant pharmacophore. Chem. Res. Toxicol. 16, 1277-1286.

Stevens, J.F. and Page, J.E. (2004) Xanthohumol and related prenylflavonoids from hops and beer: to your good health! Phytochemistry 65, 1317-1330.

Stevens, J.F., Taylor, A.W. and Deinzer, M.L. (1999) Quantitative analysis of xanthohumol and related prenylflavonoids in hops and beer by liquid chromatography-tandem mass spectrometry. J. Chromatogr. A 832, 97-107.

Strauss, R.S. and Pollack, H.A. (2001) Epidemic increase in childhood overweight, 1986-1998. JAMA 286, 2845-2848.

Stravitz, R.T. and Sanyal, A.J. (2003) Drug-induced steatohepatitis. Clin. Liver Dis. 7, 435-451.

Stroffolini, T., Andreone, P., Andriulli, A., Ascione, A., Craxi, A., Chiaramonte, M., Galante, D., Manghisi, O.G., Mazzanti, R., Medaglia, C., Pilleri, G., Rapaccini, G.L., Simonetti, R.G., Taliani, G., Tosti, M.E., Villa, E. and Gasbarrini, G. (1998) Characteristics of hepatocellular carcinoma in Italy. J. Hepatol. 29, 944-952.

Surwit, R.S., Feinglos, M.N., Rodin, J., Sutherland, A., Petro, A.E., Opara, E.C., Kuhn, C.M. and Rebuffe-Scrive, M. (1995) Differential effects of fat and sucrose on the development of obesity and diabetes in C57BL/6J and A/J mice. Metabolism 44, 645-651.

Tabata, N., Ito, M., Tomoda, H. and Omura, S. (1997) Xanthohumols, diacylglycerol acyltransferase inhibitors, from Humulus lupulus. Phytochemistry 46, 683-687.

Targher, G. and Arcaro, G. (2007) Non-alcoholic fatty liver disease and increased risk of cardiovascular disease. Atherosclerosis 191, 235-240.

Taylor-Robinson, S.D., Foster, G.R., Arora, S., Hargreaves, S. and Thomas, H.C. (1997) Increase in primary liver cancer in the UK, 1979-94. Lancet 350, 1142-1143.

Teli, M.R., Day, C.P., Burt, A.D., Bennett, M.K. and James, O.F. (1995) Determinants of progression to cirrhosis or fibrosis in pure alcoholic fatty liver. Lancet 346, 987-990.

Tien, K.M. and Savaraj, N. (2006) Roles of reactive oxygen species in hepatocarcinogenesis and drug resistance gene expression in liver cancers. Mol. Carcinog. 45, 701-709.

Tobe, H., Muraki, Y., Kitamura, K., Komiyama, O., Sato, Y., Sugioka, T., Maruyama, H.B., Matsuda, E. and Nagai, M. (1997) Bone resorption inhibitors from hop extract. Biosci. Biotechnol. Biochem. 61, 158-159.

Vallabhapurapu, S. and Karin, M. (2009) Regulation and function of NF-kappaB transcription factors in the immune system. Annu. Rev. Immunol. 27, 693-733.

Van Cleemput, M., Cattoor, K., De Bosscher, K., Haegeman, G., De Keukeleire, D. and Heyerick, A. (2009) Hop (Humulus lupulus)-Derived Bitter Acids as Multipotent Bioactive Compounds. J. Nat. Prod. 72, 1220–1230.

Van Horssen, H.R., Ten Hagen, T.L. and Eggermont, A.M. (2006) TNF-alpha in cancer treatment: molecular insights, antitumor effects, and clinical utility. Oncologist. 11, 397-408.

Vanhoecke, B., Derycke, L., Van, M., V, Depypere, H., De Keukeleire, D. and Bracke, M. (2005a) Antiinvasive effect of xanthohumol, a prenylated chalcone present in hops (*Humulus lupulus* L.) and beer. Int. J. Cancer 117, 889-895.

Vanhoecke, B.W., Delporte, F., Van, B.E., Heyerick, A., Depypere, H.T., Nuytinck, M., De Keukeleire, D. and Bracke, M.E. (2005b) A safety study of oral tangeretin and xanthohumol administration to laboratory mice. In Vivo 19, 103-107.

Vergnes, L., Phan, J., Strauss, M., Tafuri, S. and Reue, K. (2003) Cholesterol and cholate components of an atherogenic diet induce distinct stages of hepatic inflammatory gene expression. J. Biol. Chem. 278, 42774-42784.

Villanueva, A., Newell, P., Chiang, D.Y., Friedman, S.L. and Llovet, J.M. (2007) Genomics and signaling pathways in hepatocellular carcinoma. Semin. Liver Dis. 27, 55-76.

Vinson, J.A., Mandarano, M., Hirst, M., Trevithick, J.R. and Bose, P. (2003) Phenol antioxidant quantity and quality in foods: beers and the effect of two types of beer on an animal model of atherosclerosis. J. Agric. Food Chem. 51, 5528-5533.

Vogel, S. and Heilmann, J. (2008) Synthesis, cytotoxicity, and antioxidative activity of minor prenylated chalcones from *Humulus lupulus*. J. Nat. Prod. 71, 1237-1241.

Vogel, S., Ohmayer, S., Brunner, G. and Heilmann, J. (2008) Natural and non-natural prenylated chalcones: synthesis, cytotoxicity and anti-oxidative activity. Bioorg. Med. Chem. 16, 4286-4293.

Wang, Q., Ding, Z.H., Liu, J.K. and Zheng, Y.T. (2004) Xanthohumol, a novel anti-HIV-1 agent purified from Hops *Humulus lupulus*. Antiviral Res. 64, 189-194.

Watanabe, M., Houten, S.M., Wang, L., Moschetta, A., Mangelsdorf, D.J., Heyman, R.A., Moore, D.D. and Auwerx, J. (2004) Bile acids lower triglyceride levels via a pathway involving FXR, SHP, and SREBP-1c. J. Clin. Invest 113, 1408-1418.

Watkins, P.B. (2005) Idiosyncratic liver injury: challenges and approaches. Toxicol. Pathol. 33, 1-5.

Weiss, R.F. (2009) Herbal Medicine. Ab Arcanum, Gothenburg, Sweden.

Weiss, T.S., Jahn, B., Cetto, M., Jauch, K.W. and Thasler, W.E. (2002) Collagen sandwich culture affects intracellular polyamine levels of human hepatocytes. Cell Prolif. 35, 257-267.

Wilfred de Alwis, N.M. and Day, C.P. (2007) Genetics of alcoholic liver disease and nonalcoholic fatty liver disease. Semin. Liver Dis. 27, 44-54.

Wobser, H., Dorn, C., Weiss, T.S., Amann, T., Bollheimer, C., Buttner, R., Scholmerich, J. and Hellerbrand, C. (2009) Lipid accumulation in hepatocytes induces fibrogenic activation of hepatic stellate cells. Cell Res. Cell Res. 19, 996-1005.

Wong, E.T. and Tergaonkar, V. (2009) Roles of NF-kappaB in health and disease: mechanisms and therapeutic potential. Clin. Sci. (Lond) 116, 451-465.

Wouters, K., van Gorp, P.J., Bieghs, V., Gijbels, M.J., Duimel, H., Lutjohann, D., Kerksiek, A., van, K.R., Maeda, N., Staels, B., van, B.M., Shiri-Sverdlov, R. and Hofker, M.H. (2008) Dietary cholesterol, rather than liver steatosis, leads to hepatic inflammation in hyperlipidemic mouse models of nonalcoholic steatohepatitis. Hepatology 48, 474-486.

Wunderlich, S., Zurcher, A. and Back, W. (2005) Enrichment of xanthohumol in the brewing process. Mol. Nutr. Food Res. 49, 874-881.

Yamaguchi, N., Satoh-Yamaguchi, K. and Ono, M. (2009) In vitro evaluation of antibacterial, anticollagenase, and antioxidant activities of hop components (Humulus lupulus) addressing acne vulgaris. Phytomedicine. 16, 369-376.

Yang, J.Y., Della-Fera, M.A., Rayalam, S. and Baile, C.A. (2007) Effect of xanthohumol and isoxanthohumol on 3T3-L1 cell apoptosis and adipogenesis. Apoptosis. 12, 1953-1963.

Yilmazer, M. (2001) Xanthohumol, a flavonoid from hops (*Humulus lupulus*): in vitro and in vivo metabolism, antioxidant properties of metabolites, and risk assessment in humans. Ph.D. Thesis, Oregon State University.

Yilmazer, M., Stevens, J.F. and Buhler, D.R. (2001a) In vitro glucuronidation of xanthohumol, a flavonoid in hop and beer, by rat and human liver microsomes. FEBS Lett. 491, 252-256.

Yilmazer, M., Stevens, J.F., Deinzer, M.L. and Buhler, D.R. (2001b) In vitro biotransformation of xanthohumol, a flavonoid from hops (*Humulus lupulus*), by rat liver microsomes. Drug Metab Dispos. 29, 223-231.

Zanoli, P. and Zavatti, M. (2008) Pharmacognostic and pharmacological profile of *Humulus lupulus* L. J. Ethnopharmacol. 116, 383-396.

Zhang, S., Li, J., Jiang, Y., Xu, Y. and Qin, C. (2009) Programmed cell death 4 (PDCD4) suppresses metastastic potential of human hepatocellular carcinoma cells. J. Exp. Clin. Cancer Res. 28, 71.

Zhao, F., Nozawa, H., Daikonnya, A., Kondo, K. and Kitanaka, S. (2003) Inhibitors of nitric oxide production from hops (*Humulus lupulus* L.). Biol. Pharm. Bull. 26, 61-65.

Zhao, F., Watanabe, Y., Nozawa, H., Daikonnya, A., Kondo, K. and Kitanaka, S. (2005) Prenylflavonoids and phloroglucinol derivatives from hops (*Humulus lupulus*). J. Nat. Prod. 68, 43-49.

7 Abbreviations

α-sma	*alpha*-smooth muscle actin
a.k.a.	also known as
a.M.	am Main
ALT	alanine aminotransferase
approx.	approximately
APS	ammonium persulfate
arb.	arbituary
AST	aspartate aminotransferase
ATP	adenosine triphosphate
b.w.	body weight
BCA	bicinchonic acid
BMI	body mass index
bp	base pairs
BSA	bovine serum albumin
℃	degree Celsius
ca.	circa
cDNA	complementary DNA
coll-I	collagen type I
Ctrl.	Control
d	day
Da	dalton (= 1.66018 x 10^{-24} g)
DAPI	4',6-diamidino-2-phenylindole
DMX	desmethylxanthohumol
dest.	destilled
DMEM	Dulbecco's modified eagle medium
DMSO	dimethyl sulfoxide
DNA	deoxyribonucleic acid
DTT	dithiothreitol
e.g.	*exempli gratia*
ECM	extracellular matrix
EDTA	ethylene diamine tetraacetic acid
EGTA	ethylene glycol tetraacetic acid
ELISA	enzyme linked immunosorbent assay
et al.	*et alii*
EU	ELISA unit
FCS	fetal calf serum
FITC	fluorescein isothiocyanate
g	gram

gluc.	glucose
h	hour
$H_2O_{dest.}$	destilled water
HCC	hepatocellular carcinoma
HCl	hydrochloric acid
HRP	horse radish peroxidase
HSC	hepatic stellate cells
Hz	hertz
i.e.	*id est*
i.v.	intravenous
IC_{50}	half-maximal inhibitory concentrations
ICAM-1	inter-cellular adhesion molecule-1
IκBα	inhibitory *kappa* B *alpha*
IKK	IκB kinase
IL-1α	interleukin-1 *alpha*
IL-8	interleukin-8
IX	isoxanthohumol
kDa	kilodalton
l	liter
LDH	lactate dehydrogenase
LPS	lipopolysaccharide
M	molar, mol/l
mA	miliampere
MCP-1	monocyte chemoattractant protein-1 = CCL2
mg	miligram
Mg	magnesium
µl	microliter
µm	micrometer
ml	mililiter
MIC	minimal inhibitory concentration
min	minute
mM	milimolar
mm	millimeter
mmol	millimol
MMP	matrix metalloproteinase
mRNA	messenger RNA
NAD^+	nicotinamide adenine dinucleotide (oxidized form)
NADH	nicotinamide adenine dinucleotide (reduced form)
NaOH	sodium hydroxide
neg.	negative
NFκB	nuclear factor *kappa* B

OD	optical density
p-value	probability value (statistics)
PL	palmitic acid
PBS	phosphate buffered saline
PCR	polymerase chain reaction
PE	phycoerythrin
pH	*pondus hydrogenii*
6-PN	6-prenylxanthohumol
8-PN	8-prenylxanthohumol
PHH	primary human hepatocytes
PI	propidium iodide
PMH	primary murine hepatocytes
qRT-PCR	quantitative realtime-PCR
RNA	ribonucleic acid
RNase	ribonuclease
ROS	reactive oxygen species
rRNA	ribosomal RNA
RT	room temperature
s	second
SDS	sodium dodecyl sulfate
TC_{50}	half-maximal toxic concentrations
TE	Tris EDTA
TEMED	N,N,N',N'-tetramethylethylenediamine
TG	triglyceride
TGF-β	transforming growth factor-*beta*
TI	therapeutic index
TIMP-1	tissue inhibitor of metalloproteinases-1
TNF	tumor necrosis factor
Tris	tris(hydroxymethyl)aminomethane
TWEEN	Polyoxyethylene sorbitan monolaurate
U	unit
UV	ultraviolet
V	volt
v/v	volume per volume
Vol.	volume
vs.	versus
w	week
w/v	weight per volumen
w/w	weight per weight
XN	xanthohumol

8 Appendix

8.1 Curriculum Vitae

Christoph Dorn
Geburtsdatum: 25.10.1979
Geburtsort: Höchstädt a.d. Donau
Staatsangehörigkeit: deutsch

1986 - 1990	Grundschule, Volksschule Bissingen
1990 - 1999	Gymnasium Donauwörth, Allgemeine Hochschulreife (Abitur) mit Latinum, Note 2,00
1999 - 2000	Zivildienst als Altenpfleger in der ProSeniore Residenz Bissingen
Okt. 2000	Beginn des Studiums im Fach Pharmazie an der Universität Regensburg
März 2002	8-wöchige Famulatur in der Kesseltal-Apotheke Bissingen
23. Aug. 2002	Erster Abschnitt der Pharmazeutischen Prüfung in Regensburg, Note 2,75
Okt. 2002 - Feb. 2003	Studentische Hilfskraft am Lehrstuhl Pharmakologie an der Universität Regensburg
06. April 2005	Zweiter Abschnitt der Pharmazeutischen Prüfung in Regensburg, Note 2,50
Okt. 2004 - Dez. 2004	Studentische Hilfskraft am Lehrstuhl Pharmazeutische Biologie an der Universität Regensburg
Mai 2005 - Okt. 2005	Praktikum in der Apotheke im Donaueinkaufszentrum in Regensburg
Nov. 2005 - April 2006	Praktikum bei der Astellas Pharma GmbH in München
26. Juni 2006	Dritter Abschnitt der Pharmazeutischen Prüfung in Regensburg, Note 3,00; Gesamtnote der Pharmazeutischen Prüfung: 2,71
01. Juli 2006	Beginn der Promotionsarbeiten am Universitätsklinikum Regensburg, Abteilung Innere Medizin I
25. Jan. 2007	Offizieller Beginn des Promotionsvorhabens am Lehrstuhl für Pharmazeutische Biologie an der Universität Regensburg
13. Feb. 2007	Approbation als Apotheker

8.2 Advanced training courses

26. - 27. März 2007	Fortbildungsveranstaltung für Projektleiter und Beauftragte für Biologische Sicherheit (BBS) in Regensburg
05. - 08. Mai 2008	GASL Sommerkurs 2008 „Zelluläre und Molekulare Pathobiologie der Leberfibrogenese“ in Aachen
29. - 30. Jan. 2009	Falk Workshop “Translational Research in Chronic Liver Diseases“ in Heidelberg
2008	Weiterbildungsveranstaltung “Versuchstierkunde und Tierschutz” in Regensburg

8.3 Publications

■ Gäbele E., Mühlbauer M., Dorn C., Weiss T.S., Froh M., Schnabl B., Wiest R., Schölmerich J., Obermeier F., Hellerbrand C.
Role of TLR9 in hepatic stellate cells and experimental liver fibrosis. *Biochem Biophys Res Commun.* (2008) 376: 271-276.

■ Wobser H. and Dorn C., Weiss T.S., Amann T., Bollheimer C., Büttner R., Schölmerich J., Hellerbrand C.
Lipid accumulation in hepatocytes induces fibrogenic activation of hepatic stellate cells
Cell Res. (2009) 19: 996-1005.

■ Dorn C., Kraus B., Motyl M., Weiss T.S., Gehrig M., Schölmerich J., Heilmann J., and Hellerbrand C.
Xanthohumol, a prenylflavonoid derived from hops inhibits hepatic inflammation and fibrosis
Mol Nutr Food Res. [in print]

Submitted manuscripts:

■ Arndt S., Maegdefrau U., Dorn C., Schardt K., Hellerbrand C., and Bosserhoff A.K.
Iron-induced expression of BMP6 in intestinal cells is the main regulator of hepatic hepcidin expression *in vivo*
Gastroenterology [in revision]

■ Dorn C., Weiss T.S., Heilmann J., and Hellerbrand C.
Xanthohumol, a prenylated chalcone derived from hops, inhibits proliferation, migration and interleukin-8 expression of hepatocellular carcinoma cells
[submitted]

■ Dorn C., Bataille F., Gäebele E., Heilmann J., and Hellerbrand C.
Xanthohumol feeding does not affect organ function and homeostasis in mice
[submitted]

■ Weigert J., Bauer S., Wanninger J., Neumeier M., Dorn C., Hellerbrand C., Schäffler A., Zimara N., Aslanidis C., Schölmerich J., Buechler C.
Adipocyte chemerin and CMKLR1 are differentially regulated by glucose, insulin, lipopolysaccharide and free fatty acids
[submitted]

■ Dietl K. and Renner K., Dettmer K., Timischl B., Eberhart K., Dorn C., Hellerbrand C., Kunz-Schughart L.A., Oefner P.J., Andreesen R., Gottfried E., Kreutz M.
Lactic acid inhibits TNF secretion and glycolysis of human monocytes
[submitted]

8.4 Presentations

8.4.1 Oral presentations

Forschungswochenende der Klinik und Poliklinik der Inneren Medizin I, Universität Regensburg (2. - 3. Nov. 2007, Kreuth bei Rieden, Germany):

■ Dorn C., Froh M., Blank C., Mackensen A., Schölmerich J., Hellerbrand C.
Expression und Funktion von PD-L1 beim akuten Ischämie/Reperfusionsschaden der Leber

63. Jahrestagung der Deutschen Gesellschaft für Verdauungs- und Stoffwechselkrankheiten (1. - 4. Okt. 2008, Berlin, Germany):

■ Dorn C., Froh M., Schuster K., Schölmerich J., Blank C., Hellerbrand C.
Protektiver Effekt von PD-L1 beim akuten Ischämie/Reperfusionsschaden der Leber

Forschungswochenende der Klinik und Poliklinik der Inneren Medizin I, Universität Regensburg (28. - 29. Nov. 2008, Regenstauf, Germany):

■ Dorn C., Froh M., Blank C., Mackensen A., Schölmerich J., Hellerbrand C.
Expression und Funktion von PD-L1 beim akuten Ischämie/Reperfusionsschaden der Leber.

44th Annual Meeting of the European Association for the Study of the Liver
(22. - 26. April 2009, Copenhagen, Denmark):

■ Dorn C., Fleck M., Gäbele E., Weiss T.S., Blank C., Hellerbrand C.
PD1/PD-L1 protect from inflammation and fibrosis in non-alcoholic steatohepatitis

8.4.2 Poster presentations

24. Jahrestagung der Deutschen Arbeitsgemeinschaft zum Studium der Leber
(25. - 26. Jan. 2008, Frankfurt, Germany):

■ Büchler C., Schäffler A., Dorn C., Johann M., Neumeier M., Köhl P., Wodarz N., Weiss T., Kiefer P., Hellerbrand C.
Elevated adiponectin serum levels in patients with chronic alcohol abuse rapidly decrease during alcohol withdrawal

■ Dorn C., Froh M., Blank C., Mackensen A., Schölmerich J., Hellerbrand C.
Expression und Funktion von PD-L1 beim akuten Ischämie/Reperfusionsschaden der Leber
Poster Award, Category Transplantation / Liver surgery

43rd Annual Meeting of the European Association for the Study of the Liver
(23. - 27. April. 2008, Milan, Italy):

■ Dorn C., Froh M., Schuster K., Schölmerich J., Blank C., Hellerbrand C.
Protective effect of PD-L1/PD-1 in acute hepatic ischemia-reperfusion injury

■ Büchler C., Schäffler A., Dorn C., Johann M., Neumeier M., Koehl P., Weiss T.S., Wodarz N., Kiefer P., Hellerbrand C.
Elevated adiponectin serum levels in patients with chronic alcohol abuse rapidly decrease during alcohol withdrawal

Forschungswochenende der Klinik und Poliklinik der Inneren Medizin I, Universität Regensburg (28. - 29. Nov. 2008, Regenstauf, Germany):

■ Dorn C., Froh M., Schuster K., Schölmerich J., Blank C., Hellerbrand C.
Protective effect of PD-L1/PD-1 in acute hepatic ischemia-reperfusion injury.

25. Jahrestagung der Deutschen Arbeitsgemeinschaft zum Studium der Leber
(29. - 30. Jan. 2009, Heidelberg, Germany):

■ Dorn C., Blank C., Hellerbrand C.
PD-1/PD-L1 protects from inflammation and fibrosis in non-alcoholic steatohepatitis

8.5 Awards/Grants

■ EASL (European Association for the Study of the Liver) Travel Award 2008, Milano, Italy

■ GASL (German Association for the Study of the Liver) Poster Award 2008, Category Transplantation / Liver surgery, Frankfurt, Germany

■ Grant for the participation on the GASL (German Association for the Study of the Liver) Summer Lab-Course 2008 “Zelluläre und Molekulare Pathobiologie der Leberfibrogenese”, Aachen, Germany

■ EASL (European Association for the Study of the Liver) Travel Award 2009, Copenhagen, Denmark

8.6 Danksagung

Viele haben zum Gelingen dieser Arbeit beigetragen. Besonders bedanken möchte ich mich bei:

… Herrn PD Dr. Claus Hellerbrand für das große Vertrauen, dass er in mich gesetzt hat, für das Wissen und die Erfahrung, die er mit mir geteilt hat, für die konstruktive und immer positiv vorgetragene Kritik zur richtigen Zeit, für Verständnis, Rückhalt und Hilfe in jeder Situation und vor allem für seine jederzeit freundschaftliche und offene Art.

… Herrn Prof. Dr. Jörg Heilmann für die angenehme kollegiale Betreuung dieser Arbeit an der naturwissenschaftlichen Fakultät IV, für sein großes Interesse und seine Kooperationsbereitschaft, für die ertragreichen Diskussionen sowie für seine freundschaftliche und unkomplizierte Art.

… Herrn Prof. Dr. Jürgen Schölmerich für das forschungsfreundliche Umfeld in der Abteilung für Innere Medizin I am Universitätsklinikum Regensburg, das mir die Erstellung dieser Arbeit ermöglicht und erleichtert hat.

… Herrn Dr. Manfred Gehrig und den **Mitarbeitern von NATECO$_2$** für das große Interesse am Fortschritt dieser Arbeit und die vielen Hilfestellungen in Wort und Tat.

… der **Barth-Haas Group** für die gute Zusammenarbeit und die Unterstützung dieser Arbeit.

… Frau PD. Dr. Frauke Bataille für die pathologische Begutachtung der histologischen Proben.

… Herrn PD Dr. Thomas Weiss und sein Team für das große Know-How in Bezug auf Primärzellkulturen.

… Herrn Dr. Thilo Spruss für seine schnellen und brauchbaren Ratschläge zu tierexperimentellen Fragen.

…Dr. Erwin Gäbele für seine vorbildhafte Lehrmeistertätigkeit, die mir die Tür zum selbstständigen Arbeiten im Versuchstierlabor geöffnet hat.

… Dr. Matthias Froh für die freundliche, unkomplizierte und ertragreiche Zusammenarbeit.

… Herrn Peter Karl und **Herrn Herbert Gabler** für die hervorragende, sehr kollegiale und zuvorkommene Zusammenarbeit im Versuchstierlabor.

… Frau Doris Müller und **Frau Martina Meisinger** für die vielen Arbeiten, die sie mir still und leise abgenommen haben.

… Herrn Neumeier dafür, dass er stets dafür gesorgt hat, dass Hopfen und Malz bei Erstellung dieser Arbeit nie verlorengingen.

… und natürlich bei:

… der „Lebergruppe“: **Abdo Mahli, Birgitta Ott-Rötzer, Daniela Valletta, Diane Lochbaum, Georgi Kirovski, Heidi Gschwendtner, Dr. Hella Wobser, Karin Dostert, Kornelia Elser, Marina Fink, Michael Saugspier, Monika Artinger, Ruth Schewior, Sabine Kiessling und Dr. Thomas Amann** für das tolle Arbeitsklima, die tatkräftige Unterstützung, die netten Gespräche und die vielen kulinarischen Köstlichkeiten. Ein besseres Kollegium hätte ich mir nicht wünschen können. In die „Lebergruppe“ kommt man Tag für Tag gerne zur Arbeit. Ein großes Dankeschön!

… und bei **allen Kollegen im H1** für die selbstverständliche Hilfe bei den verschiedensten Fragen, die angenehme Arbeitsatmosphäre und die vielen inspirierenden Treffen und Feiern außerhalb des Forschungsbaus.

… meinen Eltern und meinen Geschwistern für alles, was sie mir ermöglicht haben, für ihr Verständnis und den Rückhalt, den sie mir gegeben haben.

… meiner Regina für die großen Entbehrungen, die sie ohne sich zu beklagen hingenommen hat, für ihr Verständnis, ihre Aufmunterungen und ihre Liebe, die ich ihr gerne wieder zurückgeben möchte!

8.7 Eidesstattliche Erklärung

Ich erkläre hiermit an Eides statt, dass ich die vorliegende Arbeit ohne unzulässige Hilfe Dritter und ohne Benutzung anderer als der angegebenen Hilfsmittel angefertigt habe; die aus anderen Quellen direkt oder indirekt übernommenen Daten und Konzepte sind unter Angabe des Literaturzitats gekennzeichnet.

Weitere Personen waren an der inhaltlich-materiellen Herstellung der vorliegenden Arbeit nicht beteiligt. Insbesondere habe ich hierfür nicht die entgeltliche Hilfe eines Promotionsberaters oder anderer Personen in Anspruch genommen. Niemand hat von mir weder unmittelbar noch mittelbar geldwerte Leistungen für Arbeiten erhalten, die im Zusammenhang mit dem Inhalt der vorgelegten Dissertation stehen.

Die Arbeit wurde bisher weder im In- noch im Ausland in gleicher oder ähnlicher Form einer anderen Prüfungsbehörde vorgelegt.

....

(Ort, Datum) (Unterschrift)